SMOOTH SUPPORT VECTOR REGRESSION (SSVR) MODELLING OF SELF-COMPACTING CONCRETE PROPERTIES

YOYOK SETYO HADIWIDODO

DOCTOR OF PHILOSOPHY

UNIVERSITI MALAYSIA PAHANG

UNIVERSITI MALAYSIA PAHANG

DECLARATION OF THESIS AND COPYRIGHT

Author's full name   : YOYOK SETYO HADIWIDODO

Date of birth   : 05 NOVEMBER 1971

Title   : Smooth Support Vector Regression (SSVR) Modelling of Self-Compacting Concrete Properties

Academic Session   : 2011/2012

I declare that this thesis is clarified as

☐ CONFIDENTIAL   (Contain confidential information under the Official Secret Act 1972)*

☐ RESTRICTED   (Contain restricted information as specified by the organization where research was done)*

☐ OPEN ACCESS   I agree that my thesis to be published as online open access (Full text)
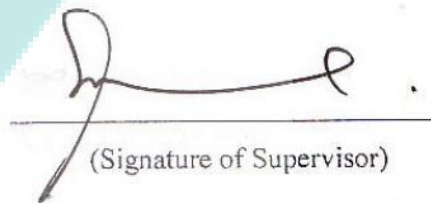
I acknowledge that Universiti Malaysia Pahang reserve the rights as follows:

1. The Thesis is the Property of Universiti Malaysia Pahang

2. The Library of Universiti Malaysia Pahang has the right to make copies for the purpose of research only

3. The Library has the right to make copies of the thesis for academic exchange

Certified by

_____   _____

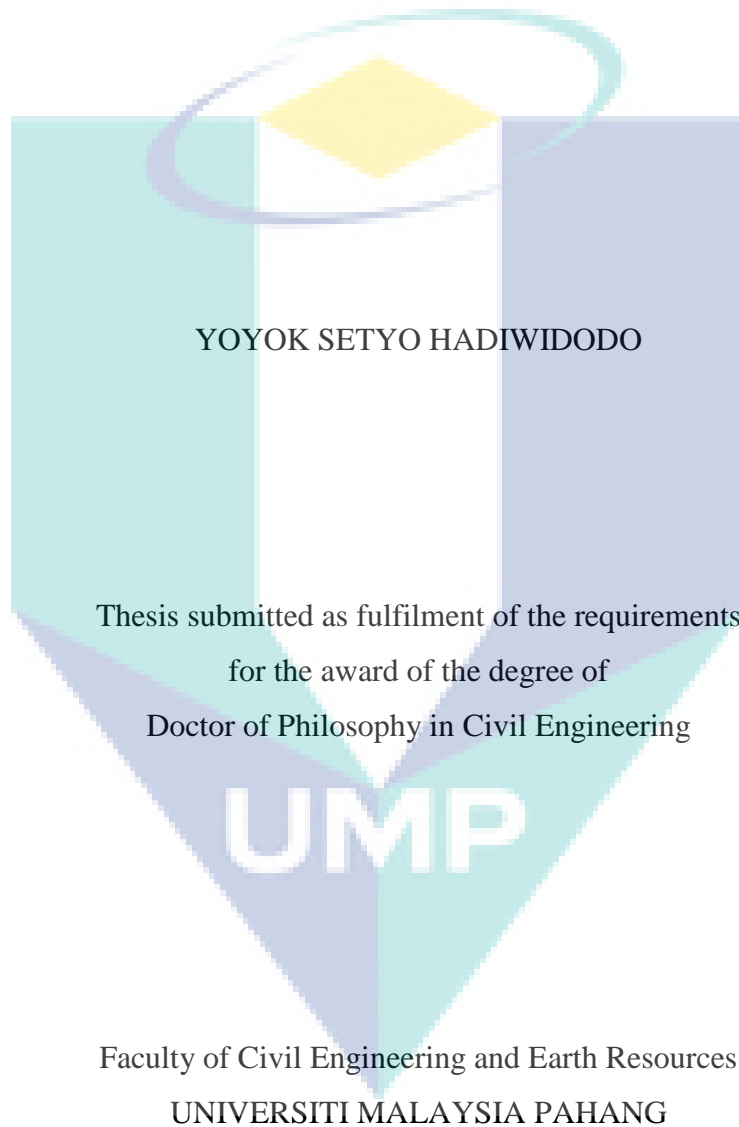(Student's signature)   (Signature of Supervisor)

S145093   Prof. Dato' Dr. Sabarudin bin Mohd

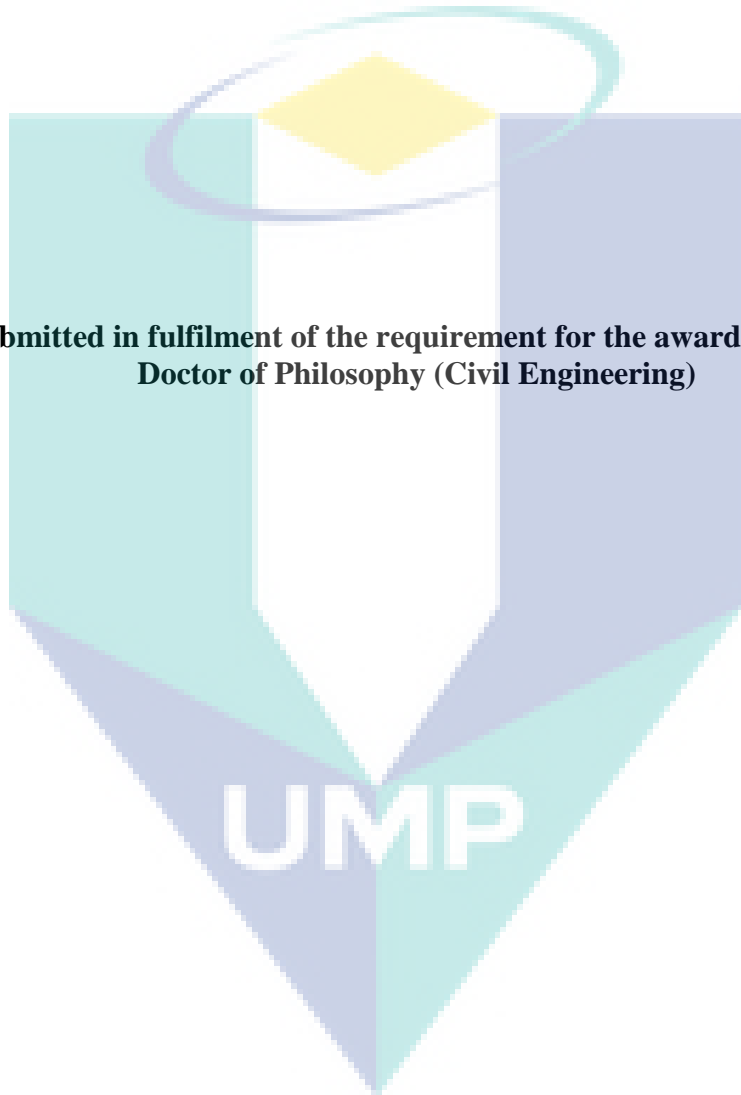(New IC/Passport Number)   (Name of Supervisor)

Date :   Date :

NOTES: If the thesis is CONFIDENTIAL or RESTRICTED, please attach with the letter from the organization with period and reasons for confidentially and restriction

SMOOTH SUPPORT VECTOR REGRESSION (SSVR) MODELLING OF SELF-COMPACTING CONCRETE PROPERTIES

YOYOK SETYO HADIWIDODO

Thesis submitted as fulfilment of the requirements
for the award of the degree of
Doctor of Philosophy in Civil Engineering

Faculty of Civil Engineering and Earth Resources
UNIVERSITI MALAYSIA PAHANG

April 2013

Thesis submitted in fulfilment of the requirement for the award of the degree of
Doctor of Philosophy (Civil Engineering)

SUPERVISOR'S DECLARATION

I hereby declare that I have checked this thesis and in my/our opinion, this thesis is adequate in terms of scope and quality for the award of the degree of Doctor of Philosophy in Civil Engineering.
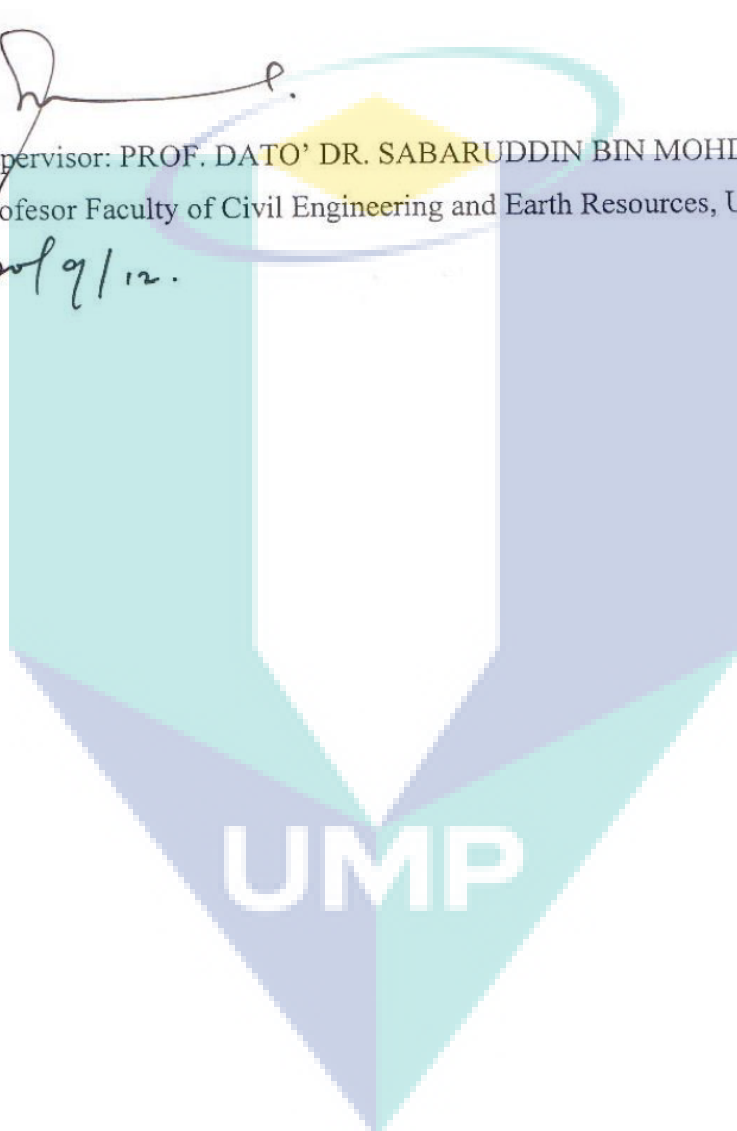
Signature:

Name of Supervisor: PROF. DATO' DR. SABARUDDIN BIN MOHD

Position: Profesor Faculty of Civil Engineering and Earth Resources, UMP

Date   : 20/9/12.

STUDENT'S DECLARATION

I hereby declare that the work in this thesis is my own except for quotations and summaries which have been duly acknowledge. The thesis has not been accepted for any degree and is not concurrently submitted for award of other degree.
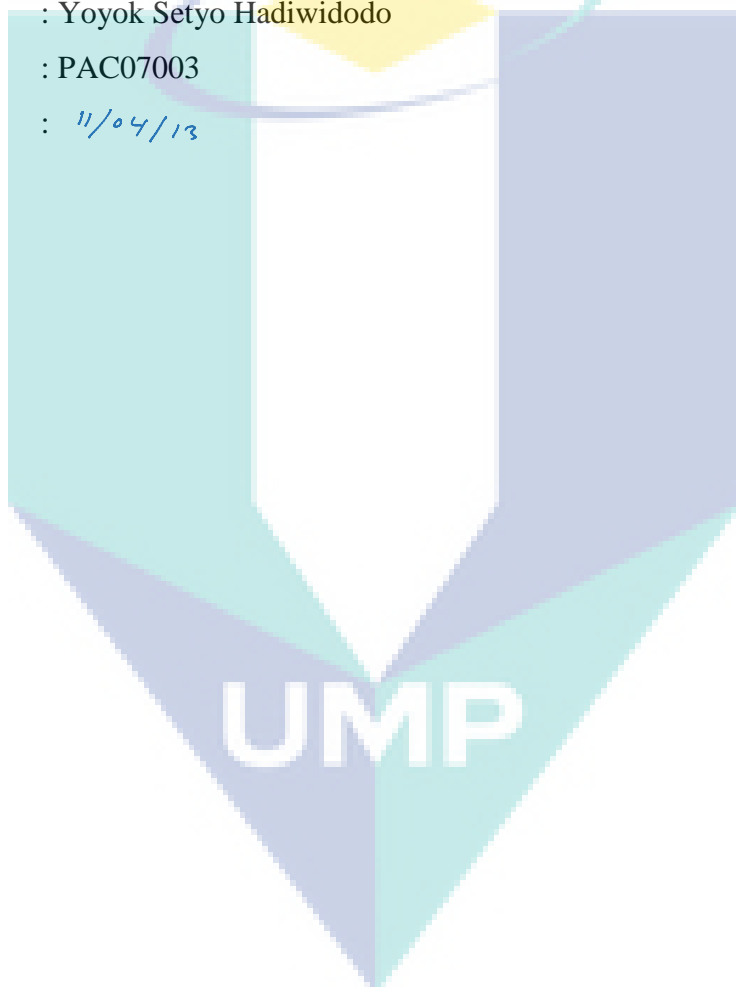
Signature:

Name   : Yoyok Setyo Hadiwidodo

ID Number   : PAC07003
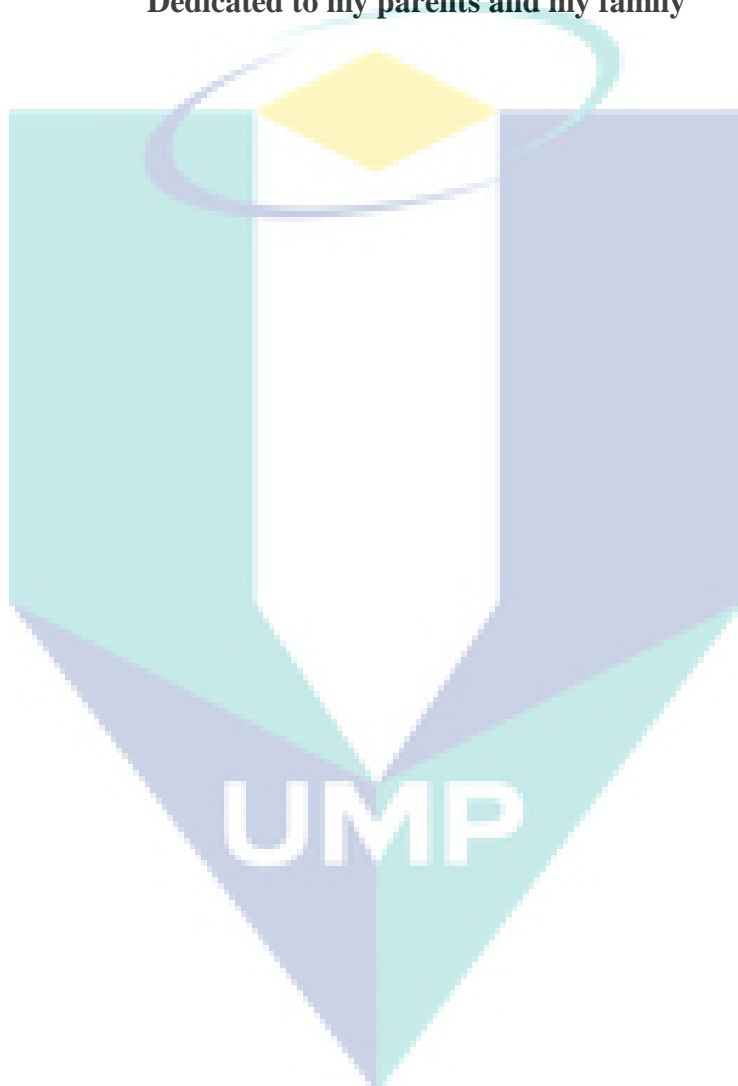
Date   : 11/04/13

PREAMBLE

Say: Though the ocean became ink for the words of my Lord, verily the sea would be used up before the words of my Lord were exhausted, even if we added another ocean like it, for its aid *(Al Qur'an, Al Kahfi 18:109)*

And if all the trees on the earth were pens and the ocean (were ink), with seven oceans behind it to add to its (supply), yet would not the words of Allah be exhausted (in the writing). For Allah is exalted in power, full of wisdom. *(Al Qur'an, Lukman 31:27)*

Behold! In the creation of the heavens and the earth, and the alternation of night and day, there are indeed signs for men of understanding. Men who celebrate the praises of Allah, standing, sitting and lying down on their sides, and contemplate the (wonders of) creation in the heavens and the earth, (with the thought): "Our lord! Not for naught hast thou created (all) this! Glory to thee! Give us salvation from the penalty of the fire *(Al Qur'an, Ali Imron 3:190-191)*

Is one who worships devoutly during the hours of the night prostrating himself or standing (in adoration), who takes heed of the hereafter, and who places his hope in the mercy of his Lord- (like one who does not)? Say: "Are those equal, those who know and those who do not know? It is those who are endued with understanding that receive admonition. *(Al Qur'an, Az Zumar 39:9)*
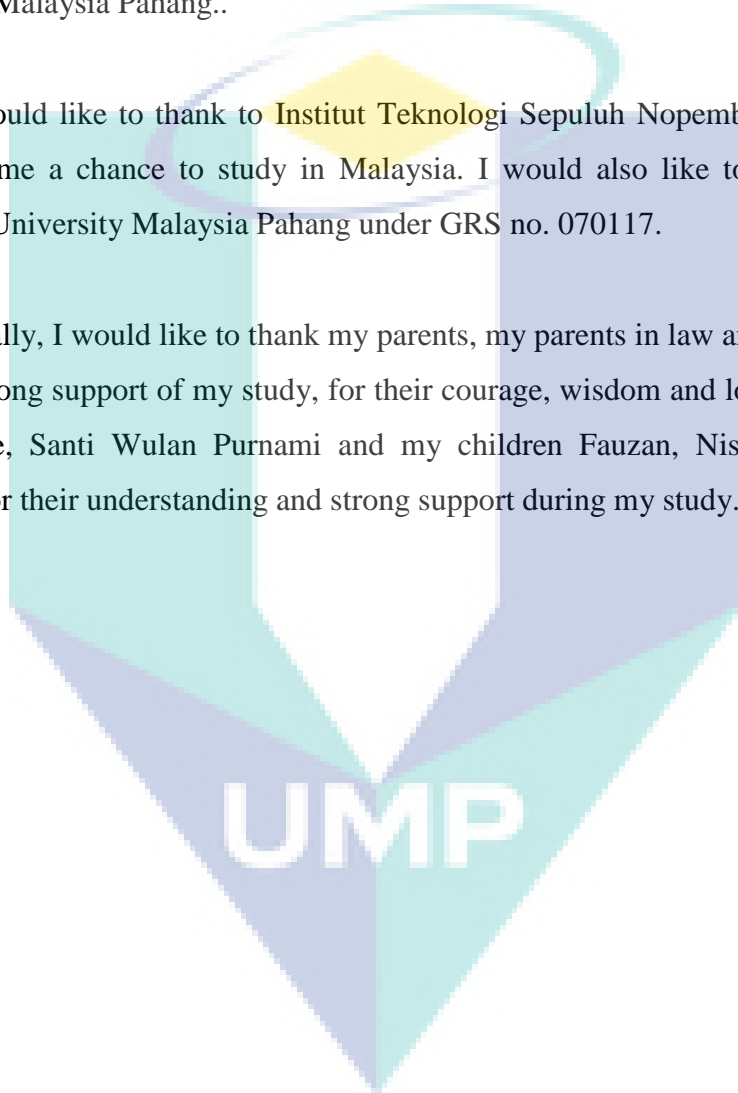
Dedicated to my parents and my family

ACKNOWLEDGMENTS

ABSTRACT

Self-compacting concrete (SCC) is a type of concrete that can flow under its own weight without vibration, filling small interstices of formwork, passing through complicated geometrical configurations, be pumped through long distances and resist segregation. SCC is a complex material, which makes modelling its behaviour a very difficult task. SCC constituent materials and mix proportions which must be properly selected to achieve these flow properties required. The effects of any changes in materials or mix proportions on fresh and hardened concrete performance must be considered in evaluating SCC. It is crucial to use a systematic approach for identifying optimal mixes and investigates the most effective factors on SCC properties under a set of constraints. Due to this reason Taguchi method with the L_{18} (3^6) orthogonal array is used in this study to investigate the properties of SCC. Taguchi method is a promising approach for optimizing mix proportions of SCC to meet several fresh concrete properties. Taguchi method can simplify the test procedure required to optimize mix proportion of SCC by reducing the number of trial mixes. This study has shown that it is possible to model SCC which fulfilling its criteria. The application of the Taguchi method gave the optimal mix design proportions for fresh properties and hardened properties as well. This study has also demonstrated the capability of regression analysis and Smooth Support Vector Regression (SSVR) modelling to predict the properties of SCC. The performance of the proposed method is evaluated using a coefficient of determination (R^2) and mean square error (*MSE*). Results have shown this model is accurate in prediction of the properties of SCC because it has maximum R^2 and minimum *MSE*. The performance of the proposed method is also verified by comparing the predicted levels with actual values. It can be concluded that SSVR method can predict properties of self-compacting concrete with higher estimation accuracy.

ABSTRAK

Konkrit Mampat Diri (SCC) merupakan jenis konkrit yang dapat mengalir di bawah beratnya sendiri tanpa getaran, mengisi celah kecil acuan, dengan melepasi geometri yang rumit, dapat dipam melalui jarak jauh dan tanpa berlaku pengasingan. Konkrit mampat diri adalah bahan yang sangat kompleks, maka tugas untuk memodelkan perilakunya menjadi sangat sukar. Bahan juzuk dan perkadaran campuran konkrit mampat diri harus dipilih dengan teliti untuk menghasilkan sifat aliran yang diperlukan. Pengaruh setiap perubahan bahan atau perkadaran campuran konkrit pada peringkat segar dan keras harus dipertimbangkan dalam menilai prestasi konkrit mampat diri. Pendekatan yang sistematik adalah penting untuk mengenalpasti campuran optimum dan mengkaji faktor yang paling berkesan pada sifat konkrit mampat diri. Atas alasan ini, kaedah Taguchi dengan susunan ortogon L_{18} (3^6) digunakan dalam kajian ini untuk menyelidik parameter yang berkesan dan perkadaran campuran optimum konkrit mampat diri. Kaedah Taguchi adalah pendekatan yang sesuai untuk mengoptimumkan perkadaran campuran konkrit mampat diri bagi memenuhi beberapa sifat segar konkrit. Kaedah Taguchi boleh memudahkan prosedur uji yang diperlukan untuk mengoptimumkan perkadaran campuran konkrit mampat diri dengan mengurangkan jumlah sampel uji kaji. Kajian ini telah membuktikan bahawa SCC dapat dimodelkan untuk memenuhi kriteria yang diperlukan. Penerapan kaedah Taguchi memberikan reka bentuk kadar campuran yang optimum untuk memenuhi sifat segar dan sifat keras. Penyelidikan ini juga menunjukkan keupayaan analisis regresi dan pemodelan regresi sokongan vektor halus (SSVR) untuk mentaksir sifat konkrit mampat diri. Prestasi kaedah yang dicadangkan dinilai dengan menggunakan pekali penentu (R^2) dan ralat min kuasa dua (MSE). Hasil kajian menunjukkan bahawa model ini mempunyai ketepatan yang tinggi karena mempunyai maksimum R^2 dan minimum MSE. Maka disimpulkan bahawa kaedah SSVR boleh memodelkan sifat konkrit mampat diri dengan ketepatan anggaran yang lebih tinggi.

TABLE OF CONTENTS

CHAPTER 6   SUMMARY AND CONCLUSIONS

REFERENCES

APPENDICES

LIST OF TABLES

LIST OF FIGURES

LIST OF SYMBOLS

N	Number of Trials
L	Number of Levels for Each Factor
m	Number of Factors Involved
Y_i	Measured Value of Each Responses
Y_o	Target Value
$\bar{Y}$	Average Value of Y_i
$\hat{Y}_i$	Predicted Value of Each Responses
N	Data Points
ε	Error Term
β	Parameter of Regression
x_i	Independent Variable
e_i	Residual/error
R^2	Coefficient of Determination
A	Data Points
w	Normal Vector of The Hyperplane
γ	Distance Hyperplane to the Origin
y	Slack Variable
e	Column Vector of One of Arbitrary Dimension
C	Regularization Parameter of SVM
u_i	The Dual Variable Corresponds to a Training Point A_i
μ	Parameter of RBF Kernel
$(x)_+$	Plus Function
$p(x,\alpha)$	Integral of Sigmoid Function
$K(A,A')$	Full Kernel Matrix

LIST OF ABBREVIATIONS

ae	Air-Entraining
ANN	Artificial Neural Networks
ANOVA	Analysis of Variance
C	Cement
EFNARC	European Federation of National Trade Associations
EPA	Expanded Perlite Aggregate
FA	Fly Ash
GGBS	Ground-Granulated Blast Slag
G_g	Specific Gravity of Coarse Aggregate
G_s	Specific Gravity of Fine Aggregate
G_c	Specific Gravity of Cement
G_w	Specific Gravity of Water
HPC	High Performance Concrete
HRWR	High Range Water Reducer
JSCE	Japan Society of Civil Engineers
MPa	Megapascals
MR	Modulus of Rupture
MSE	Mean Square Error
NN	Neural Networks
OA	Orthogonal Array
OPC	Ordinary Portland Cement
PC	Portland Cement
PCI	Precast/ Prestressed Concrete Institute
PF	Packing Factor
RBF	Radial Basis Function
S/A	Sand-Aggregate Ratio
SCC	Self-Compacting Concrete
S/N	Signal-to-Noise
SF	Silica Fume
Sp	Superplasticizer
SRM	Structural Risk Minimization
SSD	Saturated Surface Dry

SVM	Support Vector Machine
SVR	Support Vector Regression
SSVR	Smooth Support Vector Regression
V_a	Air Content
VIF	Variance Inflation Factor
VMA	Viscosity Modifying Agent
Vpp	Volume of Pozzolanic Particle
VSI	Visual-Surface Index
w/c	Water-Cementitious Ratio
W_g	Weight of Coarse Aggregate
W_s	Weight of Fine Aggregate
W_c	Weight of Water Required by Cement
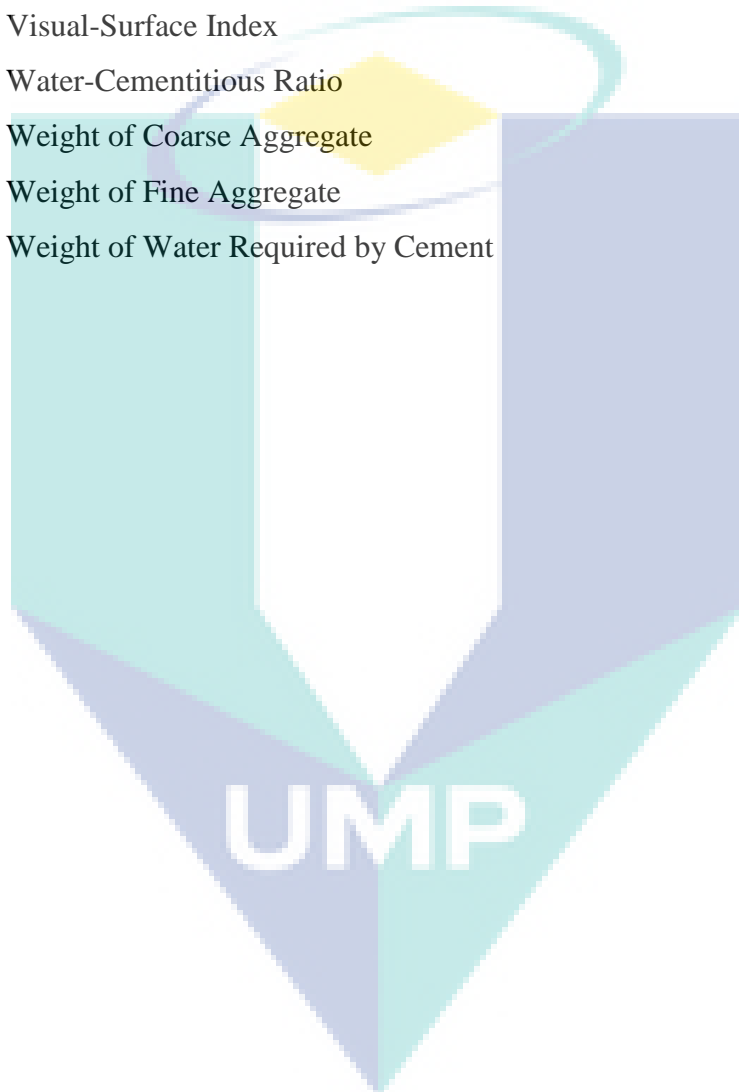
CHAPTER I

INTRODUCTION

1.1.   BACKGROUND

Self-Compacting Concrete (SCC) or self-consolidating concrete is a new generation of High Performance Concrete (HPC) that can be placed and compacted under its own weight with little or no vibration effort. SCC is produced using a high-range water-reducing admixture in combination with a stabilizer. It is a type of concrete that can flow through and fill gaps of reinforcement and corners of moulds without any need for vibration and compaction during the pouring process. The concrete, of course, has to flow without segregation. The use of SCC is beneficial in precast fabrication due to its ease of placement, minimal labour requirements, and reduced noise levels. In addition, SCC can produce a good surface finish.

The concept of SCC was first proposed by Professor Hajime Okamura of Kochi University of Technology, Japan, in 1986 as a solution to concrete's durability concerns. Inadequate consolidations of concrete and unskilled labour were the main causes for poor durability performances of Japanese structures (Okamura, 1997). The developments of self-consolidating concrete would eliminate the cumbersome process of construction, unskilled labour, and the drivers of poor durability performance of concrete.

In the last decade, SCC has become very popular in structural applications in Japan and Europe, and recently in the United States. Housing and tunnelling as well as bridge construction for the Swedish National Road Administration were the main areas of use for SCC. In the Netherlands and Germany, the precast industry is mainly driving

the development of SCC. In the United States, the precast concrete industry is also leading SCC technology implementation. Double tee girders, piles and reduced size slabs constitute the main applications for SCC in North America. Furthermore, several state departments of transportation in the United States are already involved in the study of SCC (Ouchi et all, 2003).

One of the practical advantages of SCC over conventional concrete is lower viscosity and, thus, improved flow rate when pumped. As a consequence, the pumping pressure is lower, reducing wear and tear on pumps and the need for cranes to deliver concrete in buckets at the job site (Khayat, 1999). This also significantly reduces the construction period and the amount of personnel necessary to accomplish the same amount of work. The construction of the Akashi-Kaikyo Bridge in Japan, which considered the longest span suspension bridge in the world, is a good example of SCC application. The casting of the two bridge-anchorages consumed a total of 380,000 yd^3 (290,000 m^3) of SCC that allowed reducing the anchorage construction period by 20 percent (Okamura and Ouchi, 1999).

Currently, the use of self-compacting concrete is being rapidly adopted in many countries. The use of self-compacting concrete could overcome concrete placement problems associated with the concrete construction industry. However, there still is a need for conducting more research and development work for the measurement and standardization of the methods for the evaluation of the self-compacting characteristics of SCC.

The main reason for research concerning SCC is the current lack of standards for it. However, some considerations about mix design and quality control tests are covered in a recent publication by Precast/Prestressed Concrete Institute (PCI) in their "Interim Guidelines for the Use of Self-Consolidating Concrete" (PCI, 2003). Also, EFNARC in the "Specification & Guidelines for Self-Compacting Concrete", (EFNARC, 2002, EFNARC 2005) and the Japan Society of Civil Engineers (JSCE, 1997) in "Recommendation for Self Compacting Concrete".

Three functional requirements are internationally recognized as the main properties of SCC in fresh state (EFNARC, 2002), (PCI, 2003):

1) Filling ability. This is the ability of the concrete to flow under its own weight both horizontally and vertically upwards without honeycombing around any shape.

2) Passing ability. This is the ability of the concrete to flow freely through dense reinforcement without blocking.

3) Resistance to segregation. This is the ability of SCC to maintain a homogenous mix during and after placement, without separation of aggregate from the paste, or water from solids.

Several methods have been developed to assess each of these characteristics of SCC. Most established material properties behaviour models are based on extensive data and knowledge of materials existing in a particular region or country. These models are not adequate for modelling many factors that need to be considered when designing SCC mixes. For example, advances in recent years have been assisted by the use and understanding of chemical admixtures, especially superplasticizer, and cementitious materials, especially silica fume, fly ash, blast furnace slag, etc. Modelling properties behaviour for the concrete containing these materials is essentially more difficult compared with the concrete without them.

Yeh (2007) used a second order regression and the Artificial Neural Networks (ANN) to model the slump flow, but the accuracy is still lower than 85%. The ANN has a good application in the strength modelling (Yeh, 1998a, Yeh, 1998b, Kim et.al, 2004). However, the ANN-based prediction model has a possibility of getting trapped in local minima in training, convergence slow rate and often a risk of getting over-fitting (Yanzhong et.al, 2007). Furthermore, there is no proper method to determine the number of hidden layers.

Within last few years, a new modeling technique called Support Vector Machines (SVMs) (Vapnik, 1995) has been applied in the field of civil engineering (Dibike et. al., 2001, Zhang et. al., 2006, Chen et.al., 2009). Dibike et. al. (2001) investigates the method of SVM on two different practical problems in civil engineering. The first application is for image analysis by feature classification of

remote sensing data, while the second application is for modelling of rainfall-runoff transformations in three different catchments. Zhang et. al (2006) used a support vector regression for large-scale structural health monitoring. Chen et.al (2009) studied on the estimation of exposed temperature of fire damaged concrete by using support vector machine for hydrated cement paste classification at elevated temperature.

The support vector machine (SVM) is a new, efficient and noble approach to improve generalization performance and attain a global minimum. SVMs achieve good generalization ability by adopting a structural risk minimization induction principle that aims at minimizing a bound on generalization error of a model rather than minimizing the error on the training data only. It has ability to avoid overtraining, and has better generalization capability than ANN model. Moreover, the SVMs can always be updated to get better results by presenting new training examples as new data become available (Yan and Shi, 2010). A new method of prediction based on Smooth Support Vector Regression (SSVR) is introduced to resolve the properties modelling of self-compacting concrete (SCC).

1.2.   PROBLEM STATEMENT

SCC can be described as a high performance material which flows under its own weight without requiring vibrators to achieve consolidation by complete filling of formworks even when access is delayed by narrow gaps between reinforcement bars (Zhu et al., 2003). SCC can also be used in situations where it is difficult or impossible to use mechanical compaction for fresh concrete, such as underwater concreting, cast in-situ pile foundations, machine bases and columns or walls with congested reinforcement. The high flowability of SCC makes it possible to fill the formworks without vibration (Khayat et al., 2006). Since its beginning, it has been widely used in large construction in Japan (Okamura and Ouchi, 2003). The last decade, this concrete has gained wide use in many countries for different applications and structural configurations (Bouzoubaa and Lachemi, 2001)

SCC is a complex material exhibiting several sensitive interactions between the constituent materials (Nunes, 2006) which make modeling its behaviour a very difficult task. Moreover, there is no explicit formulation for estimating the properties of self-compacting concretes. For this purpose, statistical formulations are proposed by applying the response surface model and SSVR model on the experimental dataset for prediction of slump flow diameter, flow time, V-funnel flow time, blocking ratio, segregation resistance, compressive strength, tensile strength and flexural strength of self-compacting concretes containing materials composition.

1.3.   AIM AND OBJECTIVES

The aim of this work is to enhance modelling properties of SCC using SSVR.
The specific objectives of this work are as follows:

1. To develop suitable mix design using local materials to satisfy the requirement of SCC.
2. To determine the optimum fresh and hardened characteristic of SCC.
3. To enhance the modelling of SCC characteristic using SSVR method.

1.4.   SCOPE OF WORK

The scope of this work is limited to the development of an optimum mix material to satisfy the requirements of SCC in the fresh stage using local materials and then to determine the hardened properties. The study is focused on obtaining optimum mix design for SCC using Taguchi method. The modelling of SCC properties based on SSVR.

1.5.   ORGANIZATION OF THE THESIS

Chapter 1 introduces self-consolidating concrete and asserts the purpose and main objectives of the research. Figure 1.1 shows the structure of the research that complies with the conventional steps of planning, designing, implementing and evaluating any projects.

Chapter 2 describes self compacting concrete (SCC) and their characteristics, including fresh properties and hardened properties. In this chapter, the Taguchi experiment design is explained. Finally, the statistical analysis: classical modelling and intelligent modelling using Smooth Support Vector Regression are described.

Chapter 3 describes the research methodology adopted for current work. Research methodology is a set of procedures or methods used to conduct research. It focuses primarily on providing help with the tools and techniques used in the research process.

Chapter 4 discusses the Modified Nan Su Mix Design for SCC. Next, the experimental plan based on Taguchi design and the results of properties of self-compacting concrete are described.

Chapter 5 presents the experimental results of properties of self-compacting concrete and analysis of the experimental results. The summary and conclusions of the research are presented in Chapter 6.
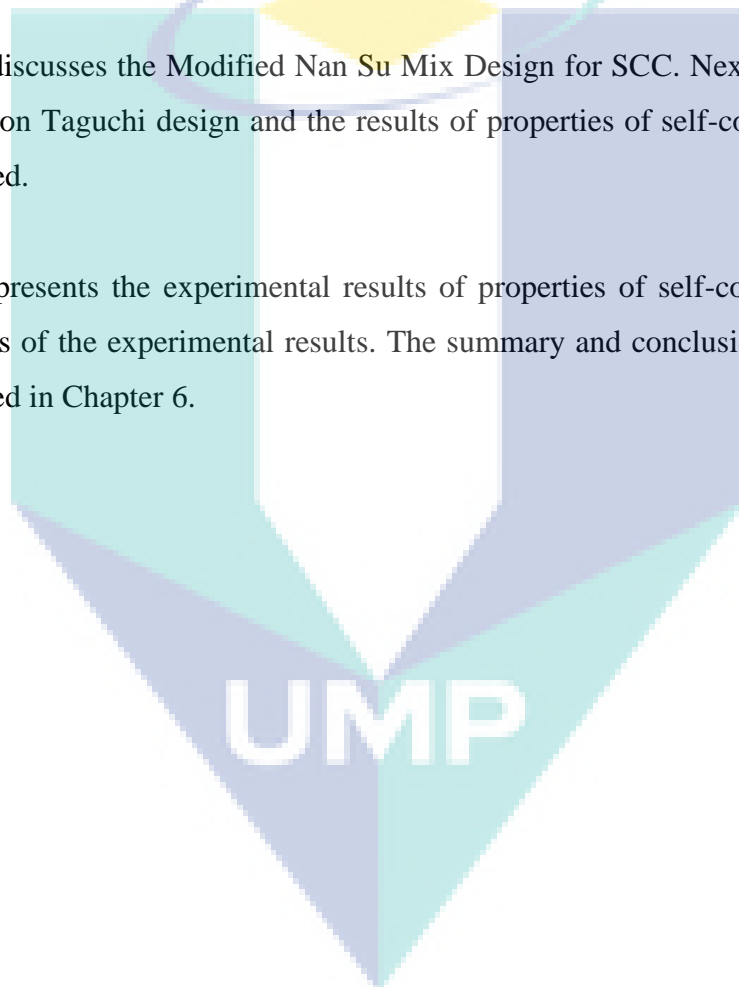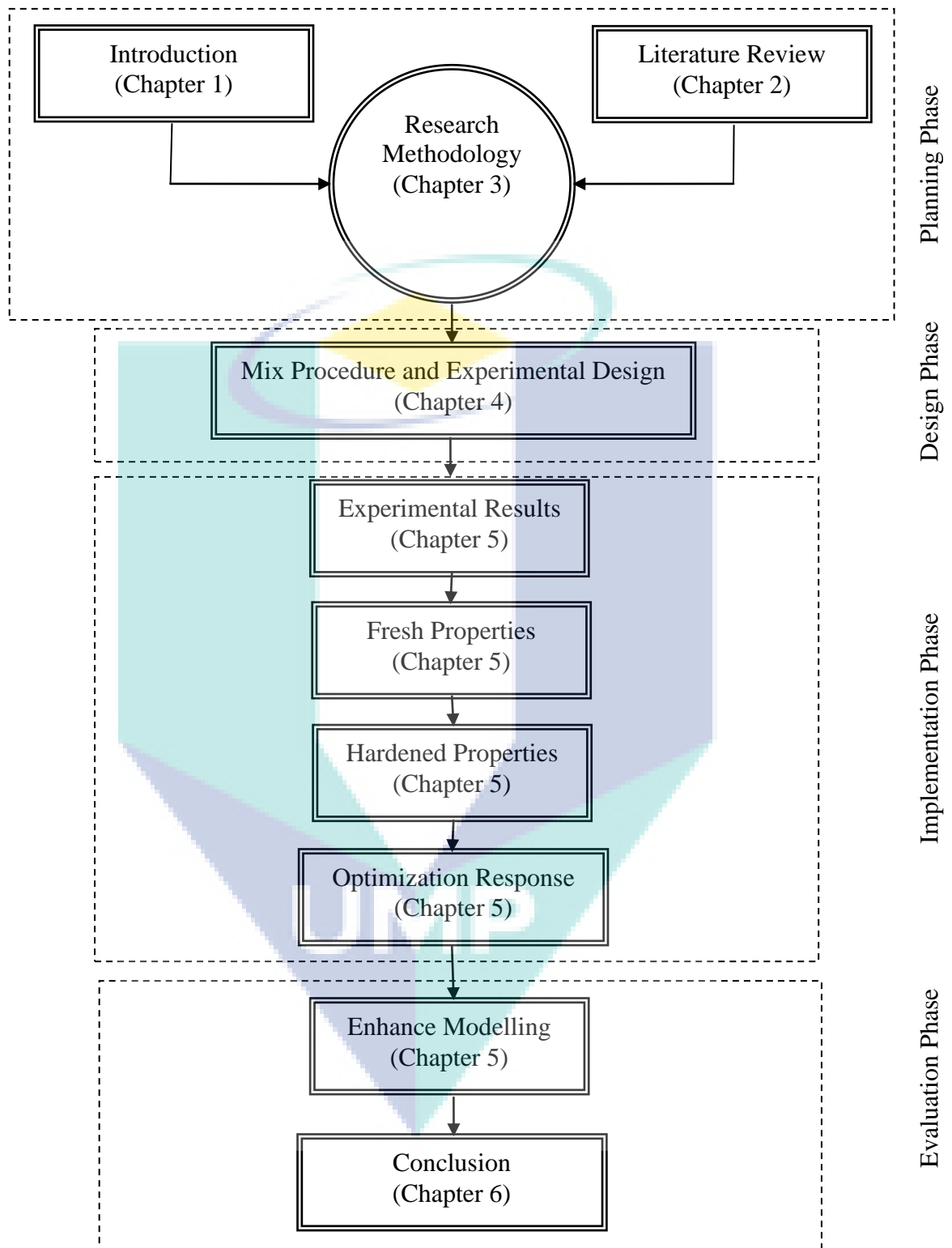
Figure 1.1: Organization of the research

CHAPTER 2

LITERATURE REVIEW

2.1   INTRODUCTION

This chapter describes self-compacting concrete (SCC) and their characteristics, including fresh properties and hardened properties. In this section, the Taguchi experiment design is explained. Finally, the statistical analysis: classical modelling and intelligent modelling using smooth support vector regression are described as well.

2.2   REVIEW OF SELF COMPACTING CONCRETE (SCC)

Self-compacting concrete (SCC) is considered as concrete which can be cast and compacted under its self-weight with little or no vibration effort, at the same time SCC is cohesive enough to be handled without segregation or bleeding. It is used to facilitate and ensure proper filling and good structural performance of restricted areas and heavily reinforced structural members. SCC was developed in Japan (Ozawa, K. et al, 1989) in the late 1980s to be mainly used for highly congested reinforced concrete structures in seismic regions. In the last decade, this concrete gained wide use in many countries for different applications and structural configurations. SCC also provide a better working environment by eliminating the vibration noise (Bouzoubaa, N., and Lachemi, M., 2001).

Since the development of the prototype of self-compacting concrete in 1988, the use of self-compacting concrete in actual structures has gradually increased. The main

reasons for the employment of self-compacting concrete can be summarized as follows (NRMCA, 2004):

- Can be cast at a faster rate with no mechanical vibration and less screeding, resulting in savings in placement cost.

- Improved and produce more uniform architectural surface finish with little to no remedial surface work.

- Ease filling of restricted sections and hard-to-reach areas. Opportunities to create structural and architectural shapes and surface finishes which are not achievable with conventional concrete.

- Improved consolidation around reinforcement and bond with reinforcement.

- Improved pump-ability.

- Improved uniformity of in-place concrete by eliminating variable operator-related effort for consolidation.

- Labor savings.

- Shorter construction periods thus resulting cost savings.

- Quicker concrete truck turn-around times enables the project more efficiently.

- Minimizes movement of ready mixed trucks and pumps during placement.

- Increased jobsite safety by eliminating the need for consolidation.

Grube and Rickert, (2002) compared the compositions between normal vibrated concrete and SCC as illustrated in Figure 2.1 in percentages by weight and by volume have the same cement contents (c = 330 kg/m3) and the same water/cement ratios (w/c ≈ 0.55). The study shows that the SCC contains almost twice the amount of ultrafines content of the vibrated concrete and has a substantially increases addition of super-plasticizer. Cementitious material was used here as the ultrafines.

The literature review of forty-two publications from 2006 to 2007 are given in Table 2.1. The detailed information of component materials, the mixture proportion and the resulting concrete properties illustrate the roadmap of the current research of SCC. As Tumidajski and Gong (2006) had pointed out that the maximum aggregate size influence the performance of the flow of concrete. Whilst the mixture proportion of Okamura and Ouchi (2003) is the most significant part of the SCC to remain homogenous. The summary of Table 2.1. can be found in the following paragraphs.
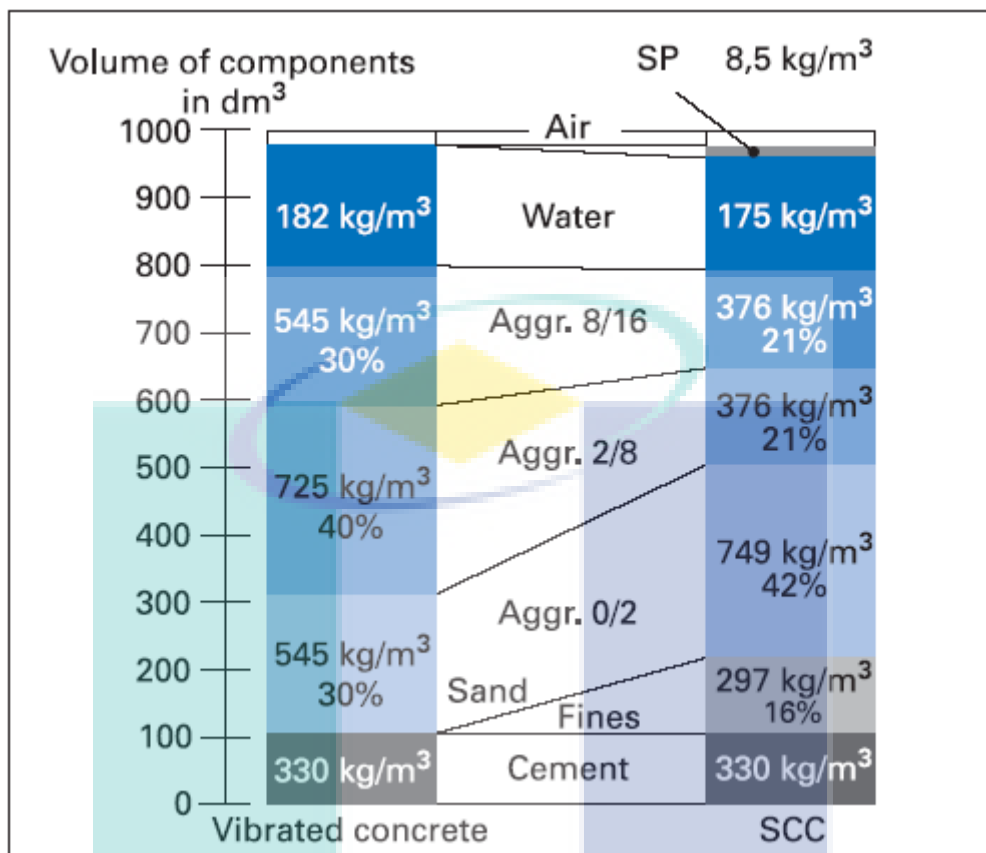
Figure 2.1: Percentage of components by volume in the vibrated concrete used and in the self compacting concrete with w/c = 0.55 (source: Grube and Rickert , 2002)

The general principles of achieving the required combination of properties of SCC mixes comprise the analysis of mixture proportions. Table 2.2 shows the mixture proportion of sand-aggregate ratio (S/A), water-cementitious ratio (w/c) and admixture content. Twenty-five cases (about 54% of the total) used S/A in the range 0.46-0.55. Seven cases used larger 0.56 of S/A, and 14 cases used 0.36-0.40. The coarse aggregate content is sufficiently low for reducing the risk of aggregate over passing and hence concrete blocking when passing through narrow gaps, as a result increasing the passing ability. Water-cementitious ratio ranged from 0.36 to 0.60 with 75% falling in the

Table 2.1: Compilation of SCC studies

Ref.	Date	Country	Application	Aggregate			Sand	S/A	Powder		w/p	Admixture		Sl flow	T50	others	strength
				Max Size, mm	Type	Kg/m³	Kg/m³		Composition	Kg/m³		Splast	VMA	(mm)	(s)		MPa@ 28 days
Assaad	2006	Canada	Experiment	10	crushed	850-900	720-760	0.46	tc+sf+fa	450	0.36-0.40	ae+wr	y	635-665			L-box
Assaad	2006	Canada	Experiment	10	crushed	870-900	740-770	0.46	pc+fa+sf	450	0.40	wr+ae	y	540-745			L-box
Assie	2006	France	Experiment	20	crushed	771-793	884-900	0.46	pc+lp	70-150	0.40-0.65	sp		670-740			L-box
Aydin	2007	Turkey	Experiment	10	natural	750	900	0.55	pc+sf+cf+qp	600	0.48	sp		400-750	2-7.3	L-box, V-funnel, J-ring	15-44
Barros	2007	Portugal	Experiment	12	crushed	669,28	108.59	0.14	pc+lp	676.52		sp		725	4.6		61.60
Bassuon	2007	Canada	Experiment	19	crushed	625-1015	625-1015		pc+fa+sf+gbfs	470	0.38	wr+ae		620-680			L-box
Castel	2006	France	Experiment	20	crushed	742-792	811-857	0.51	pc+lp	315-350	0.66	wr	y	680-700			L-box
Choi et al	2006	Korea	Lightweight	20	NC, LC	117-810	158-861	0.53	pc+ala	460	0.38	ae+wr		630-680			35-60
Cunha	2007	Portugal	SFRC	12	crushed	768.1-817.6	624.8-665.2	0.58	pc+lf	671.6-745.9	0.29	sp		700			56.70
El Chabib	2006	Canada	Experiment	19	crushed	700-1000	700-1000	0.41	pc+sf+fa	350-600	0.35-0.60	wr	y	480-745		L-box, V-funnel	
Elinwa	2007	Negeria	Experiment	20	crushed	662-719	662-719	0.50	pc+sda	441-480	0.42-0.60	sp		665-680	9.8-9.9	L-box, U-box, V-funnel	20-35
Felekoglu	2006	Turkey	Experiment	8	crushed	657-682	884-914	0.57	pc+fa	504	0.37	sp	y	700-740	1.5-6.0	L-box, VSI	
Felekoglu	2007b	Turkey	Experiment	15	crushed	562-630	861-963	0.61	pc+lp	616-649	0.22-0.37	sp		650-800	1-4	L-box, V-funnel	36-56
Felekoglu	2007a	Turkey	Experiment	15	crushed	411-588	855-1024	0.64	pc+fa+lp	555	0.27-0.48	sp		650-790	2.7-4.4	L-box, VSI	30-55
Geikera	2002								pc+sf+fa		0.40	sp+ae				Rheology	
Khayat	2006	Canada	Experiment	10	crushed	820-900	700-760	0.46	pc+sf+fa	450	0.36-0.46	ae+wr	y	640-660		L-box	
Lachemi	2006	Canada	Column	12	crushed	729	1060	0.59	pc+fa	185	0.41	ae+wr	y	655-695	3.2-3.9	L-box	49-54
Mnahoncakova	2007	Czech	Experiment	16	limestone	746	746	0.50	pc+lp+fa	632-657	0.24-0.28	sp		610-780	4.5-7.5	J-ring	43-54
Khatib	2007	UK	Experiment	10	crushed	876	751-876	0.46-0.50	pc+fa	180-500	0.36	sp		635-700		Density, Absp	10-65
Noumowe	2006	France	Experiment	20	crushed	932-1162	652-796	0.36-0.46	pc+sf+cf	450-500	0.42	sp					75-81
Nunes	2006	Portugal	Experiment	12	crushed	769-850	768-802	0.48-0.52	pc+lp	547-616	0.25-0.31	sp		525-750	1.47-14.44	V-funnel, Box	54-75

Table 2.1: Compilation of SCC studies (*continued*)

Ref.	Date	Country	Application	Max Size, mm	Type	Kg/m³	Kg/m³	S/A	Composition	Kg/m³	w/p	Splast	VMA	(mm)	(s)	others	MPa@ 28 days
					Aggregate		**Sand**	**S/A**	**Powder**			**Admixture**		**Sl flow**	**T50**	**others**	**strength**
Oliveira	2006	Portugal	Experiment	15	crushed	863-891	836-874	0.49	pc+sf+fa+hl	422-448	0.33-0.36	sp		650-680		L-box, V-funnel	25-34
Ozbay	2007	Turkey	Experiment	16	crushed	827.7-934.6	684.8-826.1	0.50	pc+fa+gbfs+sf	450-550	0.32-0.44	sp		630-750		V-funnel	
Peter	2006	India	Ream piled	12.5	crushed	700	790	0.53	pc+fa	650	0.34	sp	y	700	5.0	L-box, V-funnel	70.1
Petit	2007	France	Experiment	12	crushed	850	940	0.53	pc+fa+sf	400	0.52	wr		600			48-62
Reinhardt	2006a	Germany	Concrete in fire		qurtzitic	1524-1865			pc+lp+fa	320-636.5	0.33-0.71	ae+wr	y	680-780		J-ring, V-funnel	
Reinhardt	2006b	Germany	Concrete in fire	16	crushed	819-928	705-775	0.48	pc+lp+fa	402-650	0.28-0.48	sp	y	720-780	4.0-10.0	J-ring, V-funnel	20-65
Roussel	2006	France	Experiment	8	crushed	642	786	0.55	pc+nsf	810	0.20	sp		640			
Roziere	2007	France	Experiment	8	rolled	732-964	621-817	0.46	pc+lf	435-683	0.32	sp	y	680-800	1-25	Density, sieve	33-47
Safiuddin	2006	Canada	Experiment	19	crushed	830-902.4	826.5-898.3	0.50	pc+rhc	422.3	0.35	ae+wr		670-720			
Sahmaran	2007	Turkey	Experiment	19	crushed	530-550	889-925	0.63	pc+lp+fa	570	0.40	sp	y	630-700	2-2.9	V-funnel	19-22
Schindler	2007	US	Prestressed	20	crushed	907-1165	614-790	0.47	pc+fa+ggbf+sf	380-551	0.28-0.42	ae+wr	y	660-737	2.6-13.4	VSI	38-66
Shi et al.	2006	Canada	Experiment		LA	503	575	0.53	pc+gp	539	0.34	wr		560		Density	26.3
Sonebi	2007	UK	Experiment	16	crushed	462-1090	478-1100	0.31-0.70	pc+lp	552-635	0.30-0.40	sp		273-945	0.80-6.74	L-box, V-funnel Orimet	
Sukumar	2007	India	Experiment	12	crushed	746-772	813-842	0.52	pc+fa+qf	525	031-034	sp	y	675-773	1-2	L-box, V-funnel	30-70
Torrijos	2007	Argentina	SFRC	18	crushed	775	939	0.55	pc+lf	434	0.38	sp		310-610	1.7	J-ring, V-funnel	42-50
Turcry	2006a	France	Experiment	20	crushed	742-906	768-950	0.54	pc+lp	480	0.41	wr	y	680-760		Shrinkage	30-48
Turcry	2006a	France	Experiment	20	crushed	742-825	857-950	0.47	pc+lp	440	0.37-0.41	sp	y	680-700			35-55
Turkmen	2007	Turkey	Experiment	16	Basalt	1032	389-598	0.37	pc+sf	450	0.40	sp		580-610		L-box, orimet	38-54
Wustholz	2006	Germany	Experiment	16	gravel	960-1000	640-	0.40	pc+lp+fa	530-621	0.31	sp		750-770	10.5-12.5	J-ring, V-funnel	41-78
Yazici	2007	Turkey	Experiment	15	limestone	701-746	804-847	0.53	pc+sf+fa	600	0.28	sp		710-825	3.5-7.0	V-funnel	28-72.5
Yeh	2007	Taiwan	Experiment		crushed	708-1049	650-902	0.39-0.51	pc+fa+gbfs	137-827	0.25-0.70	sp		200-700			

range of 0.36-0.45. The choice of w/c ratio value has very significant effect on both fresh and hardened properties of SCC.

All mixes included a superplasticizer (Sp) or high range water reducer (HRWR). Ten cases used superplasticer incorporated with air-entraning (ae) agent, 16 cases used superplasticer, air-entraning agent, and viscosity modifiying agent (VMA). The results in analysis of mixture proportions are:

- Lower coarse aggregate content,
- Increased paste content,
- High powder content
- Low water-cementitous ratios,
- High superplasticizer doses,
- (Sometime) an air entraining or/and viscosity modifiying agent (VMA).

Table 2.2: Mixture proportion

S/A	Number of cases	w/c	Number of cases	admixture	Number of cases
0.36–0.40	6	0.36–0.40	35	Sp	46
0.41–0.45	8	0.41–0.45	14	Sp+ae	10
0.46–0.50	13	0.46–0.50	9	Sp+ae+VMA	16
0.51–0.55	12	0.51–0.55	5		
0.56–0.60	7	0.56–0.60	6		

The maximum aggregate size and the fresh concrete testing method are shown in Table 2.3. All cases used maximum aggregate size lesser than 20 mm. Nineteen cases used in the range of 16-20mm, fifteen cases used in the range of 11-15 mm, and eight cases used in the range of 8-10mm.

All cases used slump flow test, seven cases used slump flow test individually, and twenty-four cases used slump flow included flow time inspection, T50. Eighteen cases used slump flow incorporated with L-box test, 15 cases with V-funnel test and the eight cases used slump flow combine J-ring (6 cases), Orimet (2 cases), and visual-surface index, VSI (2 cases), respectively.

Table 2.3: Aggregate size and testing methods

Aggregate size (mm)	Number of cases	Testing method	Number of cases
8 – 10	8	Slump flow	42
11 – 15	15	T50	24
16 – 20	19	L-box	18
		V-funnel	15
		J-ring	6
		Orimet	2
		VSI	2

2.2.1 Fresh State Properties

The main characteristics of SCC are the properties in the fresh state. SCC mix design is focused on the ability to flow under its own weight without vibration, the ability to flow through heavily congested reinforcement under its own weight, and the ability to obtain homogeneity without segregation of aggregates.

Several test methods are available to evaluate these main characteristics of SCC. The tests have not been standardized by national or international organizations. The more common tests used for evaluating the compacting characteristics of fresh SCC in accordance with the draft standards of the EFNARC (2002) and Japan Society of Civil Engineers (JSCE, 1999) are described below.

Table 2.4: Comparison of guidelines for SCC

		EFNARC (2002), (2005)	JSCE (1999) Okamura (1999)	PCI (2003)	Hwang et al (2006)	BriteEuRam Grauers (2000)
Slump flow	mm	650 – 800	600-700	610 - 660	620 – 720	600 - 725
T_{50cm} slump flow	sec	2 - 5	5 - 10	3 – 5	no specification	2 - 7
Slump flow with J-Ring	mm	no specification	not mentioned	not mentioned	no specification	no specification
T_{50cm} slump flow with J-Ring	sec	no specification	not mentioned	not mentioned	no specification	no specification
J-Ring, BJ	mm	0 -10	not mentioned	10 - 15	no specification	no specification
Slump flow-Slump flow with J-Ring	mm	not mentioned	not mentioned	not mentioned	no specification	no specification
V-funnel	Sec	8 - 12	5 - 10	6 - 10	< 8	5 - 15
L-box (h_2/h_1)		0.8 - 1.0	no specification	0.75 – 1.0	no specification	0.8 – 1.0
U-box (h2-h1)	mm	30	no specification	no specification	no specification	no specification
U-box (h1)	mm	no specification	> 300	> 305	no specification	no specification
Fill box	%	90 - 100	90 - 100	no specification	80	no specification
GTM Screen stability test	%	0 - 15	no specification	5 - 15	< 15	no specification
Orimet	sec	0 - 5	no specification	0 - 5	no specification	2 - 20
VSI		not mentioned	not mentioned	0 - 3	0 or 1	no specification
Bleeding	cm/s	not mentioned	not mentioned	no specification	no specification	no specification

Various test methods to assess workability characteristics of SCC are summarized in Table 2.4, which also includes some limit values recommended by the European Federation of National Trade Associations (EFNARC, 2002), Precast/ Prestressed Concrete Institute (PCI, 2003) Interim Guidelines, (Hwang, 2006), BriteEuRam, (Grauers, 2006) and the Japan Society of Civil Engineers (JSCE, 1999). For each workability characteristic (deformability, passing ability, filling capacity, and static stability), various test methods recommended in the aforementioned specifications. The recommended test methods and performance specifications are normally used in combination for various types of SCC. Many specifications require the combination of slump flow, T50 and L-box to specify performance of SCC in fresh state. For example, according to (EFNARC, 2002) the use of SCC for civil engineering structures should have a slump flow of 650 to 880 mm, T-50 time of 2 to 5 seconds, and L-box blocking ratio ($h2/h1$) greater than 0.8.

2.2.1.1 Slump Flow

The deformability and flowability of fresh SCC in absence of obstructions can be evaluated by using slump flow test. The fresh SCC can be filled in one layer in the standard slump cone without any consolidation. The slump flow value represents the mean diameter (measured in two perpendicular directions) of SCC spread after lifting the standard slump cone and concrete stopped flowing. The schematic baseplate for slump flow test (EFNARC, 2002) is as shown in Figure 2.2.

According to EFNARC, (2002), the slump flow value of concrete should be in the range between 650 and 800 mm to qualify for the SCC. Hwang et al. (2006) suggested a slump value of 650 mm and 720 mm for SCC under conditions of no aggregate segregation. JSCE (1999) suggested limit of 600 to 700 mm for SCC. The SCC may segregate at slump flow higher than 800 mm while less than 600 mm slump flow may be insufficient to pass through highly congested reinforcement.
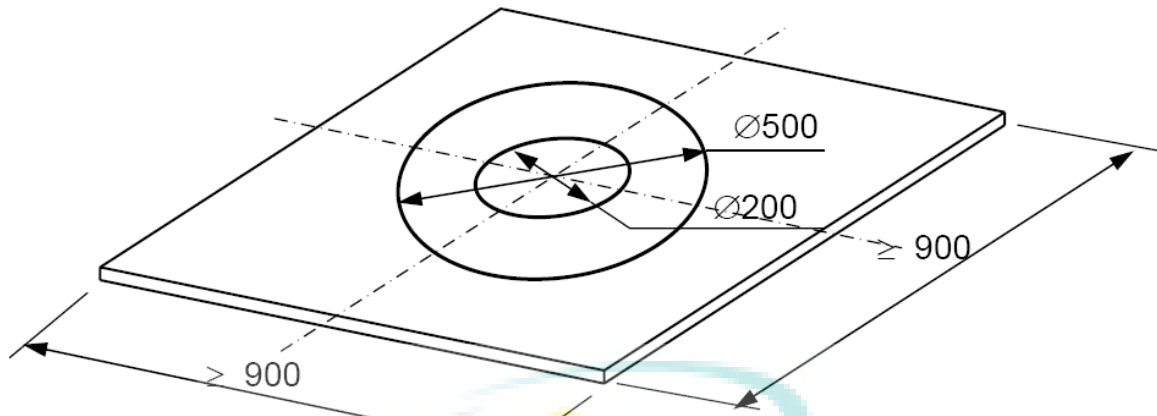
Figure 2.2: Schematic base plate for slum flow test (EFNARC, 2002)

All cases used slump flow test to measure the flow capacity. Figure 2.3 shows nearly 80% of the slump flow was in the range between 650-800mm. This fact verifies slump flow limit values as recommended by EFNARC (2002). The slump flow value provides a good idea about the fresh concrete filling ability which is related to yield stress and the T50 or time to reach a flow of 500mm provides a good idea about the relative plastic viscosity.
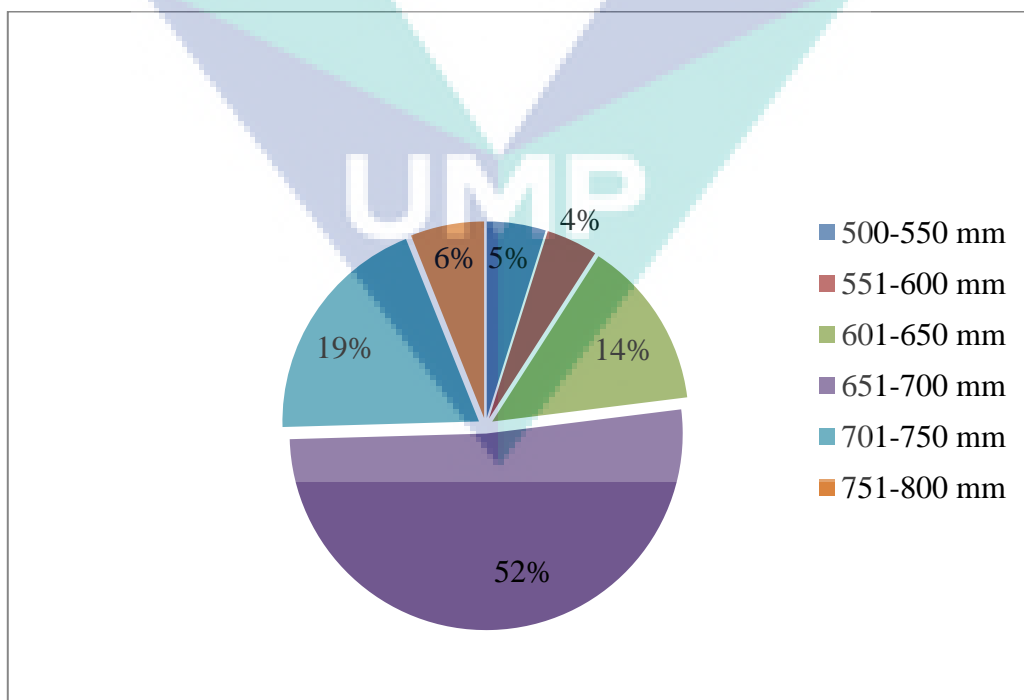
Figure 2.3: Slump flow from case studies of literature review

2.2.1.2 V-Funnel

The deformability of SCC through restricted areas can be evaluated by using V-funnel test (EFNARC, 2002). The schematic representation of V-funnel test apparatus is shown in Figure 2.4. In this test, V-shaped funnel is filled completely with fresh SCC without any consolidation and then the bottom outlet is opened, allowing concrete to fall out under gravity. The time of flow from the opening of bottom outlet to the complete fit of flow is considered as a V-funnel flow time. The V-funnel flow time is longer as the viscosity of SCC increases.

Figure 2.4: Schematic V-funnel test (EFNARC, 2002)
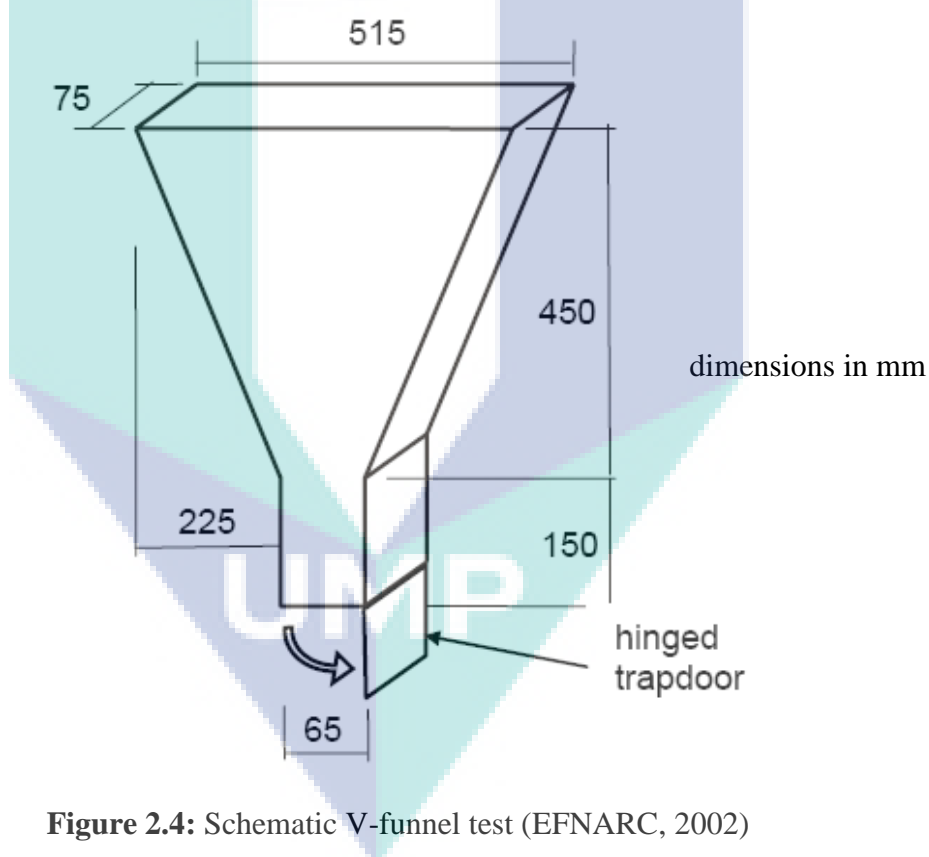
2.2.1.3 L-box

The L-box test is proved useful to determine the ability of SCC to flow through the gaps between reinforcing bars (EFNARC, 2002). The vertical part of the box is filled with fresh concrete and left to rest for one minute. After that, the gate is opened to allow the concrete to flow out of the vertical part through three reinforcing bars (12 mm diameter

with 34 mm gap). The time taken for the leading edge of concrete to reach a distance of 200 and 400 mm along the horizontal part, and the height H_1, and H_2 of concrete are measured and used to determine the H_2/ H_1 ratio. Schematic L-box test is shown in Fig 2.5.
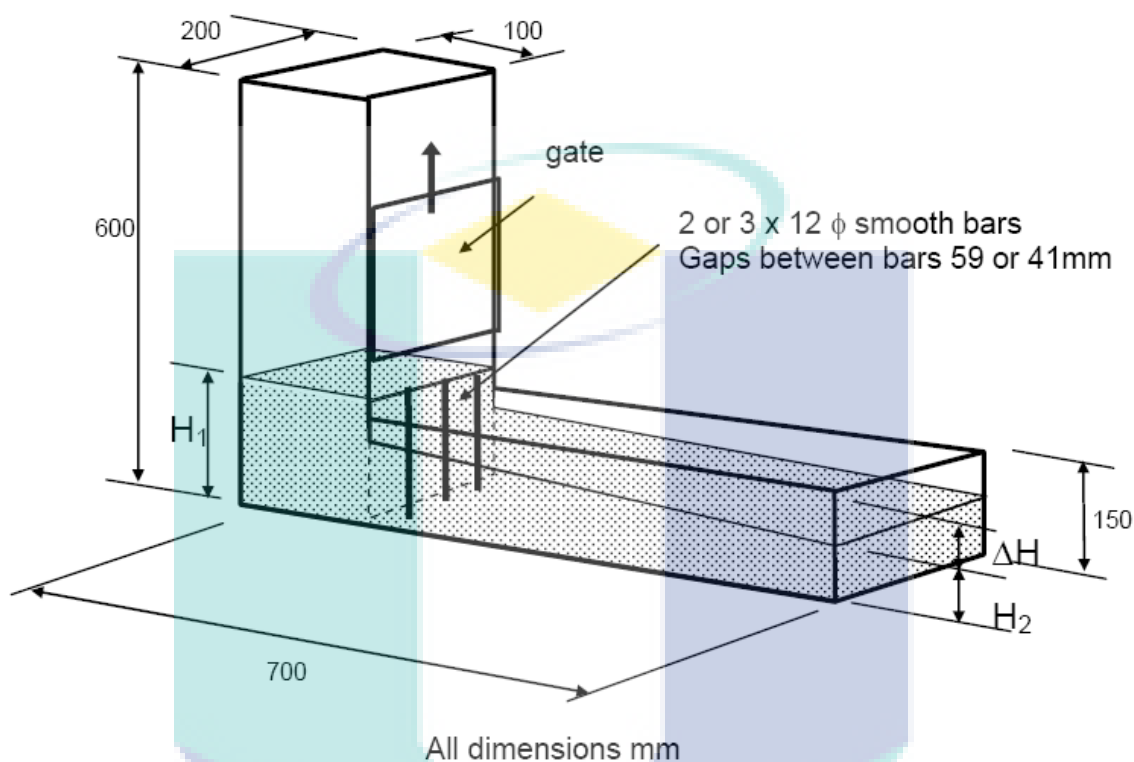
Figure 2.5: Schematic L-box test (EFNARC, 2002)

2.2.2   Hardened Properties

The basic ingredients used in SCC mixes are practically the same as those used in the conventional High Performance Concrete (HPC) vibrated concrete, except they are mixed in different proportions and the addition of special admixtures to meet the projected specifications for SCC. The hardened properties are expected to be similar to those obtainable with HPC concrete. The previous laboratory and field tests have demonstrated that the SCC hardened properties are indeed similar to those of HPC (Table 2.1).

2.2.2.1 Compressive Strength

The hardened property is associated in the 28-day compressive strength. Figure 2.6 gives values of compressive strength occurrence of Table 2.1. Values ranged from 20 to

nearly 80 MPa with about 60% of mixes having strengths in excess of 40 MPa. This confirms that it is possible to produce SCC with medium strength.
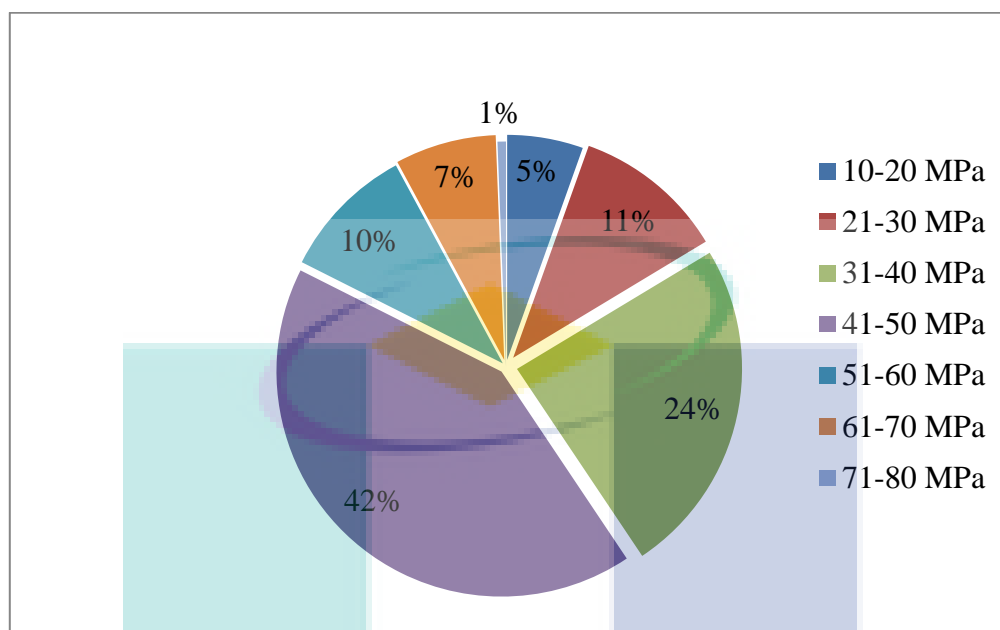
Figure 2.6: Compressive strength ranges used from case studies of literature review

The strength of SCC tends to be always high due to the high cementitious content, low water content and high Superplasticizer dosage. SCC compressive strengths are comparable to those of conventional vibrated concrete made with similar mix proportions and water/cement ratio. There is no difficulty in producing SCC with compressive strengths up to 50MPa. Turkmen and Kantarci (2007), reported the effect of special aggregate such as Expanded Perlite Aggregate (EPA) on compressive strength of SCC. They stated that the compressive strength of EPA concrete generally decreases with increasing EPA ratios.

Khatib (2007) studied the influence of cementitious material such as fly ash on the performance of SCC. The Portland Cement (PC) was partially replaced with 0–80% Fly Ash (FA). The water to binder ratio was maintained at 0.36 for all mixes. Properties included workability, compressive strength, ultrasonic pulse velocity (V), absorption and shrinkage. The results indicate that high volume FA can be used in SCC to produce high strength and low shrinkage.

2.2.2.2 Tensile Strength

Tensile strength values associated with the characteristic compressive strengths classes are explicitly defined in most codes. However, the application of the tensile strength as design parameter in international design codes varies (Mijnsbergen, 2000). Tensile strength is based on the indirect splitting test on cylinders. Since the invention and the utilisation of self-compacting concrete (SCC) many studies attended also to the creep behaviour of SCC under sustained compressive load. In contrast, less attention is paid to the behaviour under sustained tensile load. However, the response of concrete subjected to tensile load is an important factor (Wustholz and Reinhardt, 2006).

Druta (2003) reported of his research about comparison of the splitting tensile strength and compressive strength values of self-compacting and normal concrete specimens and to examine the bonding between the coarse aggregate and the cement paste using the Scanning Electron Microscope. In his work the water – cement ratios varied from 0.3 to 0.6 while the rest of the components were kept the same, except the chemical admixtures, which were adjusted for obtaining the self-compactability of the concrete. All SCC mixtures exhibited greater values in both splitting tensile and compressive strength after being tested, compared to normal concrete. The splitting tensile strength increased by approximately 30%, whilst the compressive strength was around 60% greater on normal concrete. In addition, the SCC tensile strengths after 7 days were almost as high as those obtained after 28 days for normal concrete. This was possible due to the use of mineral and chemical admixtures, which usually improve the bonding between aggregate and cement paste, thus increasing the strength of concrete.

Zaina et.al. (2002) predicted tensile strength of high performance concrete. They proposed the equation with the concrete age parameter for predicting the tensile strength. Sekhar and Rao (2008) formulate a relationship between the splitting tensile strength, flexural strength and compressive strength from the experiment test results.

2.2.2.3 Flexural Strength

It is the ability of a beam or slab to resist failure in bending. It is measured by loading unreinforced 150 x 150 x 1000 mm or 100 x 100 x 500 mm concrete beams with a

span three times the depth. The flexural strength is expressed as "Modulus of Rupture" (MR) in MPa and is determined by standard test methods ASTM C 78 (third-point loading) or ASTM C 293 (center-point loading). Flexural MR is about 12 to 20 percent of compressive strength depending on the type, size and volume of coarse aggregate used.

Designers of pavements or slab use a theory based on flexural strength. Therefore, laboratory mix design based on flexural strength tests may be required, or a cementitious material content may be selected to obtain the needed design Modulus of Rupture (MR).

Ding, et.al (2007) had study the flexural strength of SCC. They used steel fibres to improve flexural strength of SCC. The results showed that the steel fibre can represent optimal fibre reinforcement for self-compacting-high-performance-concrete. Bassuoni and Nehdi (2009) explored durability of SCC on flexural loading. They tested five mixture design variables (type of binders, air-entrainment, sand-to-total aggregates mass ratio, and hybrid fibre reinforcement). Their results show limestone binder exhibited inferior performance of flexural loading, air-entrainment agent reducing the rate of damage and sand-to-total aggregate ratio had insignificant effect on flexural loading.

2.3   TAGUCHI EXPERIMENT DESIGN

In an experimental study, in order to determine the effects of various factors, which are affecting the results of experiment, different methods and approaches are used. The fundamentals of these methods are the full factorial design and fractional factorial design concept (Montgomery, 2004). In the traditional approach, which is also known as full factorial design, the experiments are performed for each condition, which consists of all factors. The number of possible design N (number of trials) is

$$N=L^m \tag{2.1}$$

Where L= number of levels for each factor, m= number of factors involved

Assume an engineering experimental study requires six control factors and three control levels per control factor to understand the influence and interaction of its input data on the output results. By using a traditional experimental process, usually at least all the

possible 3^6 = 729 tests need to be carefully conducted and finished before an optimal performance can be concluded. The number of tests can get very large really fast.

A complete factorial design requires experiments including all possible combinations of the levels of the factors, which can be very expensive and time-consuming. Therefore, Taguchi design can be used as an efficient alternative. A Taguchi design requires running only a fraction of experiments in the complete factorial design. They also help to identify factors that have significant effects.

Taguchi's approach to parameter design provides the design engineer with a systematic and efficient method for determining near optimum design parameters for performance and cost. The objective is to select the best combination of control parameters so that the product or process is most robust with respect to noise factors. The Taguchi method utilizes orthogonal arrays from design of experiments theory to study a large number of variables with a small number of experiments. Using orthogonal arrays significantly reduces the number of experimental configurations to be studied. (Unal, and Dean, 1991).

The experiments were designed based on orthogonal array technique. Factors and its levels affecting on SCC properties were decided based on the previous study on the subject. Six factors and three levels of each factor have been taken for experimentation. In the orthogonal array technique, the minimum required experiments for six factors at three levels are 18, so it is designed in $L_{18}(2^1 \times 3^7)$. Some standard orthogonal array can be found at Appendix-E.

In Table 2.5, there are eight parameters A, B, C, D, E, F, G and H, each at three levels. This is called an "L_{18}" design, with the 18 indicating the eighteen rows, configurations, or prototypes to be tested. Specific test characteristics for each experimental evaluation are identified in the associated row of the table. Thus, L_{18} means that eighteen experiments are to be carried out to study eight variables at three levels. The number of columns of an array represents the maximum number of parameters that can be studied using that array. Note that this design reduces 6561 (3^8) configurations to 18 experimental evaluations. There are greater savings in testing for the larger arrays. For example, using an L_{27} array, 13 parameters can be studied at 3 levels by running only 27

experiments instead of 1,594,323 (3^{13}). The Taguchi method can reduce research and development costs by improving the efficiency of generating information needed to design systems that are insensitive to usage conditions, manufacturing variation, and deterioration of parts. As a result, development time can be shortened significantly and important design parameters affecting operation, performance, and cost can be identified. (Unal, and Dean, 1991).

Table 2.5: Standard $L_{18}(2^1 \times 3^7)$Taguchi orthogonal array (OA)

Exp No.	Control factors							
	A	B	C	D	E	F	G	H
1	1	1	1	1	1	1	1	1
2	1	1	2	2	2	2	2	2
3	1	1	3	3	3	3	3	3
4	1	2	1	1	2	2	3	3
5	1	2	2	2	3	3	1	1
6	1	2	3	3	1	1	2	2
7	1	3	1	2	1	3	2	3
8	1	3	2	3	2	1	3	1
9	1	3	3	1	3	2	1	2
10	2	1	1	3	3	2	2	1
11	2	1	2	1	1	3	3	2
12	2	1	3	2	2	1	1	3
13	2	2	1	2	3	1	3	2
14	2	2	2	3	1	2	1	3
15	2	2	3	1	2	3	2	1
16	2	3	1	3	2	3	1	2
17	2	3	2	1	3	1	2	3
18	2	3	3	2	1	2	3	1

The following steps are used for the Taguchi experiment (Antony, et al, 2001):

    1. Objective of the experiment

    2. Identification of the control factors and their levels

    3. Selection of most suitable response for the experiment

4. Choice of orthogonal array (OA)

5. Preparation of experimental layouts and run

6. Statistical analysis and interpretation of experimental results

Experimental design using Taguchi method has been successfully applied to many research of civil engineering material in the last decade. Srinivasan *et al*. (2003) using Taguchi method based on orthogonal array technique in L_9 array with three factors, namely ordinary portland cement (OPC), fineness of the cement, and type of additives, at three levels each. They need 9 number of experiments. They can reduce number of experiment 60% from $3^3 = 27$ number of experiment in factorial method. Tanyildizi and Coskun, (2008) adopted Taguchi approach with an L_{16} (4^5) to reduce the numbers of experiment. They studied the effect of silica fume on compressive and splitting tensile strength of lightweight concrete after high temperature. The mixes has two control factors (variables); percentage of silica fume with 4 level and heating degree with 3 level.

2.4 TAGUCHI APPROACH FOR OPTIMIZATION

Having completed an experiment, the procedure then is to analyse and interpret the Taguchi experimental results. The first step, it is to analyse the signal-to-noise (S/N) ratio, which measures the functional robustness of process performance. Signal-to-Noise ratios (S/N), which are log functions of desired output, serve as objective functions for optimization, help in data analysis and prediction of optimum results. There are 3 signal-to-Noise ratios of common interest for optimization:

1. *Smaller is better*

   The S/N ratio can be calculated as given in Eq. (2.1) for smaller is better.

$$S/N = -10 * \log_{10}\left(\frac{1}{n}\sum_{k=1}^{n} Y_i^2\right) \qquad (2.2)$$

Y shows the measured value of each response.

   Smaller is better is chosen when the goal is to minimize the response, e.g. minimum flow time T50 of SCC.

2. *Larger is better*

The S/N ratio is calculated as given in Eq. (2.2) for larger is better.

$$S/N = -10 * \log_{10}\left(\frac{1}{n}\sum_{i=1}^{n}\frac{1}{Y_i^2}\right)$$

(2.3)

Larger is better is chosen when the goal is to maximize the response, e.g. maximum expected slump flow, compressive, tensile and flexural strength of SCC.

3. *Nominal is better*

The S/N ratio is calculated as given in Eq. (3) for smaller the better.

$$S/N = -10 * \log_{10}\left(\frac{1}{n}\sum_{i=1}^{n}(Y_i - Y_0)^2\right)$$

(2.4)

Nominal is better is chosen when the goal is to target the response and it is required to base the S/N ratio on standard deviations only.

2.5 STATISTICAL MODELLING

2.5.1 Regression Analysis

Regression analysis includes any techniques for modeling and analyzing several variables, when the focus is on the relationship between a dependent variable and one or more independent variables. In linear regression, the model specification is that the dependent variable y_i is a linear combination of the parameters. For example, in simple linear regression (first order regression) (eq.2.5) for modeling n data points there is one independent variable x_i and two parameters, β_0 and β_1:

$$y_i = \beta_0 + \beta_1 x_i + \varepsilon_i \qquad i = 1,2,\ldots\ldots.n$$

(2.5)

Where ε_i is error term.

In the nonlinear regression/second order regression models, there are p independent variables:

$$y(x_i) = \beta_0 + \sum_{i=1}^{N}\beta_i x_i + \sum_{i<j}^{N}\sum \beta_{ij} x_i x_j + \sum_{i=1}^{N}\beta_{ii} x_i^2 + \varepsilon_i$$

(2.6)

where x_{ij} is the i_t observation on the j_t independent variable.

The least squares parameter estimates are obtained from p normal equations. The residual can be written as

$$e_i = y_i - \hat{\beta}_0 - \hat{\beta}_1 x_{1j} - \dots - \hat{\beta}_p x_{ip} \tag{2.7}$$

The normal equations is as follow

$$\sum_{i=1}^{n} \sum_{k=}^{p} x_{ij} x_{ik} \hat{\beta}_k = \sum_{i=1}^{n} x_{ij} y_i, \qquad j = 1, \dots \dots p \tag{2.8}$$

In matrix notation, the normal equations are written as

$$(X'X)\hat{\beta} = X'Y \tag{2.9}$$

where the ij element of X is x_{ij}, the i element of the column vector Y is y_i, and the j element of $\hat{\beta}$ is $\hat{\beta}_j$. Thus X is $n \times p$, Y is $n \times 1$, and $\hat{\beta}$ is $p \times 1$. The solution is

$$\hat{\beta} = (X'X)^{-1} X'Y \tag{2.10}$$

The validity of the result for a typical regression model requires the fulfillment of the following assumptions:

- the error terms are independent,
- the error terms are approximately normally distributed,
- and the error terms have a common variance.

Once a regression model has been constructed, it may be important to confirm the goodness of fit of the model and the statistical significance of the estimated parameters. Commonly used checks of goodness of fit include the R-squared (eq. 2.10) and Mean Square Error (MSE) (eq. 2.11). Statistical significance of parameter can be checked by an F-test of the overall fit, followed by t-tests of individual parameters.

$$- \quad R^2 = \frac{\sum_{i=1}^{n} \left(Y_i - \bar{Y} \right)^2}{\sum_{i=1}^{n} \left(\hat{Y}_i - \bar{Y} \right)^2} \tag{2.11}$$

$$- \quad \text{Mean Square Error, } MSE = \frac{\sum_{i=1}^{n} \left(Y_i - \hat{Y}_i \right)^2}{n - 2} \tag{2.12}$$

In regression analysis, variable-selection procedures are aimed at selecting a reduced set of the independent variables – the ones providing the best fit to the model. There are several methods for variable-selection procedures. Some of them are step-wise regression, forward selection, and backward elimination.

Backward elimination effort to find a good model with a model that includes all K candidates' regressors. Then the partial F-statistic (or a t-statistic, which is equivalent) is computed for each regressor as if it were the last variable to enter the model. The smallest of these partial F-statistics is compared with a preselected value, F-out (or F-to-remove); and if the smallest partial F-value is less than F-out, that regressor is removed from the model. Now a regression model with K-1 regressors is fitted, the partial F-statistic for this new model calculated, and the procedure repeated. The backward elimination algorithm terminates when the smallest partial F-value is not less than the preselected cutoff value F-out. Backward elimination is often a very good variable selection procedure. It is particularly 28avoured by analysis who like to see the effect of including all the candidate regressors, just so that nothing obvious will be missed.

Checking of Multicolinearity

Multicollinearity in regression occurs when predictor variables (independent variables) in the regression model are more highly correlated with other predictor variables than with the dependent variable.

Multicollinearity in multiple regression model can indicate how well the entire bundle of predictors predicts the outcome variable, but it may not give valid results about any individual predictor, or about which predictors are redundant with respect to others. A principal danger of such data redundancy is that of over fitting in regression analysis models. The best regression models are those in which the predictor variables each correlate highly with the dependent (outcome) variable but correlate at most only minimally with each other.

A high degree of multicollinearity can also cause computer software packages to be unable to perform the matrix inversion that is required for computing the regression coefficients, or it may make the results of that inversion inaccurate.

Indicators that multicollinearity may be present in a model:

1) Large changes in the estimated regression coefficients when a predictor variable is added or deleted

2) Insignificant regression coefficients for the affected variables in the multiple regression, but a rejection of the joint hypothesis that those coefficients are all zero (using an F-test)

3) Some authors have suggested a formal detection-tolerance or the variance inflation factor (*VIF*) for multicollinearity:

$$VIF = \frac{1}{1 - R^2}$$

(2.13)

$$Tolerance = \frac{1}{VIF} = 1 - R^2$$

(2.14)

Where R^2 is the coefficient of determination of a regression of 29xplanatory *j* on all the other explanators. A tolerance of less than 0.20 or 0.10 and/or a VIF of 5 or 10 and above indicates a multicollinearity problem (O'Brien , 2007).

2.5.2 Smooth Support Vector Regression (SSVR)

Support Vector Machine (SVM), firmly grounded in the framework of statistical learning theory Vapnik (1995), have been proposed by Vapnik. For a short over view on the statistical learning theory, refer to Vapnik (1998). As a new learning system, SVM is based on the Structural Risk Minimization (SRM) principle, which seeks to minimize an upper bound of the generalization error rather than minimize the empirical error. With the introduction of Vapnik's ε-insensitive loss function, SVM has been extended to solve nonlinear regression estimation problems, which is named support vector regression (SVR), Vapnik (1996), and then is introduced to practical problems in civil engineering by Dibike et. Al. (2001).

Based on the research of SVR algorithm, Smooth Support Vector Regression (SSVR) has been imported by Lee (2005), which transforms the constrained quadratic optimization problem to an unconstrained convex quadratic optimization problem and reduces training complexity of SVR effectively Lee (2001).

Consider a given data set S that consists of m points in n-dimensional real space R^n represented by the matrix $A \in R^{mxn}$ and m observations of real value associated with each point. The data set S is:

$$S = \left\{(A_i, y_i) | A_i \in R^n, y_i \in R, \quad for\, i = 1 \cdots m\right\}$$
(2.15)

The idea of the regression problem is to find a nonlinear regression function $f(x)$, tolerating a small error in fitting this given data set. This can be achieved by utilizing the ε–insensitive loss function that sets an ε- insensitive "tube" around the data, within which errors are discarded. Also, applying the idea of support vector machines (SVM), the function $f(x)$ is made as flat as possible in fitting the training data set. With the linear case that is the regression function $f(x)$ and it is defined as $f(x) = x^T \omega + b$ This problem can be formulated as an unconstrained minimization problem given as follows:

$$\min_{(w,b) \in R^{n+1}} \quad \frac{1}{2} \omega^T \omega + C |\xi|_\varepsilon,$$
(2.16)

Where $|\xi|_\varepsilon \in R^m$, $(|\xi|_\varepsilon)_i = \max\{0, |A_i \omega + b - y_i| - \varepsilon\}$ that represent the fitting errors and the positive control parameter C here weights the tradeoff between the fitting errors and the flatness of the linear regression function $f(x)$. To deal with the ε-insensitive loss function in the objective function of the above minimization problem, conventionally, it is reformulated as a constrained minimization problem defined as follows:

$$
\begin{aligned}
\min_{(w,b,\xi,\xi^*) \in R^{n+1+2m}} \quad & \frac{1}{2} \omega^T \omega + C |\xi + \xi^*|_\varepsilon, \\
s.t. \quad & A\omega + b - y \leq \varepsilon + \xi \\
& -A\omega - b + y \leq \varepsilon + \xi^* \\
& \xi, \xi^* \geq 0
\end{aligned}
$$
(2.17)

This formulation (2.13) is equivalent to the formulation (2.12). It is a convex quadratic minimization problem with $n+1$ free variables, $2m$ nonnegative variables, and $2m$ inequality constraints. But introducing more variables and constraints in the formulation

enlarges the problem size and could increase computational complexity for solving the regression problem.

The model (2.13) is changed slightly as an unconstrained minimization problem directly without adding any new variable and constraint. That is, the squares of 2-norm ε-insensitive loss, $\| |A\omega + b - y|_\varepsilon \|_2^2$, is minimized with weight $\frac{C}{2}$ instead of the 1-norm of ε-insensitive loss as in (2.12). In addition, the term $\frac{1}{2}b^2$ is added in the objective function to induce strong convexity and to guarantee that the problem has a unique global optimal solution. These lead to the following unconstrained minimization problem:

$$\min_{(w,b)\in R^{n+1}} \quad \frac{1}{2}\left(\omega^T\omega + b^2\right) + \frac{C}{2}\sum_{i=1}^m \left|A\omega + b - y_i\right|_\varepsilon^2, \tag{2.18}$$

This formulation has been proposed in active set support vector regression and solved in its dual form. In the formulation,

$$\begin{aligned}
|x|_\varepsilon &= \max\{0, |x| - \varepsilon\} \\
&= \max\{0, x - \varepsilon\} + \max\{0, -x - \varepsilon\} \\
&= (x - \varepsilon)_+ + (-x - \varepsilon)_+ \\
|x|_\varepsilon^2 &= (x - \varepsilon)_+^2 + (-x - \varepsilon)_+^2
\end{aligned} \tag{2.19}$$

The squares of ε-insensitive loss function can be accurately approximated by a smooth function that is infinitely differentiable and defined below. Thus, we are allowed to use a fast Newton-Armijo algorithm to solve the approximation problem. In SSVM the plus function x_+ is approximated by a smooth function as follows:

$$p(x,\alpha) = x + \frac{1}{\alpha}\log\left(1 + e^{-\alpha x}\right), \alpha > 0 \tag{2.20}$$

It is straightforward to replace $|x|_\varepsilon^2$ by a very accurate smooth approximation given by:

$$p_\varepsilon^2(x,\alpha) = \left(p(x - \varepsilon, \alpha)\right)^2 + \left(p(-x - \varepsilon, \alpha)\right)^2 \tag{2.21}$$

This function is used here to replace the squares of ε-insensitive loss function; the objective function of smooth support vector regression can be given as:

$$\min_{(w,b)\in R^{n+1}} \quad \frac{1}{2}\left(\omega^T\omega + b^2\right) + \frac{C}{2}\sum_{i=1}^{m} p_\varepsilon^2\left(A_i\omega + b - y_i, \alpha\right) \tag{2.22}$$

This problem is a strongly convex minimization problem without any constraint. It is easy to show that it has a unique solution. Moreover, the objective function in (2.18) is infinitely differentiable, thus a fast Newton-Armijo method (only requiring twice differentiability) to solve the problem.

Smooth Support Vector Regression with Nonlinear Kernel

In the previous section, the smooth support vector regression constructed a linear regression function in fitting the given training data points under the criterion that minimizes the squares of the ε-insensitive loss function. That is approximating $y \in R^m$ by a linear function of the form:

$$y \approx A\omega + b \tag{2.23}$$

where $\omega \in R^n$ and $b \in R$ are parameters to be determined by minimizing the objective function in (2.18). Applying the duality theorem in convex minimization problem ω can be represented by $A^T u$ for some $u \in R^m$. Hence,

$$\min_{(w,b)\in R^{n+1}} \quad \frac{1}{2}\left(u^T u + b^2\right) + \frac{C}{2}\sum_{i=1}^{m}\left| K\left(A_i, A^T\right)u + b - y_i\right|_\varepsilon^2, \tag{2.24}$$

This motivated the nonlinear support vector regression model. In order to generalize results from the linear case to nonlinear case, it employed the kernel technique that has been used extensively in kernel-based learning algorithms (Vapnik, 1995). It is simply replace the AA^T in (2.20) by a nonlinear kernel matrix $K(A,A^T)$ where $K(A,A^T)_{ij}=$

$K(A_i, A_j^T)$ and $K(x^T, z)$ is a nonlinear kernel function. Using the same loss criterion with the linear case, this will give us the nonlinear support vector regression formulation as follows:

$$\min_{(w,b)\in R^{n+1}} \quad \frac{1}{2}\left(u^T u + b^2\right) + \frac{C}{2}\sum_{i=1}^{m} p_\varepsilon^2\left(K\left(A_i, A^T\right)u + b - y_i, \alpha\right) \tag{2.25}$$

This problem still retains the strong convexity and differentiability properties for any arbitrary kernel. All of the results of the previous sections still valid. This problem also can be solved by the Newton-Armijo Algorithm. The solution of this unconstrained minimization problem for u and b leads to the nonlinear regression function as given below:

$$\begin{aligned} f(x) &= K\left(x^T, A^T\right)u + b \\ &= u^T K(A, x) + b \\ &= \sum_{i=1}^{m} u_i K(A_i, x) + b \end{aligned} \tag{2.26}$$

Kernel function selection

The kernel function is important because it creates the kernel matrix which summarizes all the data. There are four commonly used kernels function and they are (i) linear, (ii) polynomial, (iii) RBF and (iv) sigmoid. In practice, RBF kernel with a reasonable width is a good initial trial. In this work, RBF kernel is considered.

1. Linear: $K(x_i, x_j) = x_i^T x_j$

2. Polynomial: $K(x_i, x_j) = \left(\gamma x_i^T x_j + r\right)^d, \gamma > 0$

3. Radial basis function (RBF): $K(x_i, x_j) = \exp\left(-\gamma \|x_i - x_j\|^2\right), \gamma > 0$

4. Sigmoid : $K(x_i, x_j) = \tanh\left(\gamma x_i^T x_j + r\right)$

Parameter Model selection

One of the important choices in developing an SSVR model is the selection of model parameters which include kernel parameters, the penalty of estimation error (C), the

value of ε-Insensitive (ε) and the RBF parameter (γ). The goal of model selection is to determine which combination of C, ε and γ has the maximum cross validation accuracy (minimum error). Various combinations are tried for the three parameters by sampling the search space at discrete intervals. Once the combination with minimum mean squared error is found, the search is performed around the combination with a reduced sample interval. This procedure is repeated until there is no significant improvement in the cross validation accuracy. Dibike (2001) found good generalization by setting the capacity factor C between 10 and 100. Similarly, in most cases, ε values in the range of 0.01 to 0.025 resulted in the best performing SVM. For radial basis function, $\gamma-$ values in the range of 3 to 10 were found to be appropriate.
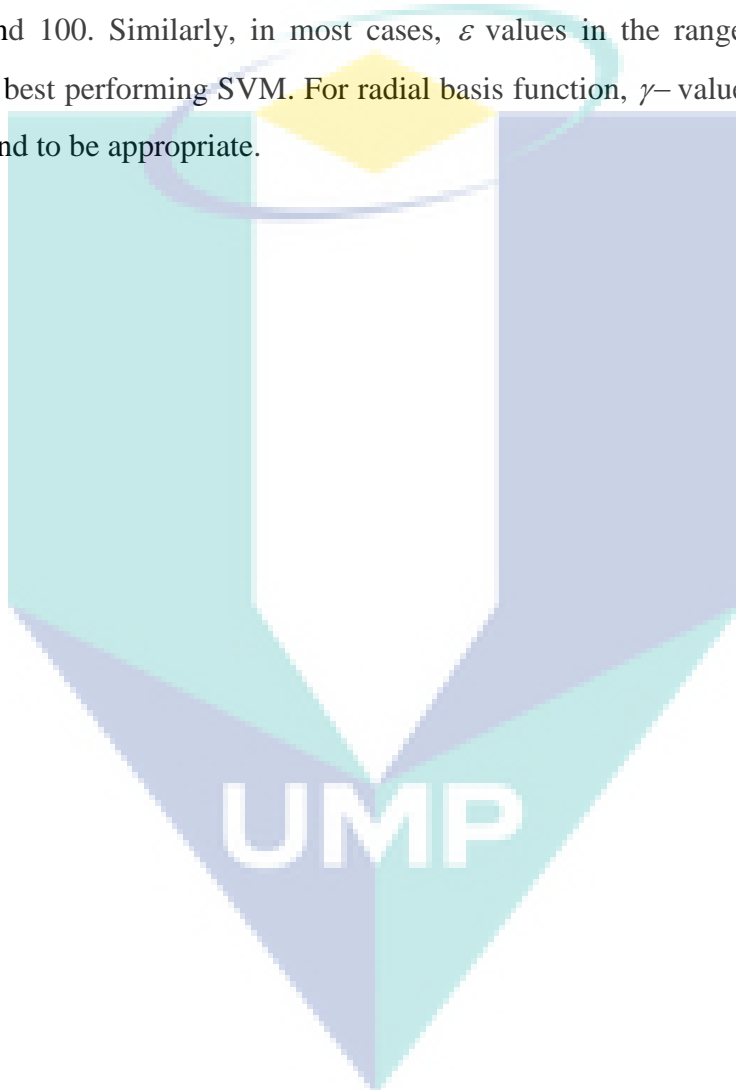
CHAPTER 3

RESEARCH METHODOLOGY

This chapter describes the research methodology used for this works. Research methodology is a set of procedures or methods used to conduct research. It focuses primarily on providing help with the tools and techniques used in the research process.

3.1   RESEARCH METHODOLOGY

The research methodology adopted in this research consists of the following steps:

1. At the first step, the researcher has undertaken intensive literature survey connected with the problem.
2. Detail study in SCC by collecting data and information about the various elements contributing to achieve the properties of SCC.
3. Development of a mix design that is suitable for SCC with local aggregate.
4. Design experiment using Taguchi method and implementation of the proposed mix design.
5. Identify optimal mixes and investigate the most effective factor of SCC properties.
6. Investigate and explore properties of SCC by Response Surface approach.
7. Finally, statistical modelling for SCC. There are two approaches used in this work. Classical modeling using Regression Analysis and modelling using Smooth Support Vector Regression (SSVR).

The flow chart of the research methodology is described in Figure 3.1.
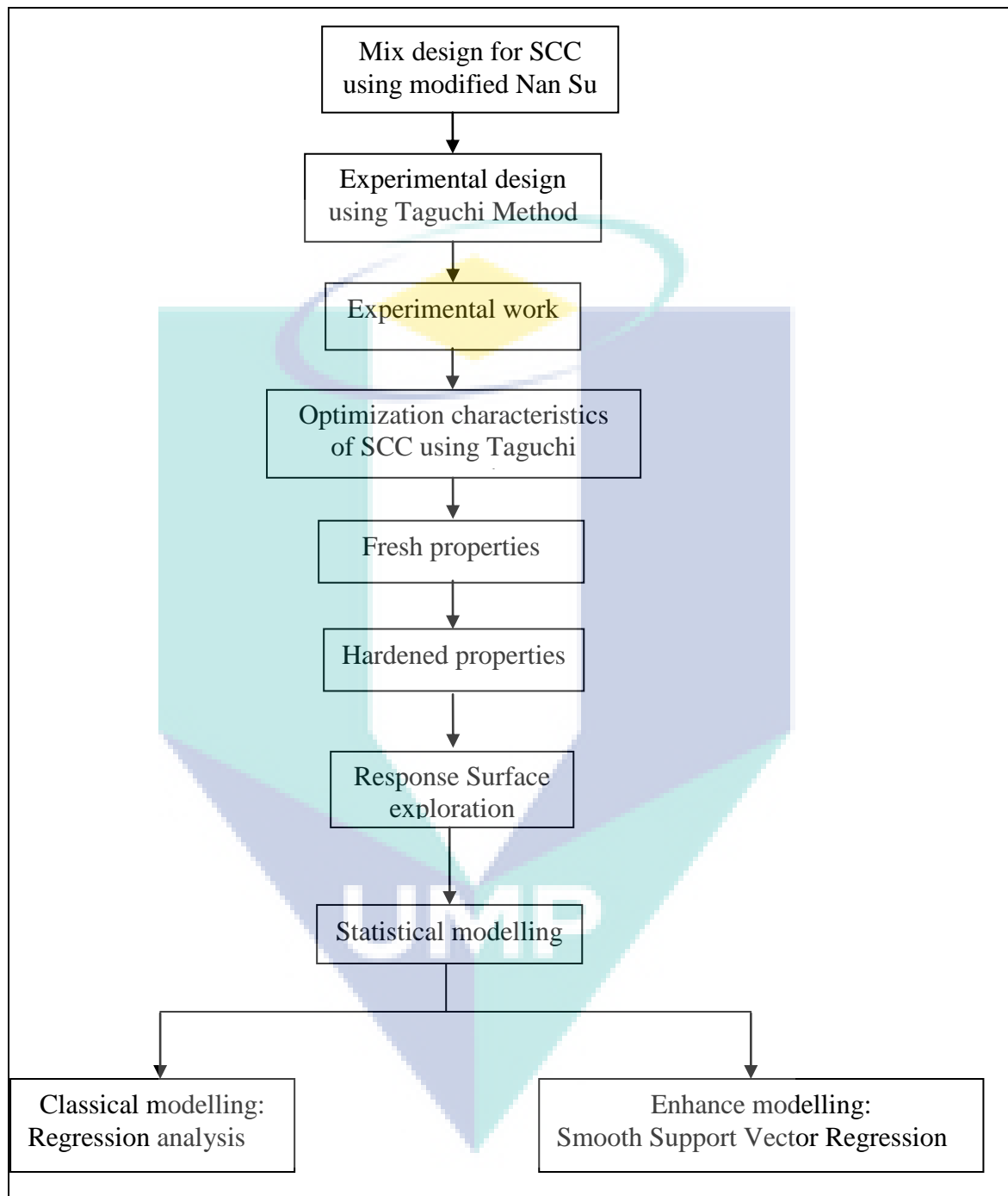
Figure 3.1: Research Methodology

The methodology presented above implicates accomplishing the following tasks:

3.1.1   Task 1: Literature Review

Conduct detailed and comprehensive literature review about the following:

1. Mix design

   Mix design of Self-compacting concrete (SCC) is a sensitive mix, strongly dependent on the composition and the characteristics of its constituents.

2. Properties of fresh concrete, including: filling ability, passing ability and segregation resistance

3. Properties of hardened concrete, specifically in compressive strength, tensile strength, and flexural strength

3.1.2   Task 2: Develop a Mix Design

In this task, the mix design of suitable SCC was carried out in an exploratory manner. The procedure underlying Nan Su Mix Design Method are reviewed and then cementitious efficiency factor was applied as Modified Nan Su Mix Design for SCC.

The Nan Su mix design method is presented in the following steps.

Step 1: Calculation of coarse and fine aggregate contents

Step 2: Calculation of cement content

Step 3: Selection of water/cement ratio

Step 4: Calculation of mixing water content required by cement

Step 5: Calculation of Pozzolanic paste volume (Ground Granulated Blast-Furnace Slag and Fly Ash content)

Step 7: Calculation of mixing water content needed in SCC

Step 8: Adjustments for aggregate moisture

Step 9: Trial batch adjustments

In this work, the Nan Su Mix method was modified by adding the "efficiency factor"(k) to get Silica Fume (SF) content in step 5. Firstly, "efficiency factor"(k) was proposed by Babu and Prakahs (1995) for normal concrete. This modified method is an

effort taken towards improving understanding of the efficiency concept of silica fume in concrete. The procedure for the modified Nan Su Mix method is given in Figure 3.2. A sample calculation of mix design can be found on Appendix D.
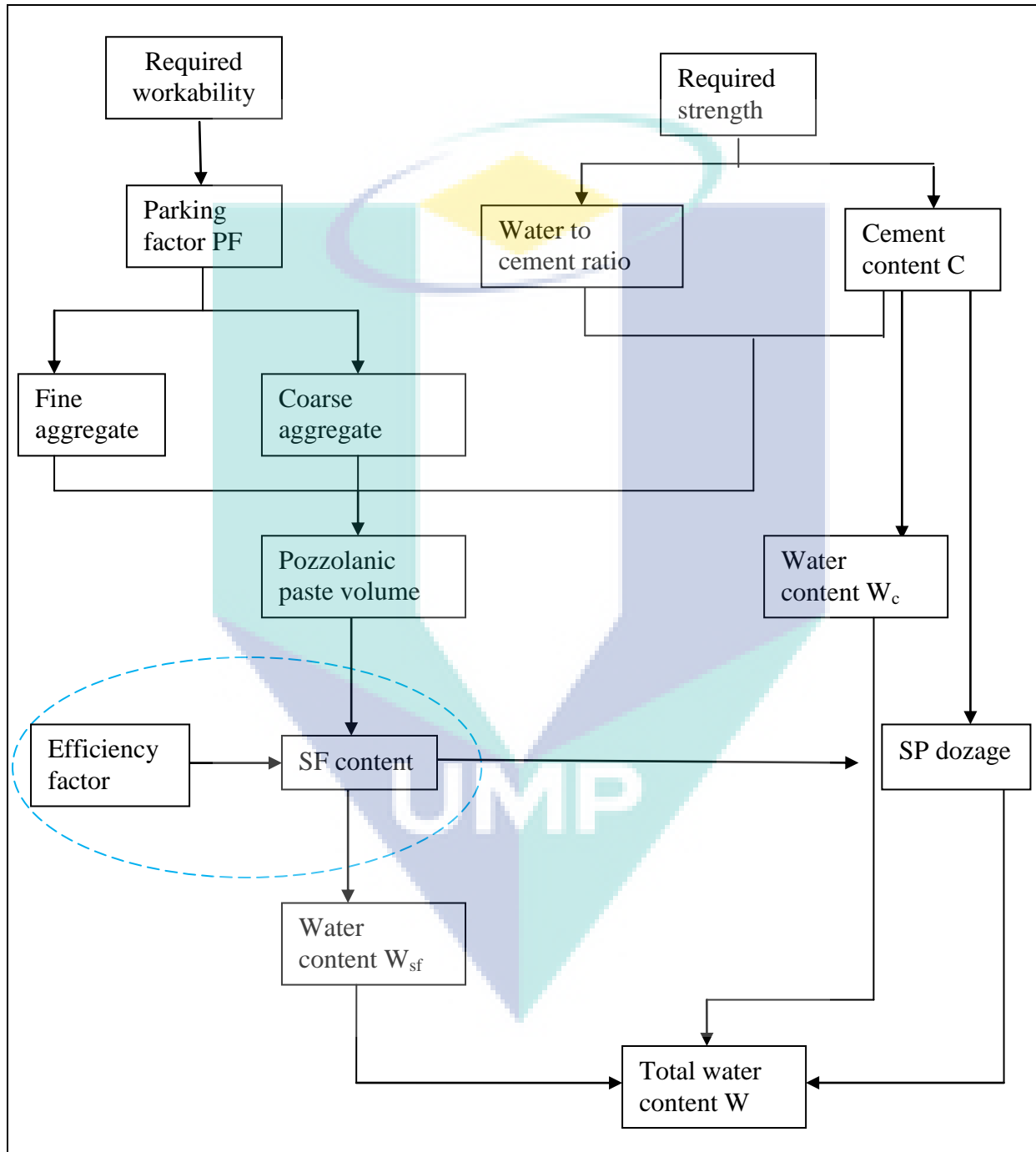
Figure 3.2: Modified Nan Su Mix Method

3.1.3. Task 3: Experimental Design by Taguchi Method

Experimental design based on Taguchi method is a powerful and effective approach to understanding the process and then optimizing the performance of the process using the statistical design of experiments. The purpose of the study was to develop suitable mix design using local materials to satisfy the requirement of SCC, both fresh and hardened properties. Taguchi method provides a systematic approach to the study of the effects of various ingredients parameters in a limited number of experimental trials.

The following steps are followed for the experiment.

Step 1: objective of the experiment

The objective of the experiment was to identify optimal mixes and investigate the most effective factors of characteristics SCC.

Step 2: identification of the control factors/parameters and their levels

The identification of control factors/parameters is crucial for the success of any engineering experiment. Table 3.1 illustrates the list of control factors. There are six factors and all factors were studied at three levels. The levels for each factor were selected based on literature study.

Tabel 3.1: Control factors and their variation levels (per m^3)

No	Control factors	Unit	Level		
			1	2	3
1	Coarse aggregate (A)	kg	759.00	767.25	775.50
2	Fine aggregate (B)	kg	833.98	826.26	818.53
3	Cement (C)	kg	538.29	546.20	554.11
4	Silica (D)	kg	43.44	45.35	47.26
5	Water (E)	kg	230.14	233.09	236.04
6	SP (F)	kg	4.11	4.48	4.84

Step 3: selection of most suitable response for the experiment

A response is an output performance characteristic of process. It is important to choose responses that can be measured quantitatively and with stability and equally important to make sure that the input control factors do have some effect on the selected response. In this work, there are five fresh properties and three hardened properties are chosen as response. (See Table 3.2)

Table 3.2: Response of characteristics SCC

No	Fresh properties		Hardened properties	
	Response	**Unit**	**Response**	**Unit**
1	Slump flow	mm	Compressive strength	MPa
2	Flow time (T_{50})	second	Tensile strength	MPa
3	V-funnel	second	Flexural strength	MPa
4	L-Box	h_2/h_1		
5	Segregation resistance	%		

Step 4: choice of orthogonal array (OA) design

Matrix experiments using OA play a crucial role to determine whether interactions are large compared to the main effects. Taguchi considers the ability to detect the presence of interactions to be primary reason for using OA. The OA experimental design method was chosen to determine the experimental plan, L_{18} (3^6) design, which is one of the standard experimental plan improved by Taguchi (see Table 3.3), since it is the most suitable for the condition being investigated, with six parameters and three levels.

Step 5: preparation of experimental layout and run

In this step, the main task is to design the experimental layout and assign the factors to appropriate columns of the chosen OA. Table 3.3 illustrates the experimental layout. The actual values are replaced by coded levels, i.e. level 1, level 2 and level 3. The experiment was conducted according to the above experimental layout.

Table 3.3: Chosen $L_{18}(3^6)$ design

Exp No.	Control factors					
	Factor 1	**Factor 2**	**Factor 3**	**Factor 4**	**Factor 5**	**Factor 6**
1	1	1	1	1	1	1
2	1	2	2	2	2	2
3	1	3	3	3	3	3
4	2	1	1	2	2	3
5	2	2	2	3	3	1
6	2	3	3	1	1	2
7	3	1	2	1	3	2
8	3	2	3	2	1	3
9	3	3	1	3	2	1
10	1	1	3	3	2	2
11	1	2	1	1	3	3
12	1	3	2	2	1	1
13	2	1	2	3	1	3
14	2	2	3	1	2	1
15	2	3	1	2	3	2
16	3	1	3	2	3	1
17	3	2	1	3	1	2
18	3	3	2	1	2	3

Step 6: statistical analysis

Having completed an experiment, it is required to analyze and interpret Taguchi experiments using statistical analysis. Statistical analysis will provide the researcher with statistically valid and reliable conclusions. For the present work, the first step was to analyze S/N ratio to determine the optimum condition. Then, response surface approach is evaluated. Finally, statistical modeling is done.

3.1.4. Task 4: Experimental Work

In this task, a set of procedure to get characteristics of SCC, such as fresh and hardened properties were done.

A. Investigation of Fresh Properties

A concrete mix can only be classified as SCC if the requirements for all the following three fresh properties are fulfilled:

1. Filling ability: It is the ability of SCC to flow into all spaces within the formwork under its own weight. Testing methods of slump flow and V-funnel are used to determine the filling ability of fresh concrete (EFNARC, 2002).

   Procedure of Slump flow test:
   a. About 6 litres of concrete is needed to perform the test, sampled normally.
   b. The base plate and inside of slump cone was moisturized,
   c. Baseplate was placed on level stable ground and the slump cone centrally on the base plate and held down firmly.
   d. The cone was filled using the scoop. Without tamping, simply strike off the concrete level at the top of the cone with the trowel.
   e. Any surplus concrete was removed from around the base of the cone.
   f. The cone vertically was lifted vertically upwards and allowed the concrete to flow out freely.
   g. Simultaneously, the stopwatch was started and recorded the time taken for the concrete to reach the 500mm spread circle. (This is the T_{50} time).
   h. The final diameters of the concrete in two perpendicular directions were measured.
   i. The average of the two measured diameters was calculated. (This is the slump flow in mm).

   Procedure of V-funnel test:
   a. About 12 litres of concrete is needed to perform the test
   b. The V-funnel was set on firm ground.
   c. The inside surfaces of the funnel were moistened.

d. The trap door remained open to allow any surplus water to drain.

e. The trap door was closed and a bucket was placed underneath.

f. The apparatus was completely filled with concrete without compacting or tamping, the concrete level was simply striked off with the trowel.

g. Within 10 seconds after filling, the trap door was opened and the concrete was allowed to flow out under gravity.

h. When the trap door was opened, the stopwatch was started and the time for the discharge to complete (the flow time) was recorded.

2. Passing ability: It is the ability of SCC to flow through tight openings, such as spaces between steel reinforcing bars, under its own weight. Passing ability can be determined by using L-box test methods. The procedure of L-box test is as follows (EFNARC, 2002)

   a. About 14 litres of concrete is needed to perform the test.

   b. The apparatus level was set on firm ground, the sliding could open and close freely.

   c. The inside surfaces of the apparatus was moistened, any surplus water was removed

   d. The vertical section of the apparatus was filled with the concrete sample.

   e. It was left to stand for 1 minute.

   f. The sliding gate was lifted and the concrete is allowed to flow out into the horizontal section.

   g. Simultaneously, the stopwatch was started and the time was recorded for the concrete to reach the 200 and 400 mm marks.

   h. When the concrete stopped flowing, the distances "*H1*" and "*H2*" were measured.

   i. Calculate the blocking ratio, *H2*/*H1*.

3. Segregation resistance: The SCC must meet the filling and passing ability with uniform composition throughout the process of transport and placing. Segregation resistance can be determined by screening test, as follows:

   a. About 10 litres of concrete is needed to perform the test, sampled normally.

b. The concrete was allowed to stand in the bucket for 15 minutes covered with a lid to prevent evaporation.

c. The mass of the empty sieve pan was determined

d. The surface of the concrete was inspected for any bleeding water and it was noted.

e. About 2 litres concrete sample within the bucket was poured on top and approximately 4.8kg ±0.2kg only into a pouring container

f. The mass of the filled pouring container was determined.

g. The mass of the empty sieve pan was determined.

h. All the concrete from the pouring container was poured onto the sieve from a height of 500mm in one smooth continuous movement.

i. The empty pouring container was weighed up.

j. Mass of concrete poured onto sieve was calculate, *Ma*. (i.e. the difference between the full weight and empty weight).

k. The mortar fraction of the sample was allowed to flow through the sieve into the sieve pan for a period of 2 minutes.

l. The sieve was removed and mass of 'filled' sieve pan was determined. Mass of sample passing sieve was calculate, *Mb*, by subtracting the empty sieve pan mass from the filled sieve pan mass.

m. The percentage of the sample-passing sieve was calculated, the segregation ratio: (*Mb*/*Ma*) x 100.

B. Investigation of Hardened Properties

The SCC hardened properties were investigated in the following tests:

1. Compression test,

The compressive strength of concrete is the most common performance measure used by the engineer in designing buildings and other structures. The compressive strength is measured by breaking cylindrical or prism concrete specimens in a compression-testing machine. The compressive strength is calculated from the failure load divided by the cross-sectional area resisting the load and reported in units of pound-force per square inch (psi) in US Customary units or megapascals (MPa) in SI units.

The compressive strength in this work was obtained on 150 x 300 mm cylindrical or 100 x 100 x 100 prism at 3, 7, and 28 days in accordance with ASTM C39. Specimens were demoulded one day after casting and then cured in water at approximately 20^0C until testing was carried out at 1, 7 and 28 days' age. Three specimens of each mixture were tested and the mean value was reported.

2. Tensile/splitting test

The splitting tensile strength was determined at 28 days on cylinders measuring 150-mm diameter and 300-mm height and cured in water until the date of test according the BS 1881: Part 117. Three specimens of each mixture were tested and the mean value was reported.

3. Flexural test

The flexural strength was attained at 28 days on 100mm X 100mm X 500mm and then cured in water until the date of test according the ASTM C293. Three specimens of each mixture were tested and the mean value was reported.

3.1.5. Task 5: Optimization Characteristic of SCC using Taguchi approach

The optimal condition is the factor settings which yield the optimum performance. In this work, it is the factor settings which provide the highest fresh and hardened properties with minimum variation. The optimal condition is obtained by identifying the levels of significant control factors which yield the highest S/N ratio. The higher the S/N ratio, the better the product performance will be. For the flow time (T_{50}) properties, the "smaller is better" is used. The S/N ratio for smaller is better response is given by the equation 2.1. While, for all other properties (slump flow, V-funnel, L-Box, Segregation resistance, compressive strength, tensile strength, flexural strength) the S/N ratio "the larger is better". The equation for the S/N ratio the larger is better is given equation 2.2.

3.1.6. Task 6: Response Surface Exploration

In this task, two characteristics of SCC (fresh and hardened properties) were evaluated using response surface approach. A response surface is the graph of system response as a function of one or more variables. These graphs offer an opportunity to visually analyse how control factors (coarse aggregate, fine aggregate, silica fume, water, cement and super plasticizer) influence multiple response of interest (fresh and hardened properties).

3.1.7. Task 7: Statistics Modelling

The performance of the SCC properties can be evaluated by conducting a comparative analysis between actual data and predicted data using statistical modeling. The first step, classical modeling using regression analysis was studied. Six component contents of SCC (coarse aggregate, fine aggregate, silica fume, water, cement and super plasticizer) were employed to build the regression formulas. The steps of regression analysis are given as follows:

1. Constructing regression equation
2. Testing of significance coefficients
3. Selecting the best regression equation
4. Checking the multicollinearity

Then, the intelligent modeling based on statistical learning regression, namely Smooth Support Vector Regression (SSVR) was proposed. The steps of this method can be described as follows:

Step 1. Selecting optimal parameter using Taguchi method

Parameter selection is one of the important steps in SSVR to improve the performance of model. There are three parameters which must be tuned in this parameter selection: the penalty of estimation error (C), the value of ε-Insensitive (ε) and the RBF parameter (γ). In this work, Radial Basis Function (RBF) kernel is applied. If the kernel function has been chosen, the next problem is choosing a good parameter setting for better

generalization ability. The Taguchi design approach is applied to select the optimal parameter. The level of each parameter and design array is given in Table 3.4.

Table 3.4: The Taguchi design of Parameter SSVR

No	C	ε	γ
1	10	0.01	2
2	10	0.0175	4
3	10	0.025	6
4	20	0.01	4
5	20	0.0175	6
6	20	0.025	2
7	30	0.01	6
8	30	0.0175	2
9	30	0.025	4

Step 2. Solving SSVR using Newton Armijo algorithm

The detail descriptions of Newton Armijo algorithm are given in section 2.5.

Step 3. Prediction

From Newton Armijo algorithm, value of u and b will be obtained. These values will be used to obtain regression equation in the equation 2.22.

Step 4. Calculation of the performance of the model

In this work, two performance models were used:

$$R^2 = \frac{\sum_{i=1}^{n}(\hat{Y}_i - \bar{Y})^2}{\sum_{i=1}^{n}(Y_i - \bar{Y})^2} \;;\; \text{ and } \quad \textit{Mean Square Error (MSE)} = \frac{\sum_{i=1}^{n}(Y_i - \hat{Y}_i)^2}{n-2} \qquad (3.1)$$

The model is called good performance if R^2 is maximum and *MSE* is minimum. The detailed procedure of SSVR is summarized in Figure 3.3.
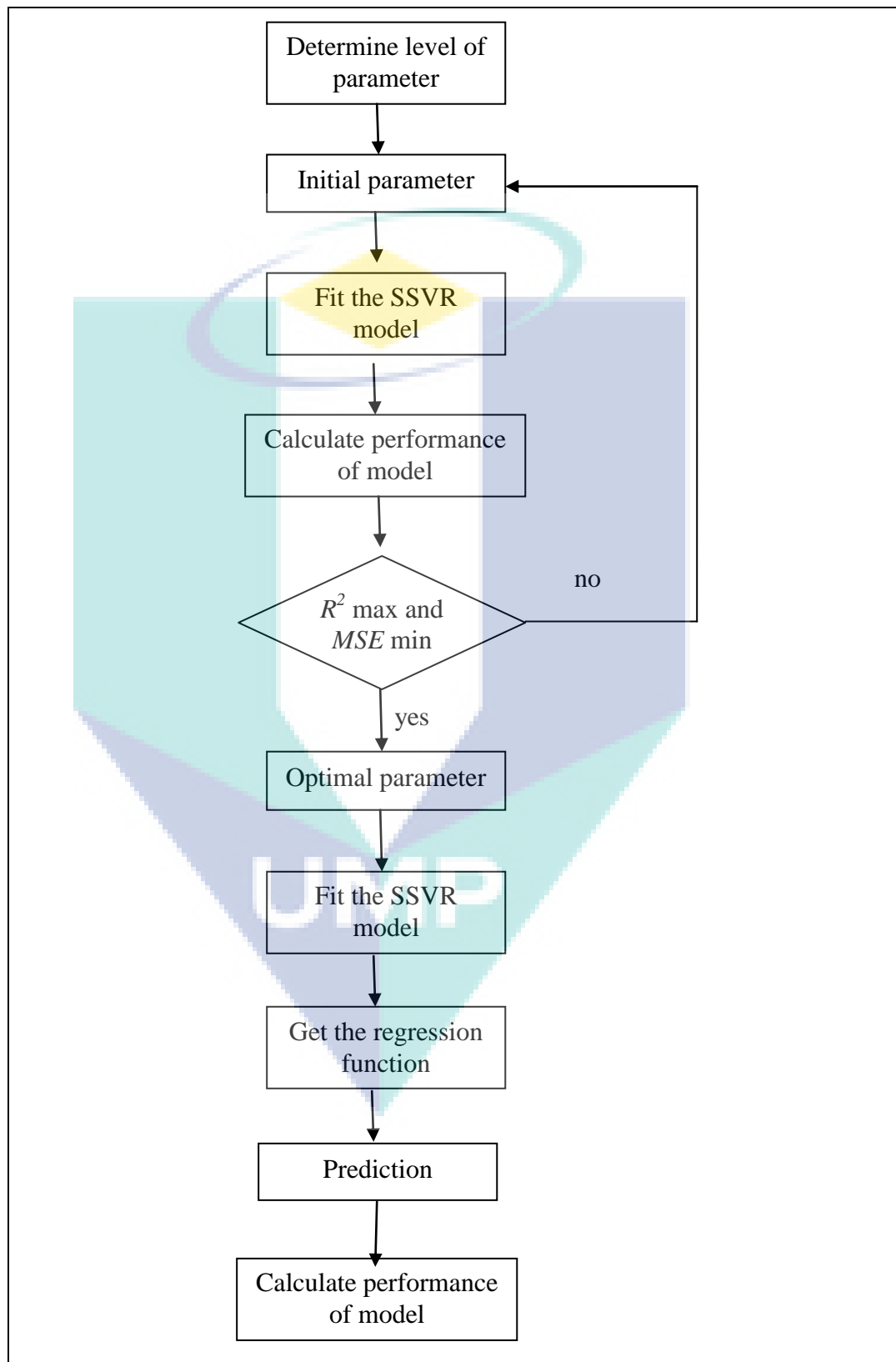
Figure 3.3: SSVR procedure

CHAPTER 4

LABORATORY RESEARCH WORK

4.1   INTRODUCTION

In this chapter the author will discuss the Modified Nan Su Mix Design for SCC. Then the experimental plan based on Taguchi design and experimental results of properties of self-compacting concrete are described.

4.2   MIX DESIGN PROCEDURE

Mix design method used for the self-compacting concrete is significantly different from the mix design method of vibrated-normal concrete. Mix design of SCC needs to consider the two opposite properties of flowability and segregation resistance ability at the same time to assure the compacting capacity of the concrete. Mix design of SCC can be a very difficult task. Initially, SCC mixtures are designed by trial and error using numerous trial mixes. Two popular design approaches are the Japanese mix design approach and the Chinese mix design.

The Japanese mix design approach was developed by Okamura and Ouchi [Okamura and Ouchi, (2003)]. Their main idea was to conduct initially the test on paste and mortar in order to examine the properties and compatibility of the mixture of superplasticizer (SP), cement, fine aggregates, and pozzolanic materials, then followed by the trial mix of SCC. The major advantage of this method is that it avoids having to repeat the same kind of quality control test on concrete, which consumes both time and labour. However, the drawbacks of Okamura's method are that firstly it requires quality control of paste and mortar prior to SCC mixing, while many ready-mixed concrete

producers do not have the necessary facilities for conducting such tests and secondly the mix design method and procedures are too complicated for practical implementation.

More Nan Su [Su et.al, (2001); Su and Miao, (2003)] developed an alternative method for composing SCC, henceforth referred to as the Chinese Method. The Chinese Method starts with the packing of all aggregates (sand and gravel together), and later with the filling of the aggregate voids with paste. The method is easier to carry out, and results in less paste. This saves the most expensive constituents, namely cement and filler, and concrete of ''normal'' strength is obtained. This will also favour the technical performance of the concrete, as the largest possible volume of aggregate is advantageous in regard to strength, stiffness, permeability, creep and drying shrinkage. Nan-Su's new method has some problems to determine the amount of cementitious or pozzolanic materials. The "cementitious efficiency factor" (*k*) has been successfully obtained from the amount of silica fume content.

4.2.1 Modified Chinese Mix Design Methods

In this study, the procedure underlying Nan Su Mix Design Method is used with the application of efficiency factor. The mix design is called Modified Nan Su Mix Design for SCC.

Nan Su Mix Design Procedure: The Nan Su mix design method is presented in the following steps.

Step 1: Calculation of coarse and fine aggregate contents

In this method, the packing factor (PF) of aggregate is defined as the ratio of mass of aggregate of tightly packed state in SCC to that of loosely packed state [Brouwers and Radix, (2005)]. The content of fine and coarse aggregates can be calculated as follows (Eqs. (4.1) and (4.2)):

$$W_g = PF \times W_{gL}\left(1 - \frac{S}{a}\right) \tag{4.1}$$

$$W_s = PF \times W_{sL}\left(1 - \frac{S}{a}\right) \qquad (4.2)$$

where W_g: content of coarse aggregates in SCC (kg/m^3); W_s: content of fine aggregates in SCC (kg/ m^3); W_{gL}: unit volume mass of loosely piled saturated surface-dry coarse aggregates in air (kg/ m^3); W_{sL}: unit volume mass of loosely piled saturated surface-dry fine aggregates in air (kg/ m^3); PF: packing factor, the ratio of mass of aggregates of tightly packed state in SCC to that of loosely packed state in air; S/a: volume ratio of fine aggregates to total aggregates, which ranges from 50% to 57%.

Step 2: Calculation of cement content

To secure good flowability and segregation resistance, the content of binders (powder) should not be too low. Therefore, the cement content to be used is (Eq. (4.3)):

$$C = \frac{f_c^{'}}{x} \qquad (4.3)$$

where C is the cement content (kg), $f'c$ is the specified compressive strength of concrete at 28 days (MPa), x is the compressive strength provided by each kilogram of cement, in MPa, 0.11–0.14 MPa (15–20 psi) for SCC used in Taiwan [Su et.al, (2001)].

Step 3: Selection of water/cement ratio

The relationship between compressive strength and water/cement ratio of SCC is similar to that of normal concrete. The water/cement ratio can be determined according to ACI 318 or other methods in previous studies. The content of mixing water required by cement can then be obtained using (Eq. (4.4)):

$$f_{cr}^{'} = \max\left(f_c^{'} + 1.34S \,,\, f_c^{'} + 2.33S - 35\right) MPa \qquad (4.4)$$

where S is the standard deviation (MPa). The ''required average compressive strength $f_{cr}^{'}$'' must first be determined from the specified strength $f_c^{'}$ and variation on concrete strength during the production in the ready-mixed concrete plant. The relationship

between $f_{cr}^{'}$ and water/cement ratio for SCC was obtained from previous experiments [Su et.al, (2001)] and is presented in Figure 4.1.
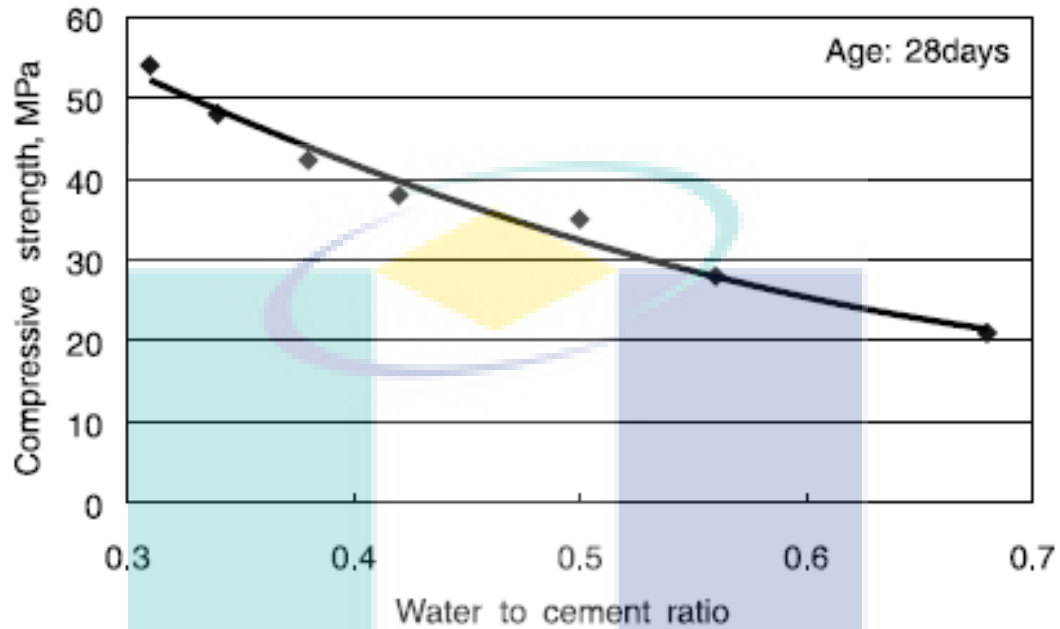
Figure 4.1: Relation between compressive strength and water to cement ratio. [Su et.al, (2001)].

Step 4: Calculation of mixing water content required by cement

The content of mixing water required by cement can then be obtained using

$$W_{wc} = \left(\frac{W}{C}\right)C \tag{4.5}$$

where W_{wc} is the content of mixing water required by cement (kg), *W/C* is the water to cement ratio by weight and *C* is the cement content (kg).

Step 5: Calculation of FA and GGBS contents

To obtain the required workability and segregation resistance, SF is used to increase the binder content. Then the paste volume of Pozzolanic materials (*Vpp*) can be calculated as follows:

$$Vpp = 1 - \frac{W_g}{1000 \times G_g} - \frac{W_s}{1000 \times G_s}$$
$$- \frac{C}{1000 \times G_C} - \frac{W_{wc}}{1000 \times G_w} - V_a \tag{4.6}$$

where *Vpp* is the volume of SF paste; *Gg*: specific gravity of coarse aggregates; *Gs*: specific gravity of fine aggregates; *Gc*: specific gravity of cement; *Gw*: specific gravity of water; *Va*: air content in SCC (%).

In order to obtain the FA and GGBS paste with water/ binder ratio of Wf/F and Ws/S as flowable as the cement paste, flow tests (ASTM C230) should be carried out. If the total amount of pozzolanic materials (FA and GGBS) in FC is P, where FA occupies A% and GGBS occupies 1- A%, the adequate ratio of these two materials can be established through testing or according to previous experience.

$$Vpp = \left(1 + \frac{W_f}{F}\right) A\% \frac{P}{1000 \times G_f} + \left(1 + \frac{W_s}{S}\right) \times (1 - A\%) \frac{P}{1000 \times G_s} \tag{4.7}$$

Where G_f, G_s, G_c, W_f/F, W_s/S and $A\%$ can be obtained from tests.

Let Eq. (4.6) equals Eq. (4.7), the total amount of Pozzolanic materials P in FC can be obtained. Hence, FA content (F) and GGBS content (S) can be calculated as follows:

$$F = A\% \times P \tag{4.8}$$
$$S = (1 - A\%) \times P \tag{4.9}$$

Mixing water content required for FA paste

$$W_f = \left(\frac{W_f}{F}\right) F \tag{4.10}$$

Mixing water content required for GGBS paste

$$W_S = \left(\frac{W_S}{F}\right) S \tag{4.11}$$

Step 6: Calculation of SP dosage

The SP can be deduced from the dosage at the saturation point from previous tests as Figure 4.2. If the dosage of SP used is *n*% of the binder (cementitious material), and the solid content of SP is *m*%, then the SP dosage (*Wsp*) by liquid can be obtained as follows:

$$SP = n(C + P)$$ (4.12)
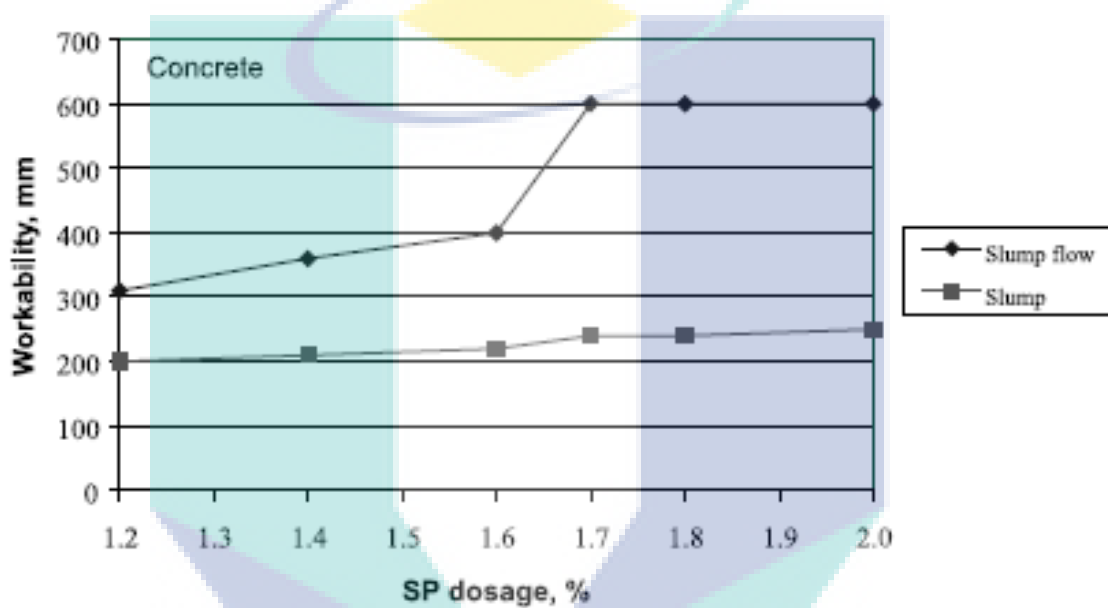
Figure 4.2: Effect of SP dosage on the workability of concrete. [Su et.al, (2001)].

Step 7: Calculation of mixing water content needed in SCC

The water content required by SCC is the total amount of water needed for cement, SF minus that in SP. Therefore, it can be calculated as follows:

$$W = W_c + W_{sf} - (1 - m)n(C + P)$$ (4.13)

Previous experiences have shown that a total water content of 168–181 kg/ m^3 is suitable for HPC [Aitcin (1998)].

Step 8: Adjustments for aggregate moisture

The mix proportions determined by steps 1–7 are therefore based on the SSD condition of aggregates. Mixing water content should be adjusted according to the moisture content of aggregates and the amount of SP at the ready-mixed concrete plant or construction site.

Step 9: Trial batch adjustments

Evaluation of the trial mixes should be based on the criteria of workability (slump and slump flow) and compressive strength. Accordingly, adjustments should be made on PF value, water to cement ratio, cement content, fine/coarse aggregate ratio, and SP dosage. When a mixture satisfying the desired criteria of workability and strength is obtained, the mix proportions of the laboratory-sized trial batch are scaled up for producing full-sized field batches.

Modified Nan Su Method: This modified method is an effort towards better understanding of the efficiency concept of silica fume in concrete. Babu and Prakahs (1995) proposed the "efficiency factor"(k) of silica fume that can be separated into two parts; the "general efficiency factor"(k_e)-a constant at all the percentages of replacement and the "percentage efficiency factor"(k_p)- varying with the replacement percentage. A value of 3.0 was found to be most acceptable for the "general efficiency factor" and it was kept constant for all the percentages of replacement. The percentage replacement calculated by applying an additional "percentage efficiency factor"(k_p). The values of k_p was evaluated the replacement percentages from 5-40% and is represented by the following relationship (Babu and Prakahs, 1995):

$$k_p = 0.0015\,\mathrm{Pr}^2 - 0.1223\,\mathrm{Pr} + 2.8502 \tag{4.14}$$

The variation of the overall efficiency factor ($k=k_e.k_p$) was presented in Figure 4.3., and then this concept was applied in step 5 in Nan Su method to obtain the silica fume content as follows;

$$SF = \frac{V_{pp}G_{pp}}{k} \tag{4.15}$$

where *SF* is the silica fume content, *Vpp* is the volume of SF paste, *Gpp* is specific gravity of SF, *k* is efficiency factor. The relationship of the strength to water-to-effecience cementitious materials ratio, $[w/(c+ k_e.k_p.s)]$ of SF concrete as presented in Fig 4.4.

4.2.2   PILOT PROJECT OF EXPERIMENTS

In order to verify the validity of the proposed mix design method, a set of SCC mixes based on the above procedures was prepared. The materials used in this study were locally available. Their properties and grading was determined in accordance with ASTM C 136 and the results are presented in Table 4.1. The coarse aggregates are crushed gravel with a maximum size of 14 mm. Natural sand was used as fine aggregate with less than 50% passing through the 0.60-mm sieve. The specific gravity and water absorption properties of natural sand and crushed gravel are 2.60, 1.63%, and 2.71, 0.39%, respectively. An F type superplasticizer admixture in conformity with ASTM C 494 standard was also employed. The solid content and the specific gravity of this superplasticizer was 39.7% and 1.10, respectively.
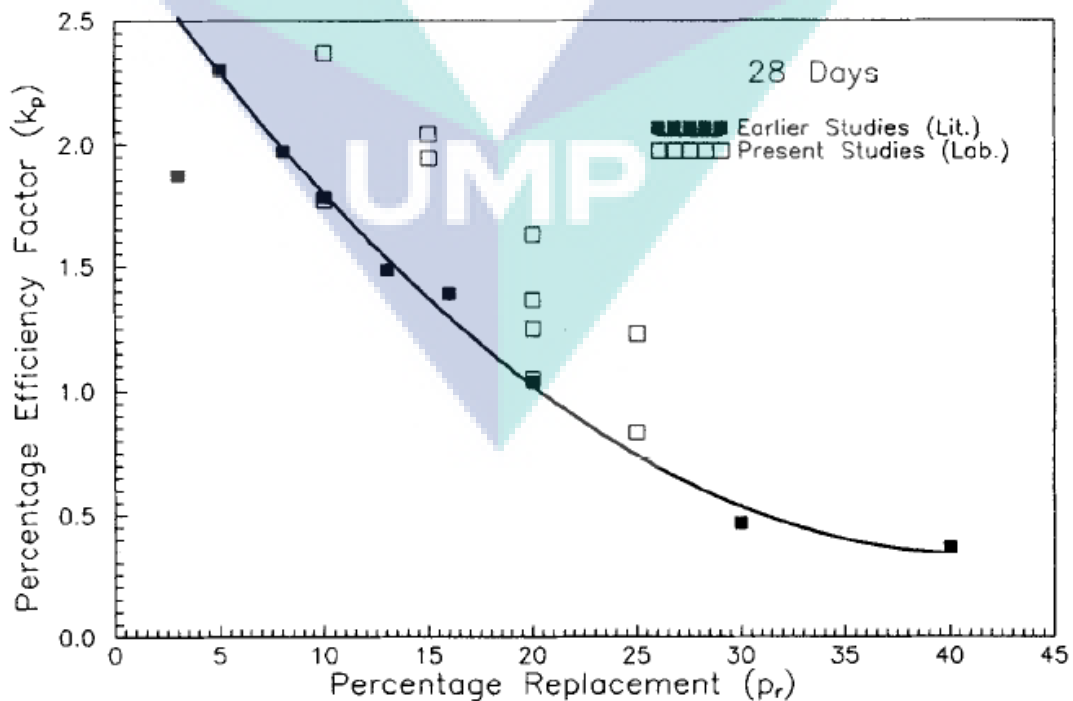
Figure 4.3: Variation of Percentage Efficiency with Silica Fume Replacement, [Source: Babu and Prakahs, (1995)]
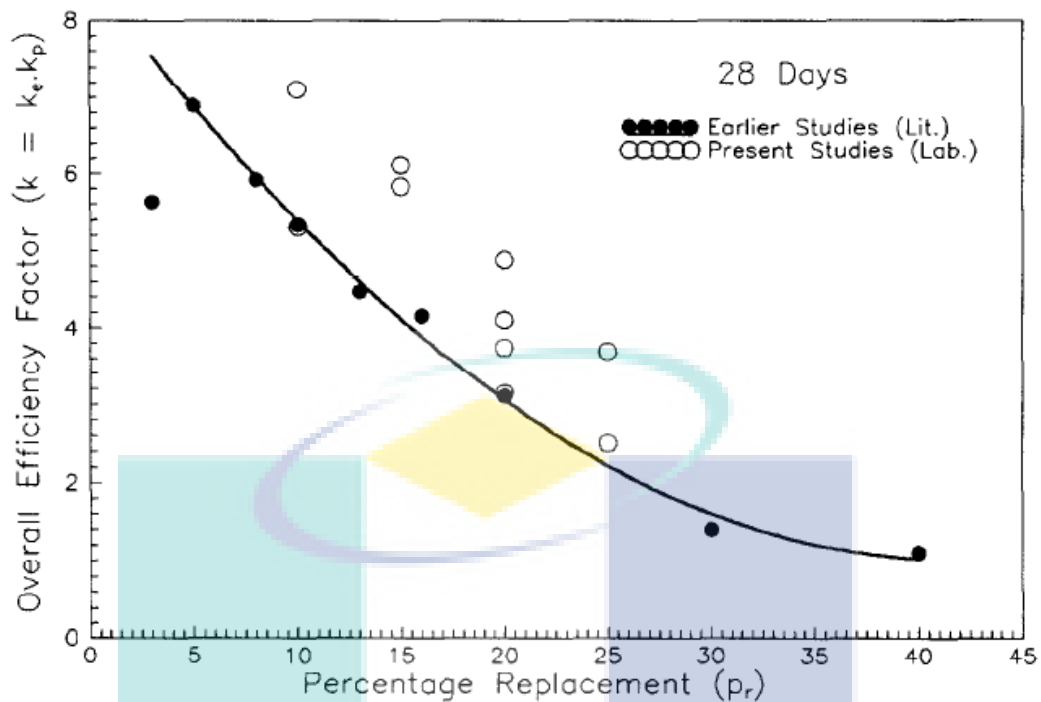
Figure 4.4: Variation of Overall Efficiency with Silica Fume Replacement, [Source: Babu and Prakahs, (1995)]

All mixtures were prepared by using an Ordinary Portland Cement (CEM II/A-M) in accordance with BS EN 197-1:2000 standard. The chemical and physical properties of cement are listed in Table 4.2. In order to enhance the paste content, a silica fume which conform to the ASTM C 1240 standard requirements was employed. Its specific gravity and Blaine fineness as given by the manufacturer were 2.2 and 290 m2/kg, respectively. The chemical properties of silica fume are also given in Table 4.2.

Nine self-compacting concrete mixtures were prepared for this study. Mixture proportions are presented in the Table 4.3. One mixture is a control mixture ID, four mixtures in Sp-series mixtures ID with vary superplasticizer; 1.15%, 1.27%, 1.39% and 1.59% of binder, four mixtures in W/B-series mixtures ID with variation of water-binder ratio; 0.386, 0.391, 0.396 and 0.401. Note that the total of binder content was kept constant at 581.73 kg per m^3.

Table 4.1: Properties of Aggregate

	Coarse Aggregate	Natural Sand
Specific gravity of coarse aggregate (kg/m^3)	2.65	2.64
Bulk density of coarse aggregate(kg/m^3)	1515	1497
Water absorption (%)		
Sieve, cumulative % passing		
20.0 mm	100	-
14.0 mm	94.0	-
10.0 mm	64.0	-
5.00 mm	52.0	100
2.36 mm	8.00	98.6
1.18 mm	0.00	69.4
0.60 mm	-	32.3
0.30 mm	-	5.6
0.15 mm	-	0.5
Pan	0.00	0.0

Table 4.2: Properties of Portland cement (OPC) and Silica Fume

Chemical Composition	OPC (%)	Silica Fume (%)
Calcium oxide (CaO)	65.0	< 1
Silicon dioxide (SiO_2)	20.1	> 90
Aluminium oxide (Al_2O_3)	4.9	< 1
Ferric oxide (Fe_2O_3)	2.5	< 1
Magnesium oxide (MgO)	3.1	< 1
Sulphur oxide (SO_3)	2.3	< 1
Potassium oxide (K_2O)	0.4	< 1
Sodium oxide (Na_2O)	0.2	< 1
Loss on ignition (%)	2.4	< 3.0
Physical Properties		
Specific Gravity	3.20	2.2-2.3
Bulk Density (kg/m^3)		150-700
Particle Size (μm)	45-150	0.15-0.50

Table 4.3: Concrete mixture proportions, (kg)

Component	C	Sp1.52	Sp1.39	Sp1.27	Sp1.15	WB0.386	WB0.391	WB0.396	WB0.401
Coarse Aggregate	759.00	759.00	759.00	759.00	759.00	759.00	759.00	759.00	759.00
Fine Aggregate	818.53	818.53	818.53	818.53	818.53	818.53	818.53	818.53	818.53
Cement	581.73	538.29	538.29	538.29	538.29	538.29	538.29	538.29	538.29
Silica Fume	-	43.44	43.44	43.44	43.44	43.44	43.44	43.44	43.44
Water	236.04	236.04	236.04	236.04	236.04	224.39	227.26	230.14	233.09
SP	8.95	8.95	8.22	7.50	6.77	8.22	8.22	8.22	8.22
W/B	0.406	0.406	0.406	0.406	0.406	0.386	0.391	0.396	0.401
SP%B	1.52%	1.52%	1.39%	1.27%	1.15%	1.39%	1.39%	1.39%	1.39%

To obtain a homogeneous SCC mix, a more complicated mixing operation was applied comparing to the conventional concrete mixing procedure. The concrete mixtures were prepared in a horizontal axis mixer. First of all, aggregates were mixed and binders (cement and SF) were added to the system. After remixing, water was added to the dry mix. Finally, superplasticizer was introduced to the wet mixture [Domone and Jin, (1999)]. In the fresh state, slump flow (S), slump flow time ($T50$), J-ring blocking step (B_J), J-ring flow spread (S_J), J-ring flow time ($T50_J$) of the SCC mixes were measured according to the EFNARC Committee's suggestions [EFNARC, (2002)]. After 24 hours, all specimens were submerged in water at 20°C. Compressive strength tests were performed on 3, 7 and 28 days old specimens.

4.2.2.1 Properties of Fresh Concrete

The results of fresh concrete test, slump flow (S), slump flow time (T_{50}), J-ring blocking step (B_J), J-ring flow spread (S_J), J-ring flow time ($T_{50})_J$ with different amounts of superplasticizer and silica fume addition are discussed in the following paragraphs.

Table 4.4: Properties of fresh concrete

Series	Flow, (S) (mm)	Time, (T_{50}) (s)	J-ring, (B_J) (mm)	J-spread, (S_J) (mm)	J-time, ($T_{50})_J$ (s)
C	722.50	1.59	4.00	720	2.87
Sp1.15	545.00	3.14	21.00	500	10.65
Sp1.27	700.00	2.29	12.75	645	3.02
Sp1.39	705.00	2.23	6.50	680	3.48
Sp1.52	790.00	2.51	12.00	700	3.50
WB0.386	590.00	6.21	23.00	500	12.48
WB0.391	635.00	3.86	16.00	590	13.53
WB0.396	665.00	4.95	19.25	555	10.50
WB0.401	575.00	5.15	23.00	535	8.76
Criteria	600-800	2-5	10-15	550-750	3.5-6

It can be seen from Table 4.4., slump flow diameters vary between 545 mm and 790 mm, which refers to the mean spread diameter of concrete following the removal of slump cone as specified by Japan Society of Civil Engineering [JSCE, (1999)]. The slump-flow test evaluates the capability of concrete to deform under its own weight against the friction of the surface with no external restraint present. It is well known that slump flow diameter indicates the yield stress [EFNARC, (2002)]. The slump flow increase with the increasing superplasticizer and water-binder content. Comparatively, Sp mixes series had improved properties, as indicated by the lesser flow time to achieve higher slump flow diameters. The effect of superplasticizer dosage, on slump flow and flow time is presented in Figure 4.5.
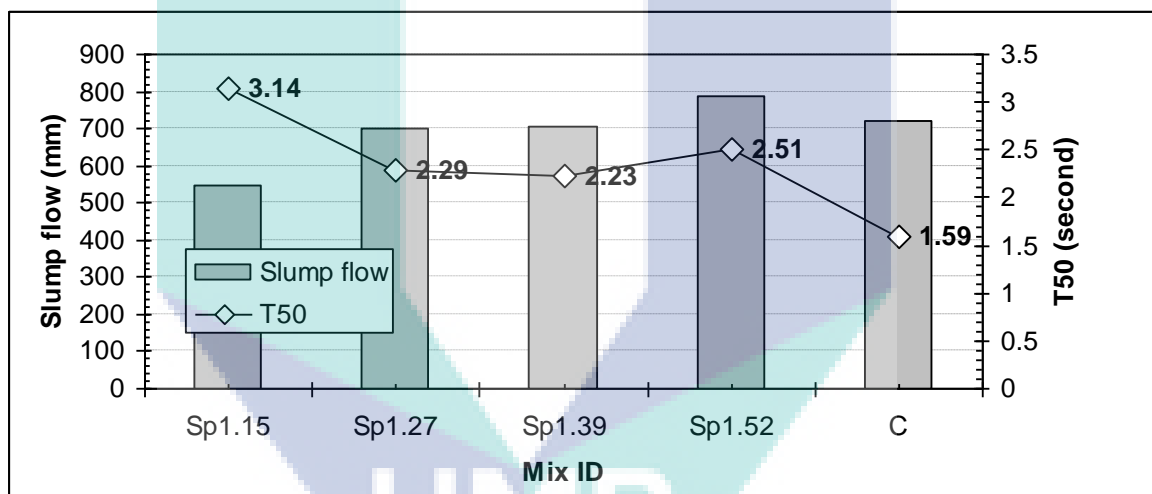
Figure 4.5: The influence of superplasticizer on slump flow and flow time

The slump-flow time (T_{50}) was measured when the concrete was slumping until it reached 500mm of flow. The slump flow time (T_{50}) vary between 1.59 second and 3.14 second. It may be seen that the (T_{50}) times, which provide an indication of the relative plastic viscosity of the SCC, increase with a decrease in the superplasticizer. This is in agreement with results found in previous study [Sahmaran, 2006]. The increase in viscosity will help to minimize the risk of segregation during and after placement.

The effect of water-binder ratio on slump flow and flow time is presented in Figure 4.6. The optimum water-binder ratio was achieved by mix WB0391 with higher slump flow and lesser flow time. With the reduction of free water content simultaneously, the increase in superplasticizer dosage is not sufficient to obtain the range of permissible slump-flow values (65–80 cm).
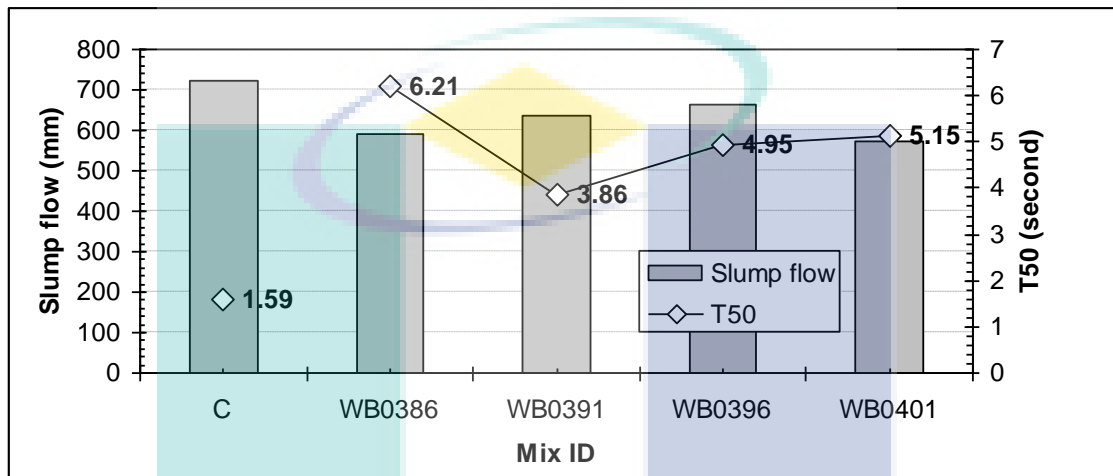
Figure 4.6: The influence of W/B ratio on slump flow and flow time

4.2.2.2 Compressive strength

The compressive strength development of Sp series within time is presented in Table 4.5. Included in that table are compressive strengths of SCC at 3, 7 and 28 days. The results show that the compressive strength decreases with the increasing superplasticizer content. It can be seen that, the compressive strength of control mix ID (0% SF) higher than all SCC mixtures in the early ages. It was proven that, SCC mixtures were good in workability. Nevertheless, the compressive strength of control mix ID and Sp1.15 mix ID were relatively equal at 28 days. It was known from that table, when compared to the control mixture, that the use of SPs generally increased the strength after 28 days.

Table 4.5: Summary of compressive strength of pilot project

Series	3 d (MPa)	7 d (MPa)	28 d (MPa)
C	45.80	50.00	54.20
Sp1.15	29.05	33.69	46.95
Sp1.27	29.49	38.07	48.90
Sp1.39	30.00	39.00	50.00
Sp1.52	30.26	41.75	54.30
WB0.386	35.13	42.15	52.25
WB0.391	38.87	47.00	55.35
WB0.396	33.48	46.95	54.80
WB0.401	30.78	43.60	52.65

Compressive strength development of W/B series up to 28 days show that, compressive strength increases with decrease of water-binder ratio. A maximum concrete strength of 54.80 MPa was achieved at a W/B ratio of 0.396 and SF content constant of 43.44 kg. It is clear that a rapid strength development can be obtained by reducing the free water content. When the strength development is an issue, water reduction is more dominant than the retardation effect of superplasticizer. To better illustrate how the concrete strength varied with the SPs and the W/B ratio, the strength results of the compacted cubes are plotted against the SPs in Fig 4.7 and next to the W/B ratio in Fig 4.8.

In the total nine concrete trial mixes for pilot project with superplasticizer content varying from 1.15% to 1.52% of binder, water-binder ratio ranging from 0.386 to 0.401 and a fixed binder content have been cast and tested. A maximum workability of 790 mm in slump flow and 2.51 seconds in flow time has been achieved at a 28 days with compacted cube strength of 46.95 MPa.

The effects of superplasticizer and W/B ratio on concrete strength and workability have been studied by comparing the results of the different trial mixes. As expected, a lower superplasticizer and W/B ratio leads to a higher strength but lower workability and vice versa. When the strength development is in issue, water reduction is more dominant than the retardation effect of superplasticizer
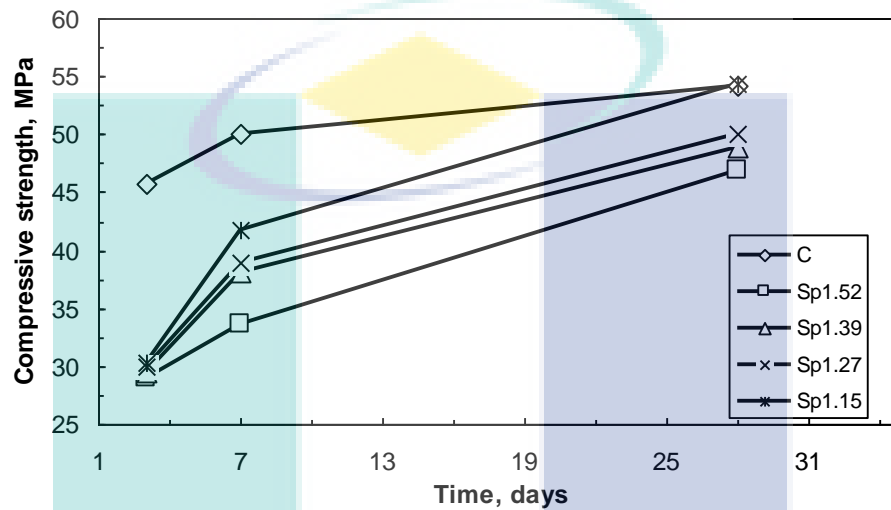
Figure 4.7: Relationship between curing time and compressive strength for varoius SPs content
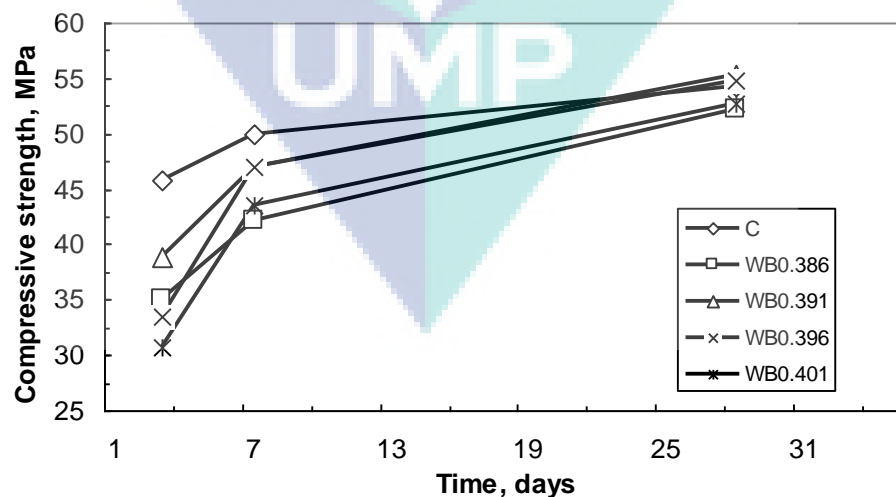
Figure 4.8: Relationship between curing time and compressive strength for varoius W/B ratio

4.3   DESIGN OF EXPERIMENT USING TAGUCHI METHOD

The work described in this thesis adopted the Taguchi's method in the design of experiment as it was the latest technique used today. Taguchi constructed a special set of orthogonal arrays (OAs) to layout the experiment. By combining the orthogonal latin squares in a unique manner, Taguchi prepared a new set of standard of OAs to be used for a number of experiment situations (Roy, 1990). Using orthogonal arrays significantly reduces the number of experimental configurations to be studied. The following section describes the experimental plan and experimental results using Taguchi method in SCC mixture.

4.3.1   Experimental Plan

In this work, L_{18} (3^6) orthogonal array (OA) is used. The L_{18} (3^6) OA (Table 3.3) has been explained in chapter 3. Six key parameters that can cause significant influence on the mix characteristics of SCC were selected to derive the mathematical models for evaluating relevant properties. The experimental levels of the variables (maximum and minimum), coarse aggregate, fine aggregate, cement, silica fume, water and SP are defined (See Table 3.1). Based on Table 3.1 and Table 3.3, 18 trials mix proportions of SCC are given in Table 4.6.

To simplify calculations and analysis, the actual variable ranges are usually transformed to dimensionless coded variables with a range of ±1. The coded forms of process control parameters were found by fixing the values for central parameter (0), maximum (+1) and minimum (-1) value of the variable. The coded values were calculated from the following relationships:

$$X_i = [2X - (X_{max} + X_{min})]/(X_{max} - X_{min}) \qquad (4.16)$$

where,

X_i= Required coded value of a variable X

X= Any value of the variable form X_{min} to X_{max}

The design matrix in coded value is shown in Table 4.7.

Table 4.6: Mix concrete proportions of Taguchi Design for one metre cube mix

Exp. No.	Factor 1 Coarse kg	Factor 2 Fine kg	Factor 3 Cement kg	Factor 4 Silica Fume kg	Factor 5 Water kg	Factor 6 Sp kg
1	759.00	818.53	538.29	43.44	230.14	4.11
2	759.00	826.26	546.20	45.35	233.09	4.48
3	759.00	833.98	554.11	47.26	236.04	4.84
4	767.25	818.53	538.29	45.35	233.09	4.84
5	767.25	826.26	546.20	47.26	236.04	4.11
6	767.25	833.98	554.11	43.44	230.14	4.48
7	775.50	818.53	546.20	43.44	236.04	4.48
8	775.50	826.26	554.11	45.35	230.14	4.84
9	775.50	833.98	538.29	47.26	233.09	4.11
10	759.00	818.53	554.11	47.26	233.09	4.48
11	759.00	826.26	538.29	43.44	236.04	4.84
12	759.00	833.98	546.20	45.35	230.14	4.11
13	767.25	818.53	546.20	47.26	230.14	4.84
14	767.25	826.26	554.11	43.44	233.09	4.11
15	767.25	833.98	538.29	45.35	236.04	4.48
16	775.50	818.53	554.11	45.35	236.04	4.11
17	775.50	826.26	538.29	47.26	230.14	4.48
18	775.50	833.98	546.20	43.44	233.09	4.84

Table 4.7: The design matrix in coded value

Exp No.	Control factors					
	Factor 1	**Factor 2**	**Factor 3**	**Factor 4**	**Factor 5**	**Factor 6**
1	-1	-1	-1	-1	-1	-1
2	-1	0	0	0	0	0
3	-1	1	1	1	1	1
4	0	-1	-1	0	0	1
5	0	0	0	1	1	-1
6	0	1	1	-1	-1	0
7	1	-1	0	-1	1	0
8	1	0	1	0	-1	1
9	1	1	-1	1	0	-1
10	-1	-1	1	1	0	0
11	-1	0	-1	-1	1	1
12	-1	1	0	0	-1	-1
13	0	-1	0	1	-1	1
14	0	0	1	-1	0	-1
15	0	1	-1	0	1	0
16	1	-1	1	0	1	-1
17	1	0	-1	1	-1	0
18	1	1	0	-1	0	1

CHAPTER 5

RESULTS AND DISCUSSION

5.1   INTRODUCTION

In this chapter, the experimental results of properties of self-compacting concrete and analysis of the experimental results were discussed. The results are mainly divided into two parts: (i) the fresh properties and, (ii) hardened properties results. In assessing the fresh concrete properties, the slump flow, flow time, V-funnel time, blocking ratio and segregation resistance were first determined. For determining the hardened properties, this study focused only on the compressive, tensile and flexural strengths.

5.2   EXPERIMENTAL RESULTS

5.2.1   Fresh Properties.

The results of slump flow, flow time, V-funnel time, L-box and segregation resistance for 18 SCC mixtures are presented in Table 5.1. The slump-flow values of all concrete mixtures were in the range of 650 to 800 mm, which refers to the mean spread diameter of concrete following the removal of slump cone, as specified by JSCE(1999). However, it is not sufficient to verify the self-compactability of these mixtures. Additionally, the speed of slump-flowing (i.e. T_{50} time), passing ability and visual stability of the mixtures was also tested.

The slump-flow time (T_{50}) of all mixtures was in the range of expected times (approximately 2 to 5 s). The slump-flow time (T_{50}) was measured when the concrete was slumping until it reached 500mm of flow. Very low T_{50}-times may cause segregation and very high T_{50} times may cause blocking. Visual stability index is a well known and the simplest detection method of any evidence of stability loss in fresh SCCs. The visual stability indices for all mixtures varied between 0 and 1, which indicates a good segregation resistance.

Table 5.1: Results of fresh properties test

Mix #	Slump flow (mm)	T_{50} (second)	V-funnel (second)	L-Box (H_2/H_1)	Segr. Resistance (%)
1	740.00	3.09	9.42	0.98	6
2	665.00	4.95	11.78	0.99	12
3	695.00	4.38	12.91	0.87	10
4	740.00	2.90	12.09	0.84	5
5	720.00	2.76	13.75	0.86	5
6	735.00	3.09	9.09	0.91	7
7	720.00	3.84	12.06	0.90	9
8	700.00	5.48	12.62	0.89	14
9	710.00	5.07	12.75	0.90	14
10	705.00	5.10	12.65	0.91	13
11	737.50	3.54	11.73	0.88	8
12	690.00	5.28	8.69	0.92	14
13	695.00	4.23	11.41	0.83	9
14	680.00	5.20	11.65	0.80	14
15	690.00	5.73	13.84	0.98	15
16	720.00	3.81	10.52	0.87	9
17	710.00	3.31	9.54	0.87	7
18	717.50	4.32	9.37	0.89	9

Additionally, satisfactory blocking resistances were obtained from the L-box tests. L-box passing ability ratios of all mixtures were higher than 0.80. If the concrete being tested was able to truly self-leveling, like water, the value of the blocking ratio would be unity.

The V-funnel test is used to measure the filling ability of self-compacting concrete and can also be used to judge segregation resistance (EFNARC, 2002). This test measures the ease of flow of the concrete; shorter flow times indicate greater flowability. For SCC a flow time of 10 seconds is considered appropriate. In this research, the V-funnel time was in the range of 8.69 to 13.84 seconds.

Empirical observations suggest that if the percentage of mortar that has passed through the 5mm sieve and the segregation ratio was in the range 5 to 15 per cent of the weight of the sample, the concrete was considered satisfactory for SCC. Below 5 per cent the resistance is considered excessive, and is likely to affect the surface finish. Above 15 per cent, and particularly above 30 per cent, there is a strong likelihood of segregation.

5.2.2   Hardened Properties

The hardened properties were tested for all 18 mixtures were compressive strength, split tensile and flexural strength. The specimens were demoulded one day after casting. Then they were cured in water at 27±3°C until three days before testing. The results of compressive strength, tensile and flexural strength are presented in Table 5.2.

Compressive strength test results are primarily used to determine that the concrete mixture as delivered meets the requirements of the specified strength- $f_c^{'}$, in the job specification. The strength is the average of at least two standard-cured strength specimens made from the same concrete sample and tested at the same age. In most cases, the strength requirements for concrete are at an age of 28 days. From these results, it may be observed that with this experimental plan a range of SCCs was covered, with compressive strength ($f'c$) 28 days from 52.65 to 64.90 MPa.

In addition to compressive strength, tensile strength is also required in the design of structures. Tensile strength is important for nonreinforced concrete structures such as a dam under earthquake excitations. Other structures such as pavement slabs and airfield runways, which are designed based on bending strength, are subjected to tensile forces. Therefore, in the design of these structures, tensile strength value is more appropriate than the compressive strength. The split tensile strength salues are observed to variy from 11.01 to 15.12 MPa for 28 days.

Table 5.2: Results of hardened properties test

Mix #	Compr. strength (3 days) (MPa)	Compr. strength (7 days) (MPa)	Compr. strength (28 days) (MPa)	Tensile Strength (MPa)	Flexural Strength (MPa)
1	38.97	43.60	52.65	13.22	5.36
2	32.71	42.05	56.30	14.23	4.30
3	33.51	44.95	60.10	13.77	5.04
4	26.62	43.55	60.20	13.94	4.67
5	28.48	41.24	62.20	15.12	4.80
6	27.47	40.60	56.94	12.45	5.18
7	29.31	39.64	55.35	14.39	4.63
8	21.66	39.98	57.75	11.85	5.56
9	30.44	39.20	56.50	12.44	4.13
10	29.53	49.25	62.40	14.11	4.97
11	32.58	47.95	61.45	11.81	4.72
12	36.92	49.20	64.90	12.06	5.49
13	33.62	49.45	63.45	12.96	5.06
14	35.91	43.75	57.80	11.48	5.16
15	33.41	44.65	57.45	11.83	4.66
16	29.63	48.90	61.35	14.13	4.98
17	29.29	45.20	63.35	11.01	5.47
18	28.22	41.12	59.05	13.08	4.82

Flexural strength is one measure of the tensile strength of concrete. It is a measure of an unreinforced concrete beam or slab to resist failure in bending. It is measured by loading a 150 x 150-mm concrete beams section with a span length of at least three times the depth. Flexural MR is approximately 10 to 20 percent of compressive strength, depending on the type, size and volume of coarse aggregate used. The flexural strength values are observed to vary from 4.13 to 5.55 MPa for 28 days.

5.3   MIX PROPORTIONING AND OPTIMISATION

In this section, the Taguchi approach is discussed in the selection of the optimal mixture proportioning of SCC based on the fresh stage requirements on the slump flow, flow time, V-funnel time, blocking ratio, segregation resistance and hardened stage requirement such as: compressive strength, splitting and flexural strength. The experimental results are then transformed into a signal-to-noise (S/N) ratio. Taguchi recommends the use of the S/N ratio to measure the quality characteristics deviating from the desired values. Several other researchers have studied the properties of concrete (Srinivasan et.al, 2003, Turkmena et.al, 2008, Tanyildizi and Coskun, 2008, Tanyildizi, 2008) by using the Taguchi method. However, they generally changed one or two constituents of concrete and investigated the effect of those parameters on concrete. Table 5.3   and 5.5 shows S/N ratio for fresh and hardened properties, respectively.

The best possible levels of mix proportions are investigated for the maximisation of slump flow, L-box ratio, compressive strength, splitting tensile strength, flexural strength, and for the minimisation of flow time, V-funnel, and segregation resistance by using the Taguchi method. The performance statistics for ''the larger is better'' situations are evaluated for maximisation properties of SCC and ''the smaller is better'' situations are evaluated for minimisation properties of SCC. This study does not take into the interactive effects of the mix parameters in SCC, as all of the parameters had interaction between them in the SCC mix.

Design expert software is used to analyse experimental data. The best possible testing conditions of the SCC properties can be determined from the main effect plot

graphs from Figures 5.1 to 5.9 for slump flow, flow time, L-box ratio, V-funnel time, segregation resistance, compressive strength, splitting tensile strength, and flexural strength, respectively. The objective is to select the best combination of control parameters so that the product or process is most robust in regard to noise factors. According to the Figures 5.1 to 5.9, the best mix proportions of the target properties are tabulated in Table 5.4.

Table 5.3: S/N ratio for fresh properties

Factor	Level	Slump flow (dB)	Flow time (dB)	Block ratio (dB)	V-funnel (dB)	SR (dB)
A	1	65.12	-25.44	8.84	-20.89	20.07
	2	64.83	-49.94	8.37	-21.48	21.75
	3	65.46	-60.91	8.50	-20.87	22.35
B	1	64.64	-28.51	8.57	-21.06	21.01
	2	65.31	-47.53	8.42	-21.42	20.32
	3	65.47	-60.26	8.73	-20.76	22.84
C	1	64.72	-39.38	8.67	-21.17	23.20
	2	65.43	-55.40	8.67	-20.86	20.88
	3	65.26	-41.51	8.37	-21.20	20.08
D	1	64.78	-39.53	8.52	-20.40	20.21
	2	65.17	-46.84	8.74	-21.19	19.79
	3	65.47	-49.93	8.45	-21.65	24.17
E	1	65.05	-52.04	8.69	-20.03	20.32
	2	65.05	-40.14	8.49	-21.33	22.85
	3	65.32	-44.11	8.53	-21.88	21.00
F	1	65.11	-41.46	8.48	-20.82	22.46
	2	65.27	-50.18	8.86	-21.11	19.97
	3	65.04	-44.65	8.38	-21.31	21.74

5.3.1 Optimization of Fresh Properties

The slump test values of all mixes are in the range of 650 to 800 mm. As mentioned in EFNARC (2002), concrete can be accepted as SCC if their slump flow values are in the range of 650 to 800 mm. It can be said that all produced concrete SCC. Based on Figure 5.1, the optimal mix proportion for slump flow SCC is obtained by A3B3C2D3E3F2 combinations with a mean 775.50 kg coarse aggregate, 818.53 kg fine aggregate, 546.20 kg cement, 47.26 kg silica fume, 274.00 kg water and 8.14 kg superplasticizer. The slump flow increased with the increase of fine aggregate and silica fume. The slump flow test is used to assess the horizontal free flow of SCC in the absence of obstructions. On lifting the concrete filled slump cone, the concrete flows freely. The average diameter of the concrete circle is a measure for the filling ability of the concrete (Aggarwal, 2008).
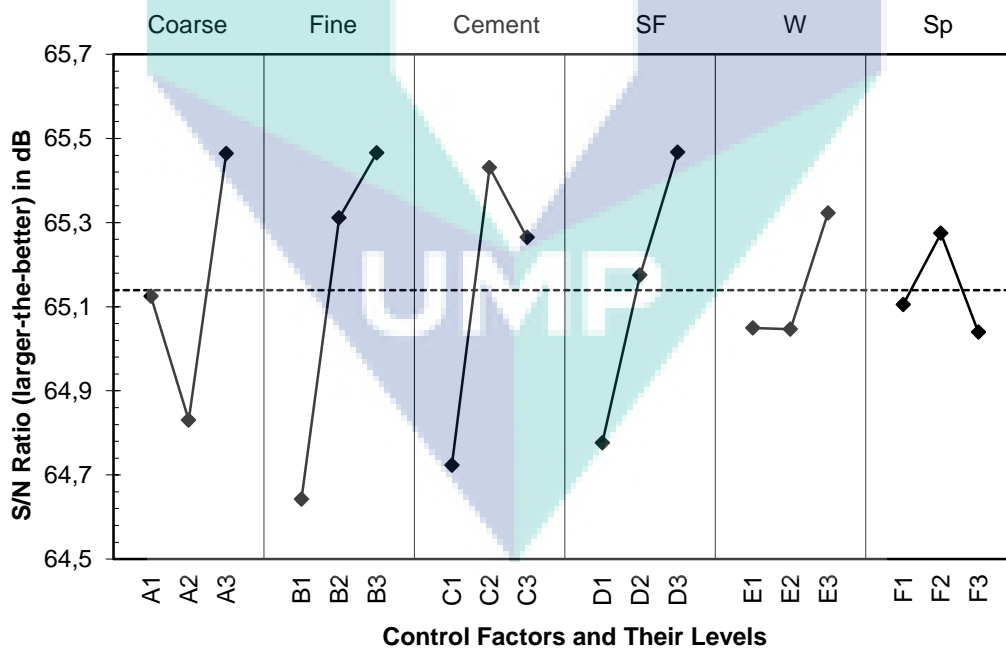
Figure 5.1: Factor effect plot for slump flow

The time T$_{50cm}$ is a secondary indication of flow. It measures the time taken in seconds from the instant the cone is lifted to the instant when horizontal flow reaches a

diameter of 500 mm. Based on Figure 5.2, the optimal mix proportion for flow time SCC is obtained by A3B3C3D2E2F2 combinations.
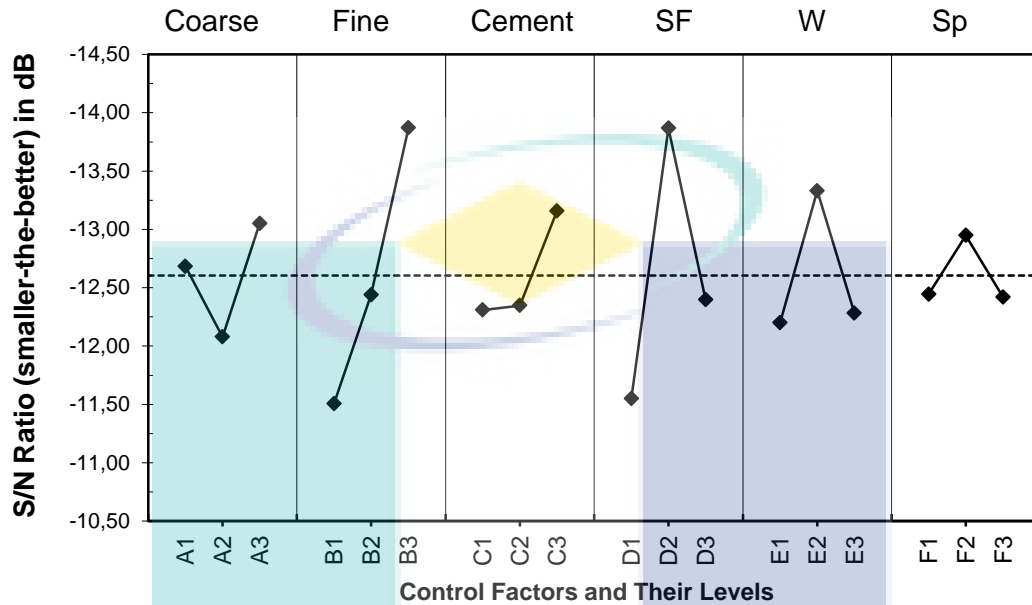
Figure 5.2: Factor effect plot for flow time (T50)
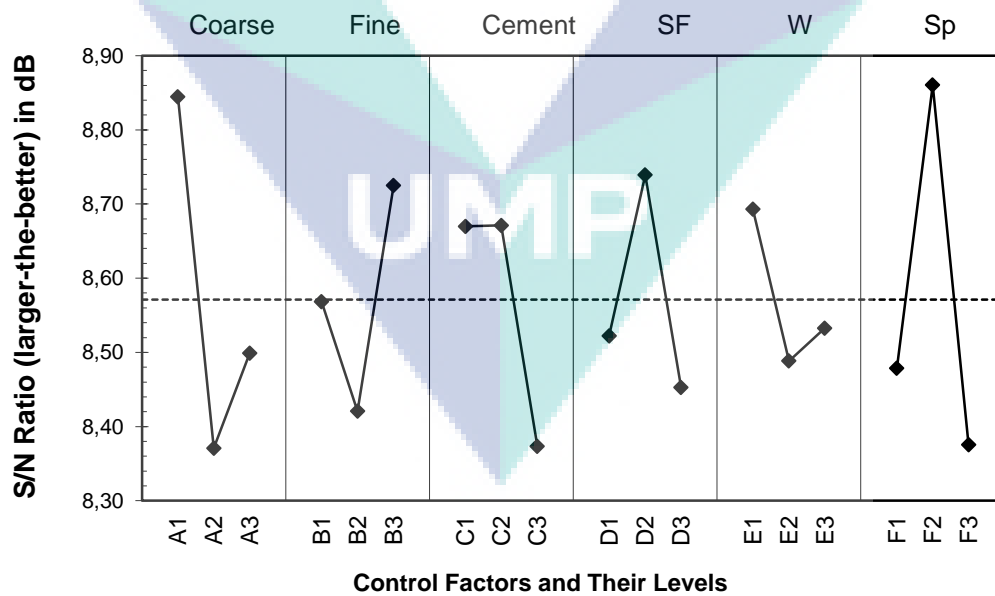
Figure 5.3: Factor effect plot for blocking ratio

The blocking ratio assesses the filling and passing ability of SCC. If the concrete flows as freely as water, at rest it will be horizontal, thus H2/H1 = 1. Therefore, the

nearer this test value, the 'blocking ratio', is to unity, the better the flow of the concrete. Figure 5.3 shows the optimal mix proportion for the blocking ratio SCC is obtained by a combination of A1B3C2D2E1F2. For the L-box test, the increase of the dosages of water and Sp led to an increase in the L-box blocking ratio. This is in agreement with results found in the previous study (Sonebi, et.al. 2007).
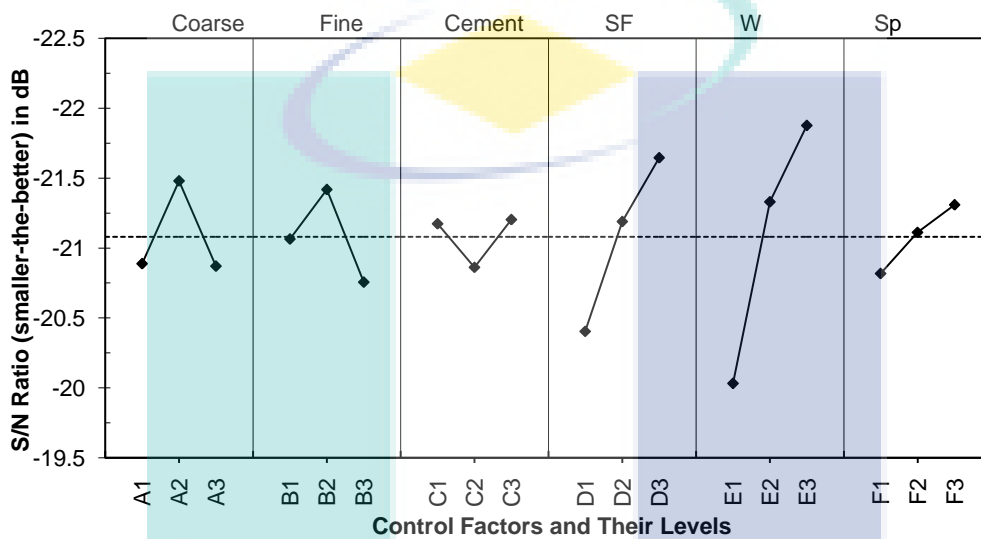
Figure 5.4: Factor effect plot for V-funnel Time

This V-funnel test measures the ease of flow of the concrete; shorter flow times indicate greater flowability. For SCC a flow time of 10 seconds is considered appropriate. Optimal conditions for V-funnel time are obtained by mixture combination A2B2C3D3E3F3, as shown in Figure 5.4. When silica fume, water, and superplasticizer content are increased in concrete mix the V-flow time is also increased.

The segregation resistance increases with the increase of cement content, but decreases the coarse aggregate. The optimal conditions for segregation resistance are obtained by mixture A1B2C3D2E1F2, as shown in Figure 5.5. The systematic experimental approach showed that partial replacement of coarse and fine aggregate could produce self-compacting concrete with low segregation potential, as assessed by the V-Funnel test (Ravindrarajah et.al., 2003).
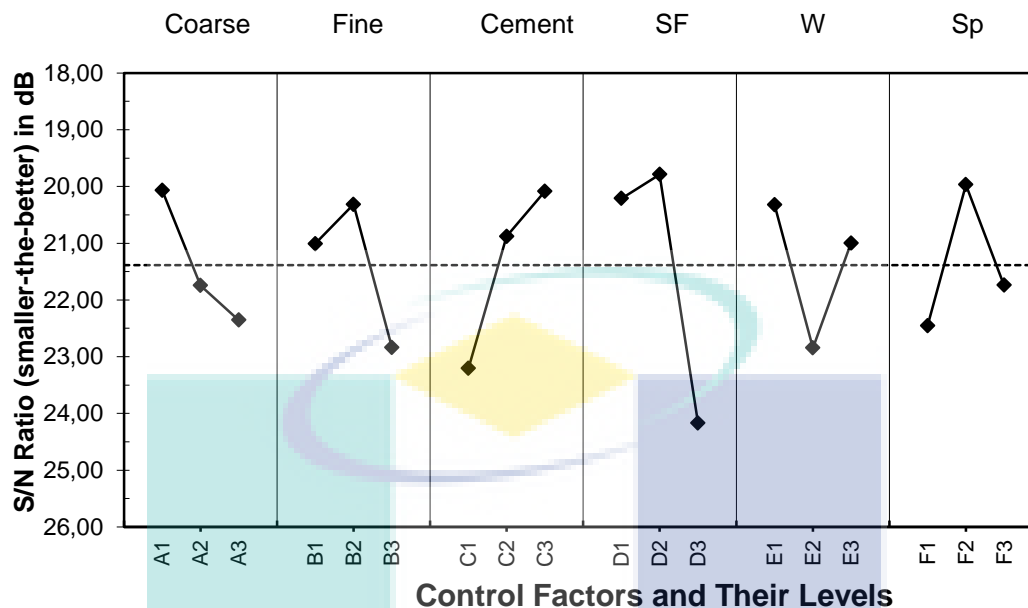
Figure 5.5: Factor effect plot for Segregation Resistance

The best possible testing conditions of the SCC fresh properties can be determined from the main effect plot graphs from Figures. 5.1 to 5.5 for slump flow, flow time, blocking ratio, V-funnel and segregation resistance, respectively. Based on Figures 5.1 to 5.5, the best mix proportions of the fresh as a target properties are tabulated in Table 5.4.

Table 5.4: Optimal mix design proportions for fresh properties

Optimal mix proportions	Coarse (kg)	Sand (kg)	Cement (kg)	SF (kg)	Water (kg)	Sp (kg)
Slump flow	775.50	818.53	546.20	45.35	233.09	4.48
Flow time	775.50	818.53	554.11	45.35	233.09	4.48
Block ratio	759.00	818.53	546.20	45.35	230.14	4.48
V-funnel time	767.25	826.26	554.11	47.26	236.04	4.84
Segregation resistance	759.00	826.26	554.11	45.35	230.14	4.48

Table 5.5: S/N ratio for hardened properties

Factor	Level	Compr. strength (dB)	Splitting strength (dB)	Flexural strength (dB)
A	1	22.20	21.76	14.34
	2	21.59	21.06	13.36
	3	22.56	22.01	13.86
B	1	21.03	20.72	13.67
	2	21.96	21.43	14.01
	3	23.38	22.68	13.89
C	1	21.82	21.24	14.08
	2	21.87	21.46	13.59
	3	22.67	22.12	13.90
D	1	21.07	20.69	13.96
	2	23.37	22.67	13.88
	3	21.92	21.47	13.73
E	1	21.72	21.21	13.75
	2	22.84	22.31	14.04
	3	21.80	21.31	13.78
F	1	21.96	21.46	13.60
	2	22.46	21.91	13.92
	3	21.94	21.46	14.04

5.3.2 Optimization of Hardened Properties

The optimal conditions for compressive strength are obtained by mixture combination A2B2C2D3E1F3 as shown in Figure 5.6. As can be seen from Figure 5.6, increasing the SF parameter increases the compressive strength. The optimal mix-design for maximisation of the compressive strength of SCC is 767.25 kg coarse, 826.26 kg sand, 546.20 kg cement, 47.26 kg SF, 230.14 kg water, and 4.84 kg Sp.
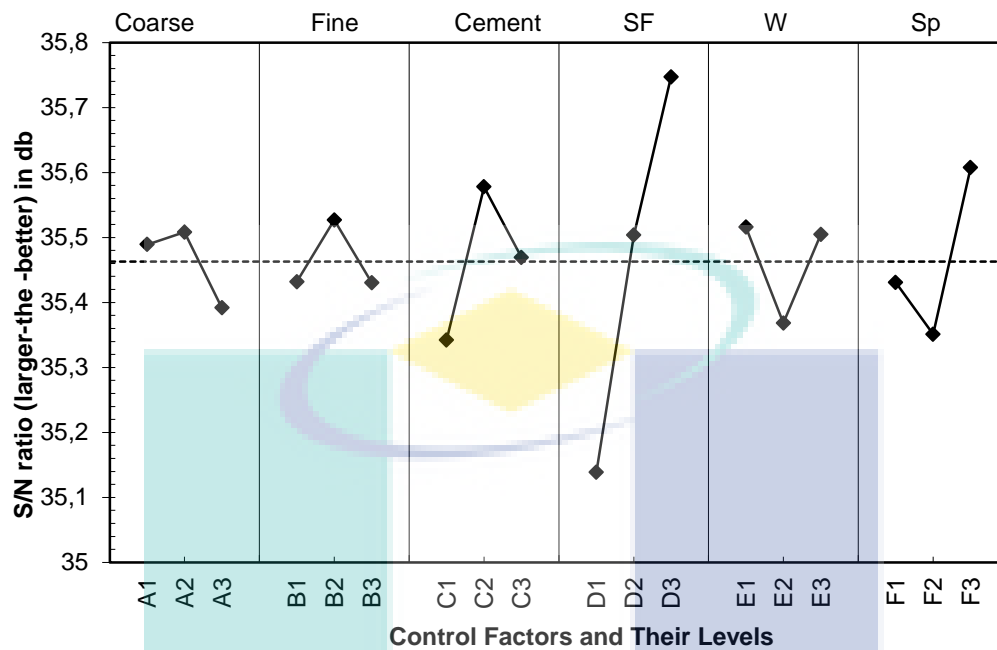
Figure 5.6: Factor effect plot for Compressive Strength

Figure 5.7 shows that, increasing the sand and cement content parameters increases the splitting strength. The optimal mix proportions for maximum splitting tensile strength is obtained by A3B3C3D2E2F2 combinations with a mean of 775.50 kg coarse, 818.53 kg sand, 554.11 kg cement, 45.35 kg SF, 233.09 kg water, and 4.48 kg Sp.
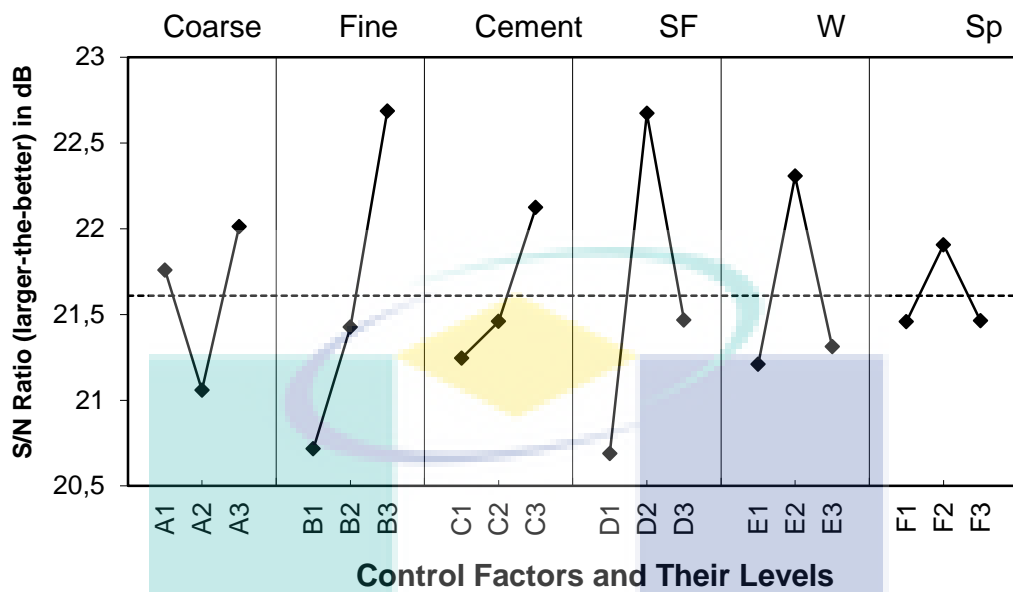
Figure 5.7: Factor effect plot for Splitting Strength
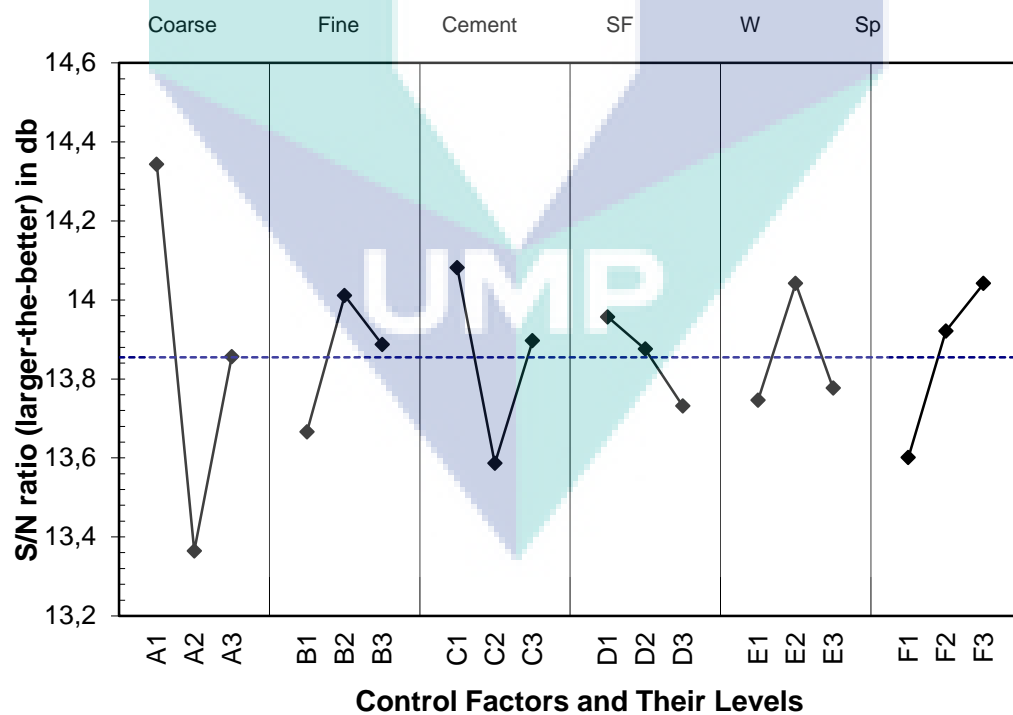
Figure 5.8: Factor effect plot for Flexural Strength

Based on Figure 5.8, the flexural strength values of the produced concrete are increased by increasing of the Sp content, but decreased by increasing the SF content. The optimum mix proportions for the maximum flexural strength of concrete are 759.00 kg coarse, 826.26 kg sand, 538.29 kg cement, 43.44 kg SF, 230.14 kg water, and 4.84 kg Sp with A1B2C1D1E2F3 combinations (see Figure 5.8).

The best possible testing conditions of the SCC for hardened properties can be determined from the main effect plot graphs from Figures. 5.6 to 5.8. Based on the these figures, the best mix proportions of the target properties are tabulated in Table 5.6.

Table 5.6: Optimal mix design proportions for hardened properties

Optimal mix proportions	Coarse (kg)	Sand (kg)	Cement (kg)	SF (kg)	Water (kg)	Sp (kg)
Compressive Strength Test	767.25	826.26	546.20	47.26	230.14	4.84
Splitting Strength Test	775.50	818.53	554.11	45.35	233.09	4.48
Flexural Strength Test	759.00	826.26	538.29	43.44	230.14	4.84

In order to verify the optimum mix-design proportion obtained using the Taguchi method, an experimental study was performed to check whether slump flow, L-box ratio, compressive strength, splitting tensile strength, and flexural strength can be actually be maximised and flow time, V-funnel, and segregation resistance can be actually be minimised by the proposed optimum mixture proportions. In order to obtain meaningful results, the same materials and conditions were used with the Taguchi analyses. These samples were tested for compressive strength, splitting tensile strength, and flexural strength at 28 days by using the related standard. The results can be seen in Table 5.7. The verification study results showed that proposed optimum mix proportions satisfied the expectance maximize for slump flow, L-box ratio, compressive strength, splitting tensile strength, and flexural strength and ultrasonic pulse velocity and minimize for the flow time, V-funnel, and segregation resistance.

Table 5.7: Optimum mix-design verification test results

Concrete Property	Test Result
Slump flow	680 (mm)
Flow time	3.5 (second)
L-box ratio	0.85
V-funnel time	11.54 (second)
Segregation Resistance	9.8 (%)
Compressive strength	56.34 (MPa)
Splitting strength	14.05 (MPa)
Flexural strength	5.20 (MPa)

5.4   REGRESSION MODELLING OF SCC

In this part of study, the statistical relation (modelling) between fresh properties (slump flow, flow time, blocking ratio, V-funnel time, segregation resistance), hardened properties (compressive strength, tensile strength, flexural strength) and mixture constituents for predicting fresh and hardened properties values is introduced. The regression analysis method is generally used to obtain this type of relation. In this study, second-order regression analysis was used to establish a model between the experimentally obtained values and mixture constituents.

5.4.1   Regression Modelling of Fresh Properties

In order to estimate the model parameters effectively, Design Expert Software was used to build the regression equation. Through the design of the experiments mentioned in Chapter 4, six control factors with three levels are presented in Table 3.1. The six control factors selected are as follows:

A: Coarse aggregate, (kg)
B: Fine aggregate/ sand (kg)
C: Cement, (kg)

D: Silica fume, (kg)

E: Water, (kg)

F: Superplasticizer, (kg)

The five selected fresh properties models are slump flow, T_{50} flow time, V-funnel, blocking ratio and segregation resistance. The final functions of the statistical model are itemized as follows:

(i). Modelling of Slump Flow

The statistical model of the slump flow was expressed as

$$Slump\ flow = +709.44 - 11.88 * A + 11.67 * B + 8.32 * C + 4.79 * D$$
$$+ 7.99 * E - 14.31 * A * B + 11.84 * A * D - 16.10 * B * D$$

(5.1)

with $R^2 = 0.939$

Based on the values of the regression coefficients obtained in Equation 5.1 the highest influence on slump flow was coarse aggregate (A) (11.88), and then, in order of contribution, fine aggregate (B) (11.67), cement (C) (8.32), water (E) (7.99) and silica fume (D) (4.79) content. The coefficient of the determination (R^2) value of the proposed model for slump flow was 0.939. The high R^2 value demonstrated high correlation between the actual value that could be correlated with the proposed model.

To verify whether the obtained statistical model is significant, analysis of variance (ANOVA) and F-ratio test were performed on them. After the ANOVA is completed, the F statistic of any specific control (A), for example F_A, which is defined as the ratio between the mean of variance square for the A control factor and the mean of error variance square, can be obtained. The value of F_A is used for the significance test. The bigger the F_A, the larger the significant influence of control factor A will be. The significance level is divided into two kinds: (1) significant ($\alpha = 5\%$) and (2) very significant ($\alpha = 1\%$) as given by Equations 5.2 and 5.3.

$$F_A > F_{0.01}, \nu_1, \nu_2 \qquad : \text{very significant} \qquad (5.2)$$

$$F_{0.01}, \nu_1, \nu_2 > F_A > F_{0.05}, \nu_1, \nu_2 \quad : \text{significant} \qquad (5.3)$$

where ν_1 and ν_2 are the degrees of freedom. The statistical F-table can be found in Appendix-C.

The ANOVA of the slump flow model is shown in Table 5.8. A five factor ANOVA for the test data was used in this model. The F-value of the statistic model and individual model terms helps to find their significance. Based on the P-values, it can be concluded that the coarse aggregate (A) and fine aggregate (B) are statistically very significant, whereas cement (C), silica fume (D) and water (E) have a statistically significant effect on slump flow.

Table 5.8: Analysis of variance for Slump Flow

Source	Sum of Squares	DF	Mean Square	F Value	P-Value	VIF
Model	7350.81	8	918.85	17.19	0.0001[a]	
A	1692.19	1	1692.19	31.65	0.0003[a]	1.00
B	1633.33	1	1633.33	30.55	0.0004[a]	1.00
C	431.08	1	431.08	8.06	0.0194[b]	1.92
D	275.52	1	275.52	5.15	0.0493[b]	1.00
E	533.75	1	533.75	9.98	0.0116[b]	1.44
AB	1203.55	1	1203.55	22.51	0.0011[a]	1.36
AD	561.21	1	561.21	10.50	0.0102[b]	2.00
BD	1441.44	1	1441.44	26.96	0.0006[a]	1.44
error	481.13	9	53.46			
Cor Total	7831.94	17				

[a]At least 99% confidence

[b]At least 95% confidence

Multicollinearity is a statistical term for a problem that is common in regression analysis. Multicollinearity is a state of very high inter-correlations or inter-associations amongst the independent variables. Multicollinearity is therefore a type of disturbance

in the data, and if present in the data the statistical inferences made about the data may not be reliable. The Variance Inflation Factor (VIF) will produce to be less than 4.0, indicating that multicollinearity is not a serious problem. Table 5.8. shows that the VIF varied from 1.32 to 2.36. This indicates that multicollinearity is not a problem.

(ii). Modelling of Flow Time

The statistical model of flow time is

$$Flow\ time\ (T50) = +4.23 + 0.64 * A - 0.67 * D + 0.89 * A * B + 1.05 * A * C$$
$$- 1.02 * A * D - 0.69 * A * E - 1.30 * B * F + 1.50 * C * E$$

(5.4)

with $R^2 = 0.939$

Table 5.9: Analysis of variance for Flow Time (T_{50})

Source	Sum of Squares	DF	Mean Square	F Value	P-Value	VIF
Model	15.08	8	1.88	17.47	0.0001[a]	
A	4.89	1	4.89	45.33	0.0001[a]	1.00
D	2.34	1	2.34	21.68	0.0012[a]	2.32
AB	4.92	1	4.92	45.57	0.0001[a]	1.30
AC	3.44	1	3.44	31.84	0.0003[a]	2.55
AD	4.42	1	4.42	40.97	0.0001[a]	1.90
AE	1.98	1	1.98	18.36	0.0020[a]	1.93
BF	4.96	1	4.96	45.97	0.0001[a]	2.74
CE	6.19	1	6.19	57.41	0.0001[a]	2.89
error	0.97	9	0.11			
Cor Total	16.05	17				

[a]At least 99% confidence

[b]At least 95% confidence

Based on the values of the regression coefficients obtained in Equation (5.4) the highest influence on flow time was coarse aggregate (A) and silica fume (D) content.

The coefficient of the determination (R^2) value of the proposed model for flow time was 0.939.

Based on the P-values (Table 5.9), it can be concluded that coarse aggregate (A) and silica fume (D) statistically have a very significant effect on flow time. Table 5.9 also shows that all of the VIF values are less than 4. This indicates that multicollinearity is not a problem.

(iii). Modelling of V-Funnel Time

The statistical model of V-funnel time is

$$V\text{-}funnel\ Time = +11.44 + 0.88*A - 0.62*B - 2.30*D$$
$$- 0.76*F - 1.32*A*B - 1.78*A*C - 0.80*A*E$$
$$- 0.85*B*C - 1.81*B*D + 2.10*B*E + 1.89*C*F \qquad (5.5)$$

with $R^2 = 0.989$

The derived model of V-funnel time for different content of coarse aggregate (A), fine aggregate (B), silica fume (D) and superplasticizer (F) is shown in Equation (5.5). The dosage of cement (C) and water (E) did not have any significant influence on V-funnel time. Table 5.10 summarises the analysis of variance for V-funnel time. The P-*Value* reveals that the effects of A and D are very significant. Table 5.10 also shows that the all value VIF less than 4. This indicates that multicollinearity is not a problem.

Table 5.10: Analysis of variance for V-funnel time

Source	Sum of Squares	DF	Mean Square	F Value	P-Value	VIF
Model	44.23	11	4.02	43.20	0.0001[a]	
A	6.85	1	6.85	73.57	0.0001[a]	1.36
B	2.25	1	2.25	24.15	0.0027[b]	2.08
D	16.44	1	16.44	176.65	0.0001[a]	3.87
F	2.34	1	2.34	25.14	0.0024[b]	2.93
AB	5.92	1	5.92	63.56	0.0002[a]	2.36
AC	11.26	1	11.26	121.00	0.0001[a]	2.26
AE	1.81	1	1.81	19.40	0.0045[a]	2.84
BC	3.36	1	3.36	36.13	0.0010[a]	1.72
BD	11.69	1	11.69	125.64	0.0001[a]	2.24
BE	15.23	1	15.23	163.60	0.0001[a]	2.31
CF	11.70	1	11.70	125.67	0.0001[a]	2.45
error	0.56	6	0.09			
Cor Total	44.79	17				

[a]At least 99% confidence

[b]At least 95% confidence

(iv). Modelling of Blocking Ratio

The statistical model of the blocking ratio test is as follows

$$Bocking\ Ratio = +0.89 + 0.034 * B - 0.044 * E + 0.027 * A * B$$
$$+ 0.031 * A * C + 0.041 * C * D + 0.032 * C * E - 0.047 * C * F \tag{5.6}$$

with $R^2 = 0.872$

Only the fine aggregate (B) and water content (E) has a significant influence on the blocking ratio. The coefficient of the determination (R^2) value of the proposed model for flow time was 0.872.

The fourth column of the ANOVA table provides a useful understanding of the value of goodness of a response surface equation. These are the mean square columns. The numerical value of the last of these columns in the statistics refers to the mean square error. An MSE equal to zero, means that the estimator predicts observations of the parameter with perfect accuracy, which is ideal, but practically never possible. The goal of experimental design is to construct experiments in such a way that when the observations are analysed, the MSE is close to zero relative to the magnitude of at least one of the estimated treatment effects. This model shows that the MSE is 0.0006.

Table 5.11: Analysis of variance table L-blocking ratio

Source	Sum of Squares	DF	Mean Square	F Value	P-Value	VIF
Model	0.0375	7	0.0054	9.699	0.0009[a]	
B	0.0079	1	0.0079	14.239	0.0036[a]	1.72
E	0.0152	1	0.0152	27.600	0.0004[a]	1.52
AB	0.0048	1	0.0048	8.733	0.0144[a]	1.24
AC	0.0054	1	0.0054	9.786	0.0107[a]	1.47
CD	0.0084	1	0.0084	15.134	0.0030[a]	1.58
CE	0.0057	1	0.0057	10.355	0.0092[a]	1.44
CF	0.0106	1	0.0106	19.191	0.0014[a]	1.66
error	0.0055	10	0.0006			
Cor Total	0.0430	17				

[a]At least 99% confidence

[b]At least 95% confidence

(v). Modelling of Segregation Resistance

The statistical model of segregation resistance is

$$\text{Segr. Resistance} = +10.04 + 1.88*A - 2.31*D$$
$$+ 2.90*A*B + 3.79*A*C - 3.81*A*D$$
$$- 2.60*A*E - 4.82*B*F + 4.97*C*E \qquad (5.7)$$

with $R^2 = 0.9205$

Based on the values of the coefficient of regression obtained in Equation 5.7, the highest influence on segregation resistance was interaction cement-water (CE), interaction fine aggregate-superplasticizer (BF), and coarse aggregate-silica fume (AD). The main factors of silica fume (D) and coarse aggregate (A) influenced the segregation resistance.

Table 5.12: Analysis of variance table for Segregation Resistance

Source	Sum of Squares	DF	Mean Square	F Value	P-Value	VIF
Model	161.1330	8	20.1416	13.018	0.0004	
A	42.2324	1	42.2324	27.295	0.0005	1.00
D	27.5157	1	27.5157	17.784	0.0022	2.32
AB	52.0030	1	52.0030	33.610	0.0003	1.30
AC	44.8663	1	44.8663	28.997	0.0004	2.55
AD	60.9760	1	60.9760	39.409	0.0001	1.90
AE	27.9781	1	27.9781	18.082	0.0021	1.93
BF	68.0394	1	68.0394	43.974	< 0.0001	2.74
CE	68.3238	1	68.3238	44.158	< 0.0001	2.89
error	13.9253	9	1.5473			
Cor Total	175.0583	17				

[a]At least 99% confidence

[b]At least 95% confidence

The ANOVA of segregation resistance model and F-test were performed to evaluate the significance of the coarse aggregate (A), fine aggregate (B), cement (C), silica fume (D), water (E) and superplasticizer (F) dosages of the SCC. A larger F-value

means a more significant contribution of the parameter to segregation resistance. The ANOVA for the segregation resistance model is shown in Table 5.12.

5.4.2 Response Surface for Fresh Properties

The response surface uses multiple regression techniques to sequentially fit the order polynomial to the sample data and conduct tests that should indicate the next appropriate action (Onyiah, 2009). A response surface is the graph of the system response as a function of one or more variables. These graphs offer an opportunity to visually analyse how certain factors influence the measurement system (Bayramov et al., 2004).

i.   Slump flow test

The content of the coarse aggregate had the greatest effect on the slump flow with a contribution of more than 29 per cent. Figure 5.9 shows that the increase in the dosage of coarse aggregate has an influence on decreasing slump flow. However, the slump flow is increased as the quantity of fine aggregate increases. The trade-off illustrates that the decrease in coarse aggregate necessitates a decrease in fine aggregate to maintain a fixed slump flow.

The orientation of response surfaces in Figures 5.9 (a) and 5.9.(b) shows the influence of water content on slump flow. The water content is either 230.14 kg or 236.04 kg and in both cases the content of the coarse aggregate varied from 759.00 kg to 775.50 kg and the fine aggregate varied from 818.53 kg to 833.98 kg; the proportion of cement, silica fume and superplasticizer is fixed at 546.20 kg, 45.35 kg and 4.47 kg, respectively. In other words, the slump flow increases as the water-cement ratio increases.

(a). Water = 230.14 kg

(b). Water = 236.04 kg
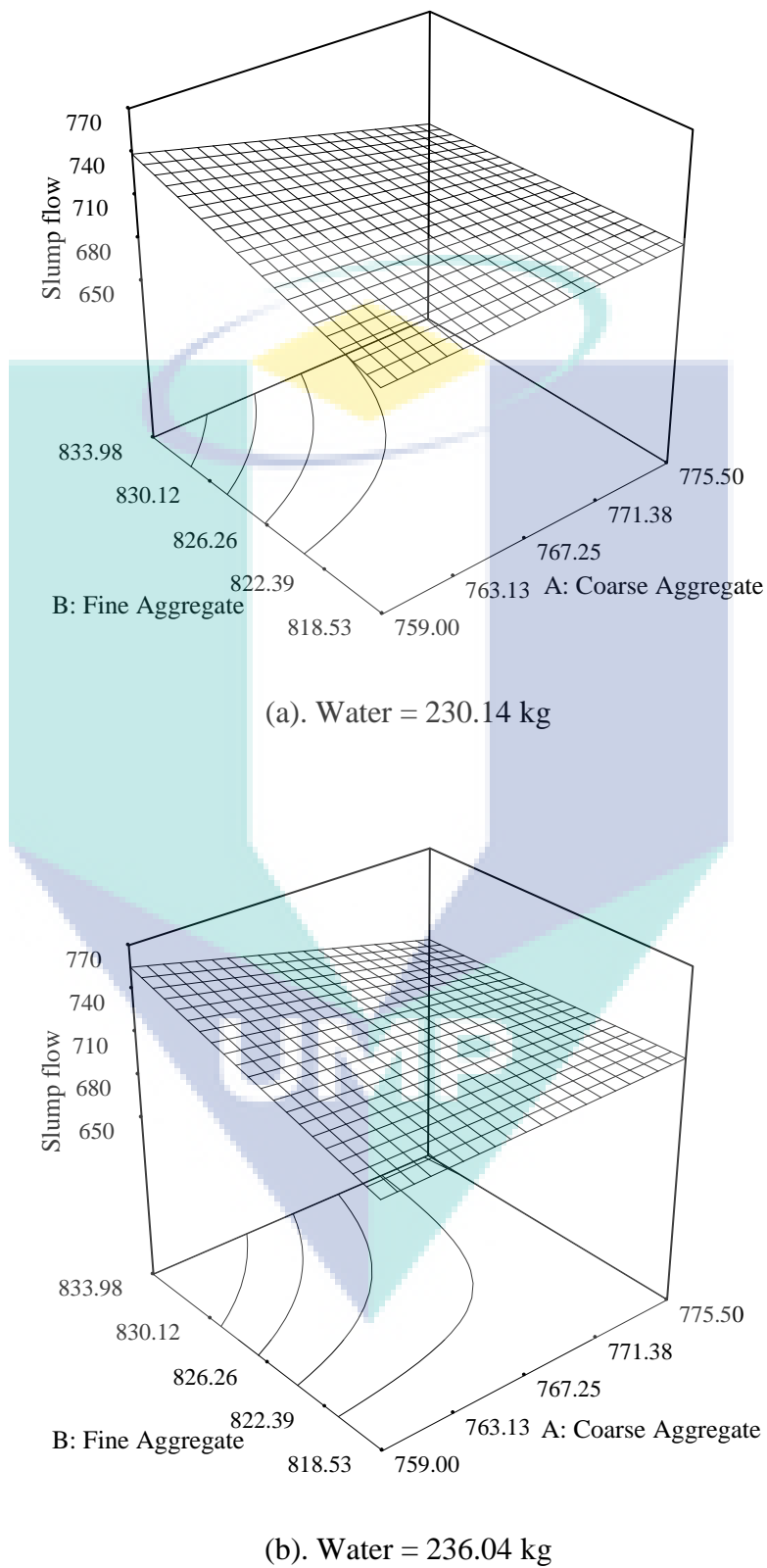
Figure 5.9: Response surface of slump flow

ii. Flow time

The main effect of the coarse aggregate and the dosage of silica fume are that it actually dominates on the flow time, with a very significant level, $\alpha = 1$ per cent. Figure 5.10 shows that, the increase in the dosage of coarse aggregate has an influence on decreasing flow time. Nevertheless, the flow time increases as the fine aggregate decreases. The trade-off illustrates that the decrease in coarse aggregate necessitates a decrease in fine aggregate to maintain a fixed flow time within a range of 3.11 to 4.46 seconds.

The significant difference of the orientation of the response surface in Figures 5.10(a) and 5.10(b) shows the high influence of superplasticizer on flow time. The response of the dosage of superplasticizer on flow time when the superplasticizer dosage is equal to 4.11 kg Figure 5.10(a) and 4.47 kg Figure 5.10(b) shows the position of the response surfaces. The flow time decreases as the dosage of superplasticizer increases.

iii. V-funnel test

The orientation of the response surface in Figure 5.11 shows that the increase of the volume of fine and coarse aggregate caused an increase in V-funnel, within a range content of aggregate 763 kg to 775 kg. It is also important to note that, the contours illustrate that the increase in coarse aggregate necessitates an increase in fine aggregate to maintain a fixed V-funnel flow time.

The lower position of the response surface in Figure 5.11(b) when the dosage of superplasticizer was equal to 4.84 kg, and the water and cement were fixed demonstrates that the V-funnel flow time is decreased by increasing the superplasticizer dosage, compared to the results in Figure 5.11(b).

(a). Sp = 4.11 kg

(b). Sp = 4.47 kg
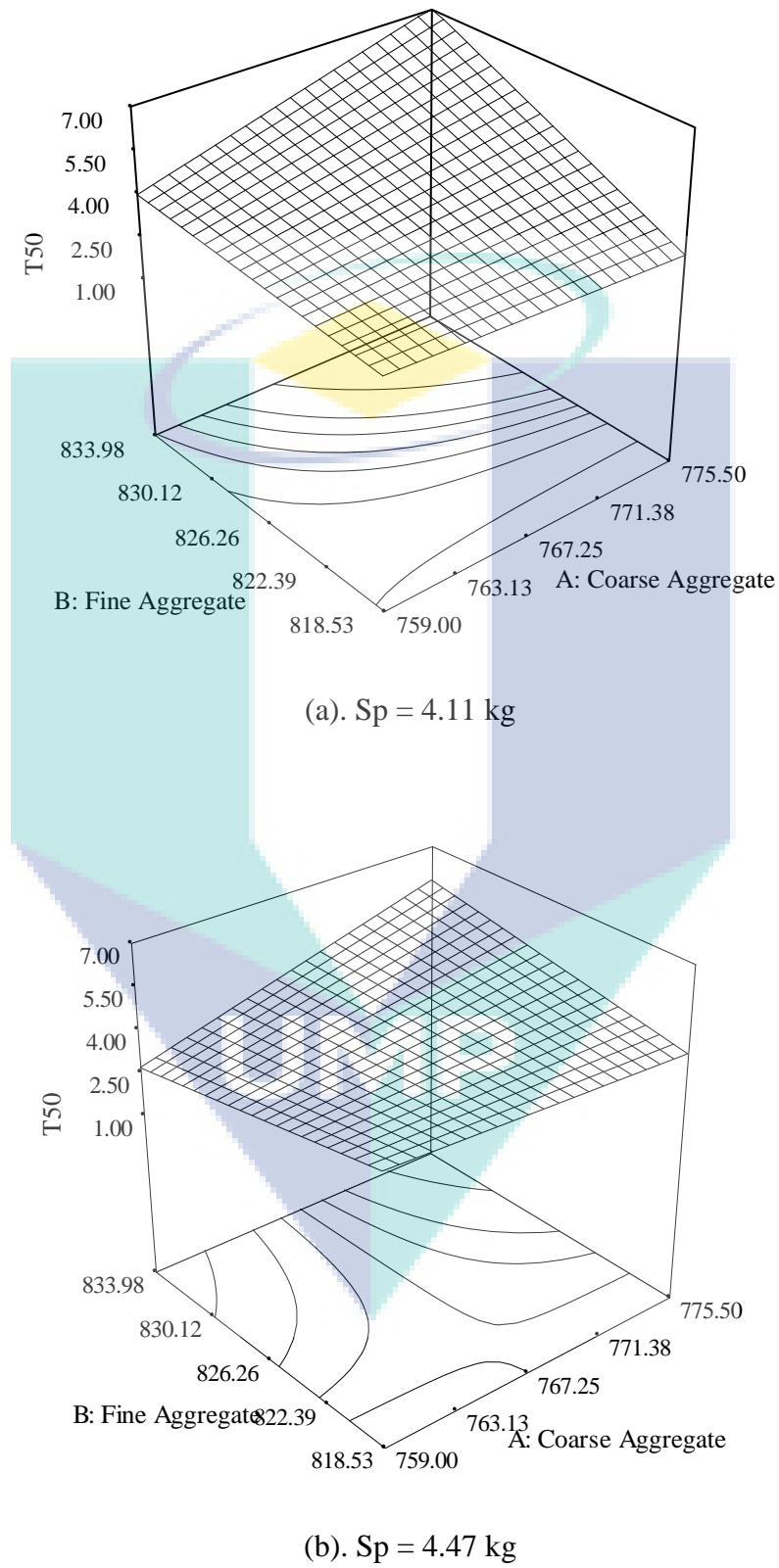
Figure 5.10: Response surface of flow time

(a) Sp = 4.47 kg

(b) Sp = 4.84 kg
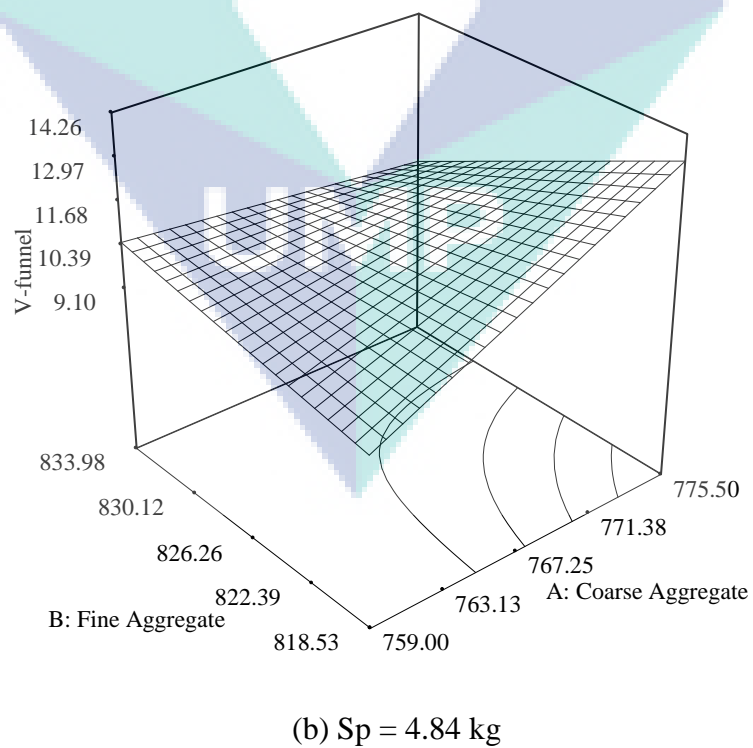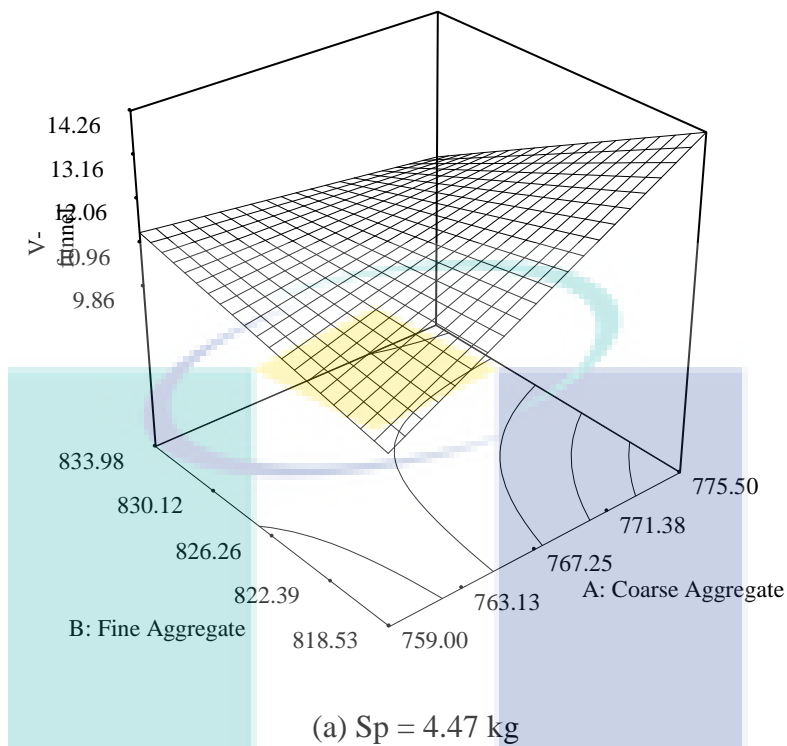
Figure 5.11: Response surface of V-funnel time

iv.   L-box test

Figure 5.12(a) shows the response surface orientation that illustrates the effect of the aggregate on the L-box test results. The blocking ratio is increased, as increasing the quantity of coarse aggregate for the content of fine aggregate varied from 818.53 kg (lower limit) to 826.26 kg (central point). However, the blocking ratio is decreased when increasing the coarse aggregate for the fine aggregate content by more than 826.26 kg. This is due to the increase of the risk of blockage with a collision of coarse aggregate particles behind reinforced bars of the L-box when the volume of coarse aggregate is high. The optimum fine aggregate content was 826.16 kg.

The same orientation of response surfaces in Figures 5.12(a) and 5.12(b) exhibited no interaction when increasing of the superplasticizer on the blocking ratio. The effect of the water content on the blocking ratio can be observed by comparing Figures 5.12(a) and 5.12(c). The higher position of the response surface in Figure 5.12(a), when the dosage of water was equal to 233.09 and the Sp was fixed at 4.47, demonstrates that the water-cement ratio is more dominant than the superplasticizer content on the blocking ratio.
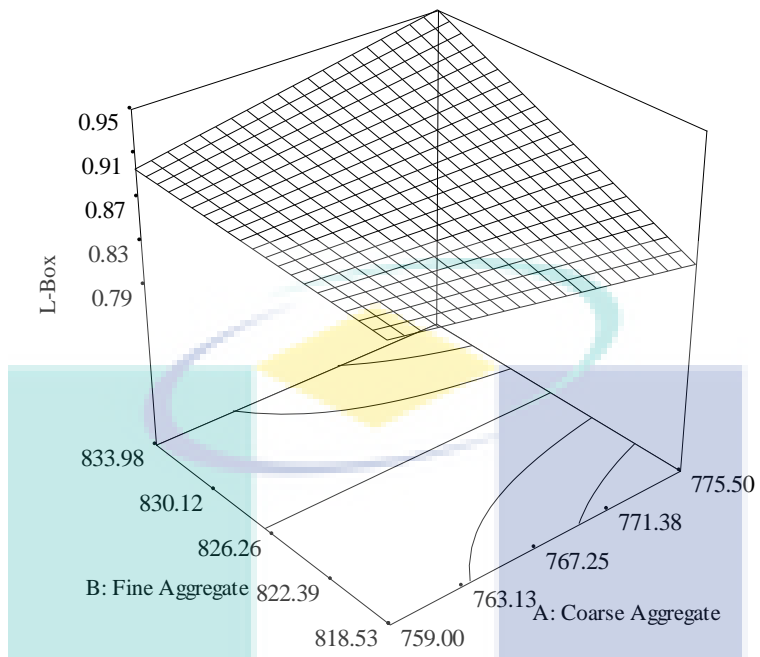
(a). Water = 233.09 kg, Sp = 4.47 kg
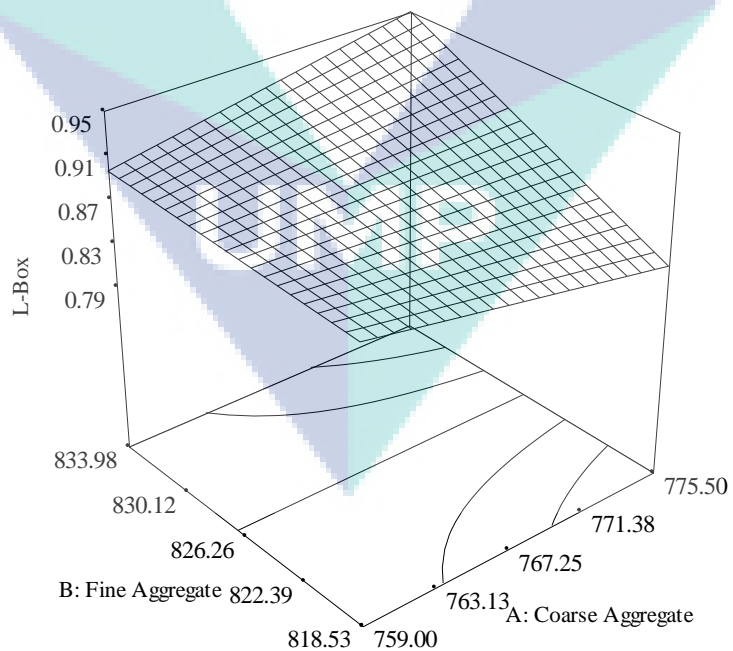
(b). Water = 233.09 kg, Sp = 4.84 kg

Figure 5.12: Response surface of blocking ratio

(c). Water = 236.04 kg, Sp = 4.47 kg
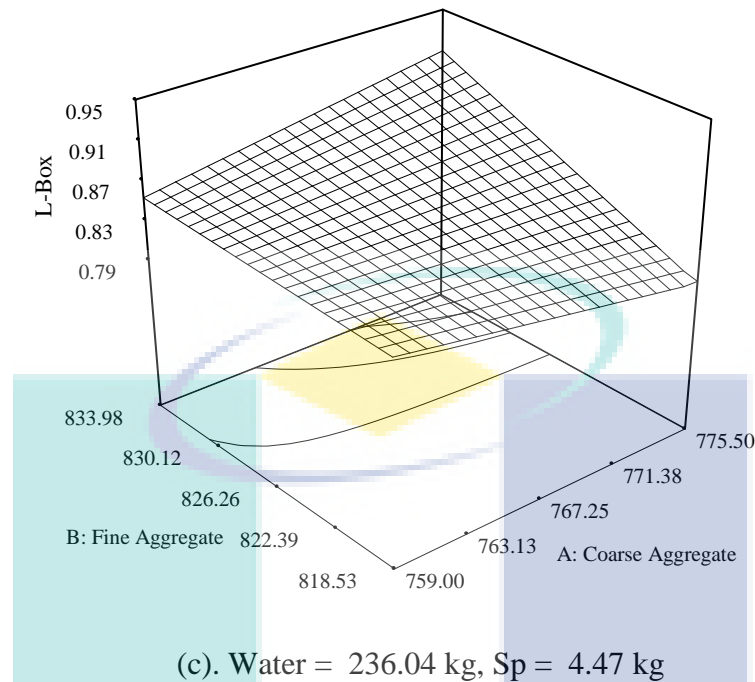
Figure 5.12: Response surface of blocking ratio

v.   Segregation resistance

The example response surface of segregation resistance is shown in Figure 5.13 (a). The segregation resistance decreases with an increase in the content of coarse aggregate and decreases with an increase in fine aggregate. In addition, the contours illustrate that the increase in coarse aggregate necessitates a decrease in fine aggregate to maintain a fixed segregation resistance.

The significant difference in orientation of the response surface in Figures 5.13(a) and 5.13(b) shows the high influence of superplasticizer on segregation resistance. The increasing of 15 per cent in water content causes a decrease of 26 per cent of segregation resistance. The comparison of Figure 5.13(b) and 5.13(c) demonstrates that the water content significantly influences segregation resistance. The segregation resistance decreases as the water content increases. The increase of 1.3 per cent in water content causes a decrease of 3.29 per cent of segregation resistance. Hence, water content is more dominant than superplasticizer content.
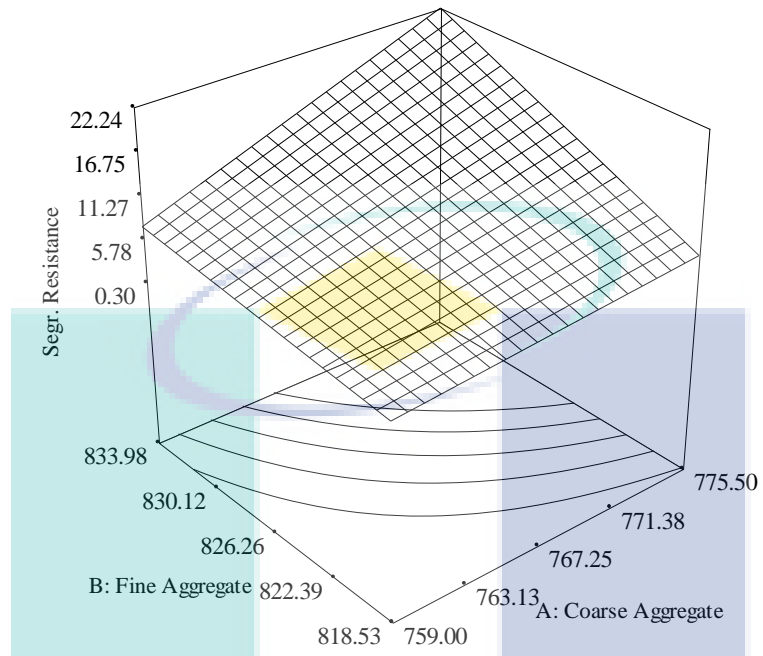
(a) Water= 230.14 Sp = 4.11
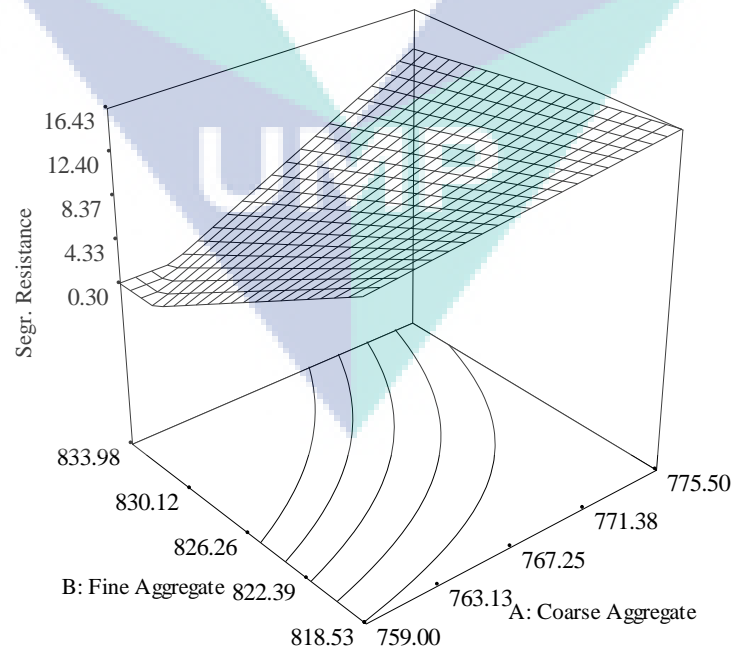
(b). Water= 230.14 Sp = 4.84

Figure 5.13: Response surface of segregation resistance

(c) Water= 233.09 Sp= 4.84
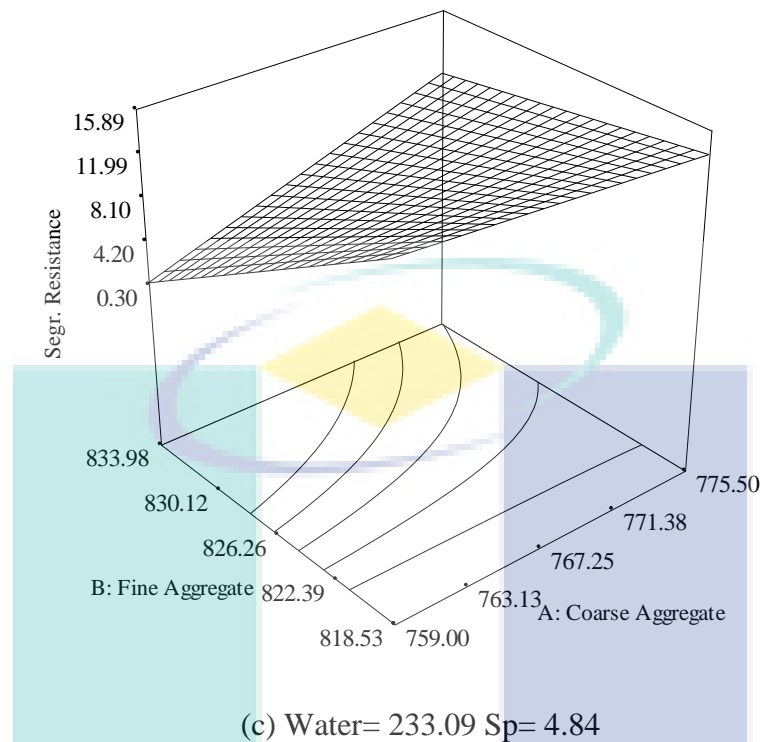
Figure 5.13: Response surface of segregation resistance

In this work, the results of 18 concrete mixes used to investigate the properties of self-compacting concrete are presented. The application of a new superplasticizer generation and powders in high-performance concrete give the opportunity to produce self-compacting concrete that easily reaches compressive strength values of more than 50 MPa. This concrete shows very high workability in the fresh state, and the hardened concrete also shows excellent quality.

This investigation shows that all of the mixtures are suitable for SCC, as they exhibited a satisfactory slump flow within the range of 665 to 740mm, and a flow time in the range of 2.76 to 5.73s. All of the mixtures suitable for SCC exhibited a V-funnel flow time of 15 seconds. The L-box test indicates the concrete's ability to flow through the gaps between the reinforcing bars. The blocking ratio for all suitable SCC mixtures varied from 0.08 to 0.99. GTM screen testing confirmed that a stable SCC should

exhibit a segregation index value lower than 15 per cent. In the present study, all of the SCC suitable mixtures exhibited segregation indices lower than 15 per cent.

5.4.3 Regression Modelling of Hardened Properties

The response function representing hardened properties can be expressed as *y=f(Coarse Aggregate, Fine Aggregate, Cement, Silica fume, Water, Sp)*. The relationship between responses (the compressive, tensile and flexural strength) and mixture constituent is itemise as follows:

(i). Modelling of compressive strength

The compressive strength model equation is as follows:

$$f_c' = +54.87\text{-}0.76 * A\text{-}1.35 * B\text{-}1.08 * C+0.98 * E$$
$$+1.35 * A^2\text{-}1.92 * B^2\text{-}2.61 * D^2+4.73 * E^2+5.24 * F^2$$
$$-5.23 * A * C\text{-}4.32 * B * D\text{-}1.58 * B * E \tag{5.8}$$

with $R^2 = 0.971$

Based on the parameter estimates in the model of Equation 5.8, the following inferences can be made about the different blends used in the experiment:

1. Four single component blends, in order of contribution; sand (B), cement (C), water (E), and coarse (A) contributes to compressive strength.
2. The order of contribution of binary blends regarding compressive strength is coarse-cement (AC), sand-silica fume (BD), sand-superplasticizer (BF). That is, by adding an equal quantity of coarse (A), sand (B), cement (C), silica fume (D), and superplasticizer (F) separately to the same weight of concrete, the compressive strength value is highest for the coarse-cement blend. Thus coarse and cement play the most significant role in increasing the compressive strength of SCC.

Table 5.13: Analysis of variance for Compressive Strength

Source	Sum of Squares	DF	Mean Square	F Value	P-Value	VIF
Model	173.41	9	19.27	15.32	0.0004[a]	
A	19.20	1	19.20	15.27	0.0045[a]	2.62
B	9.44	1	9.44	7.51	0.0254[b]	1.66
F	26.25	1	26.25	20.87	0.0018[a]	3.10
AB	45.14	1	45.14	35.89	0.0003[a]	1.16
AE	33.99	1	33.99	27.02	0.0008[a]	2.19
BD	106.22	1	106.22	84.45	0.0001[a]	1.61
BF	64.15	1	64.15	51.00	0.0001[a]	1.83
CD	43.30	1	43.30	34.43	0.0004[a]	4.32
CE	41.05	1	41.05	32.64	0.0004[a]	1.68
Residual	10.06	8	1.26			
Cor Total	183.47	17				

[a]At least 99% confidence

[b]At least 95% confidence

An ANOVA analysis was selected to investigate the effects of different factors (coarse, sand, cement, silica fume, water and superplasticizer) and their interaction on the compressive strength of SCC. Table 5.13 summarises the ANOVA results for compressive strength. Note that the main effects due to the content of coarse (A), sand (B), cement (C), and water (E) are statistically significant (P-value $< 5\%$). Nonetheless, the principal effect due to silica fume (D) and superplasticizer (F) is not significant.

In the second-order interactions, coarse-cement (AC), sand-silica fume (BD) and sand-water content (BE) are significant. The second-order quadratic, sand (B), silica fume (D), water and superplasticizer are significant, but not in the term quadratic of coarse aggregate (P-value > 5%).

Table 5.14: Analysis of variance for Tensile Strength

Source	Sum of Squares	DF	Mean Square	F Value	P-Value	VIF
Model	21.45	8	2.68	9.87	0.0012	
D	8.36	1	8.36	30.76	0.0004[a]	2.58
E	7.32	1	7.32	26.93	0.0006[a]	1.57
AB	4.13	1	4.13	15.21	0.0036[a]	1.82
AC	2.59	1	2.59	9.52	0.0130[b]	2.07
AD	3.28	1	3.28	12.06	0.0070[a]	1.36
AE	4.98	1	4.98	18.31	0.0021[a]	1.32
BC	6.53	1	6.53	24.04	0.0008[a]	1.74
BE	1.83	1	1.83	6.72	0.0291[b]	1.77
Residual	2.45	9	0.27			
Cor Total	23.90	17				

[a]At least 99% confidence

[b]At least 95% confidence

(ii). Modelling of tensile strength

For the tensile strength model the equation is:

$$f_t = +12.99 + 1.34*D + 0.98*E + 0.97*A*B + 0.82*A*C$$
$$- 0.75*A*D + 0.91*A*E + 1.19*B*C - 0.64*B*E$$

$$\text{(5.9.)}$$

with $R^2 = 0.898$

The model for tensile strength of SCC is given in Equation 5.9. Adequacy of the models was also checked by examining the coefficient of determination (R^2). The R^2 value of the proposed model for slump flow was 0.898. The analysis of variance of tensile strength model is summarized in Table 5.14. Based on the P-values shown in this table, it is concluded that silica fume (*D*) and water (*E*) are statistically significant, as is the interaction of coarse-fine aggregate (AB), coarse-cement (AC), coarse-silica fume (AD), coarse-water (AE), sand-cement (BC), and cement-water (CE).

(iii). Modelling of flexural strength

For the flexural strength model the equation is given as:

$$f_f = +4.49 + 0.15 * C - 0.30 * E + 0.51 * E^2$$
$$+ 0.18 * F^2 - 0.21 * A * C - 0.12 * A * E + 0.27 * A * F$$
$$+ 0.16 * B * D + 0.17 * B * F - 0.32 * C * F \qquad (5.10.)$$

with $R^2 = 0.926$

The derived model of flexural strength is shown in Equation 5.10. Two single component blends, water (E) and cement (C), contribute to flexural strength. The order of contribution of the binary blends regarding flexural strength is coarse-cement (AC), coarse-water (AE), coarse-superplasticizer (AF), sand-silicafume (BD), sand-superplasticizer (BF) and cement-superplasticizer (CF).

Table 5.15: Analysis of variance for Flexural Strength

Source	Sum of Squares	DF	Mean Square	F Value	P-Value	VIF
Model	2.48	10	0.25	8.72	0.0044	
C	0.20	1	0.20	7.19	0.0315[b]	1.37
E	0.47	1	0.47	16.60	0.0047[a]	2.34
E2	0.74	1	0.74	25.96	0.0014[a]	1.39
F2	0.10	1	0.10	3.37	0.1089[c]	1.32
AC	0.15	1	0.15	5.43	0.0525[c]	2.19
AE	0.08	1	0.08	2.83	0.1362[c]	1.32
AF	0.24	1	0.24	8.55	0.0222[b]	2.36
BD	0.09	1	0.09	3.20	0.1168[c]	2.21
BF	0.15	1	0.15	5.29	0.0550[c]	1.60
CF	0.35	1	0.35	12.32	0.0099[a]	2.36
Residual	0.20	7	0.03			
Cor Total	2.68	17				

[a]At least 99% confidence

[b]At least 95% confidence

Table 5.15 shows that the VIF factor varied from 1.32 to 2.36. This indicates that multicollinearity is not a problem. Overall, some multicollinearity appear to be present, but it is not serious. The variance inflation factor will produce to be less than 4.0, indicating that multicollinearity is not a serious problem.

5.4.4 Response Surface for Hardened Properties

The mathematical models above can be used to predict the concrete strength by substituting the values, in coded form, of the respective factors. The responses calculated from these models for each set of coded strength concrete variables are represented in graphical form in Figures. 5.14 to 5.16.

i. Compressive strength

The response surface of compressive strength is shown in Figure 5.14.(a). The contour illustrates that the compressive strength increases as the amount of aggregate increases. In other words, the increase of coarse aggregate necessitates a decrease of fine aggregate to maintain a fixed compressive strength. A comparison between Figure 5.14(a) and 5.14(b) shows that the highest surface position decreases by 6.95 per cent with an added water content of 1.28 per cent. Figure 5.14(b) and (c) show that the compressive strength decreases by 8.3 per cent when increasing the superplasticizer dosage by 8.88 per cent. Furthermore, water content has a greater effect on compressive strength than superplasticizer.

ii. Tensile strength

Examples of the response surface of tensile strength are shown in Figure 5.15. The effect of interaction between the silica fume-fine aggregate and silica fume-coarse aggregate represent the different orientation of response surface in Figure 5.15(a) and 5.15(b), where the dosages of cement and silica fume are variable, the superplasticizer is fixed at 4.47 kg and the proportion of cement and silica fume are 538.29-545.99 kg and 43.44-45.20 kg, respectively. The influence of silica fume on tensile strength can be

observed in Figures 5.15 (b) and (c). From those figures, the influence of silica fume on tensile strength is lower than the effect of extra cement on concrete. Furthermore, the cement content is more dominant than the silica fume content on tensile strength
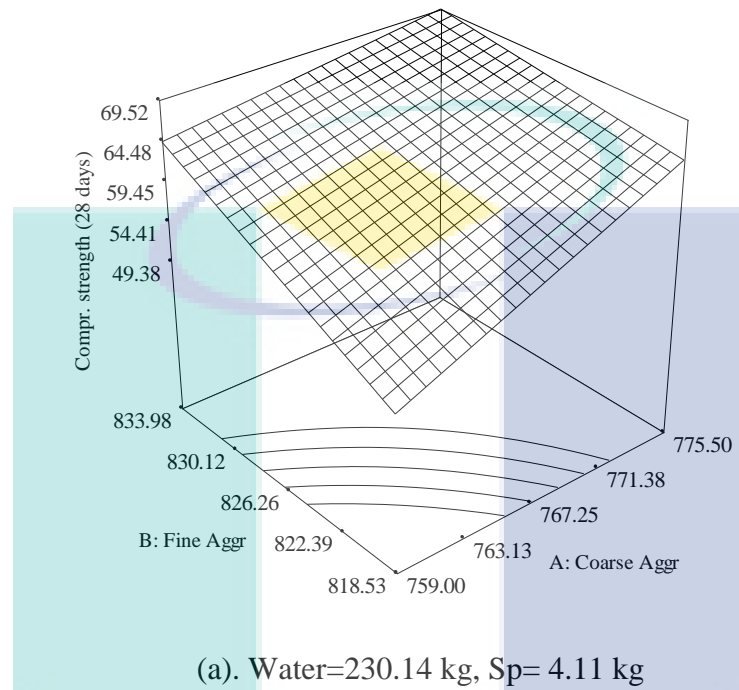
(a). Water=230.14 kg, Sp= 4.11 kg

Figure 5.14: Response surface of compressive strength

(b). Water=233.09 kg, Sp= 4.11 kg
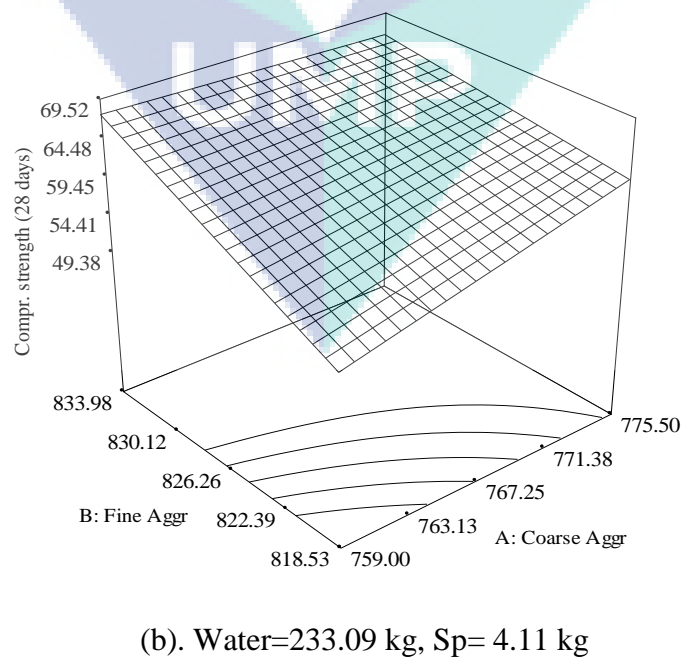
Figure 5.14: Response surface of compressive strength
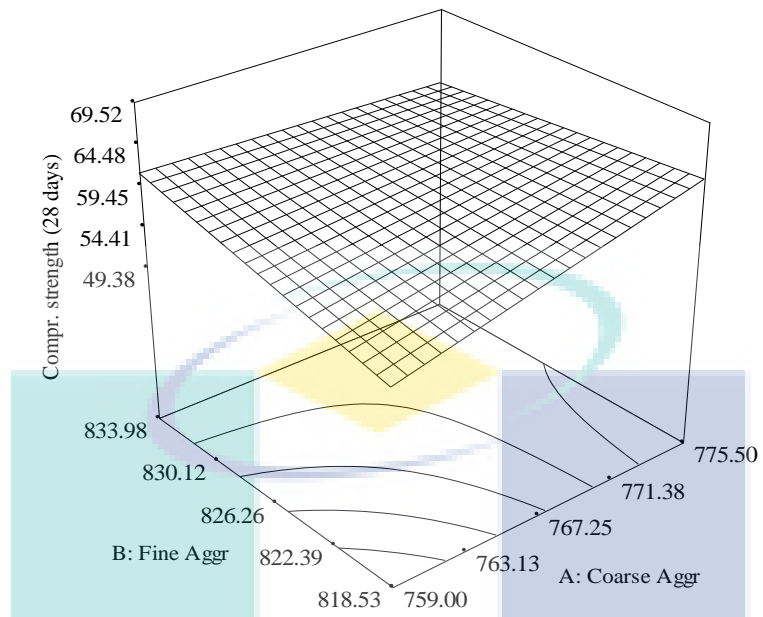
(c). Water=233.09 kg, Sp= 4.47 kg

Figure 5.14: Response surface of compressive strength
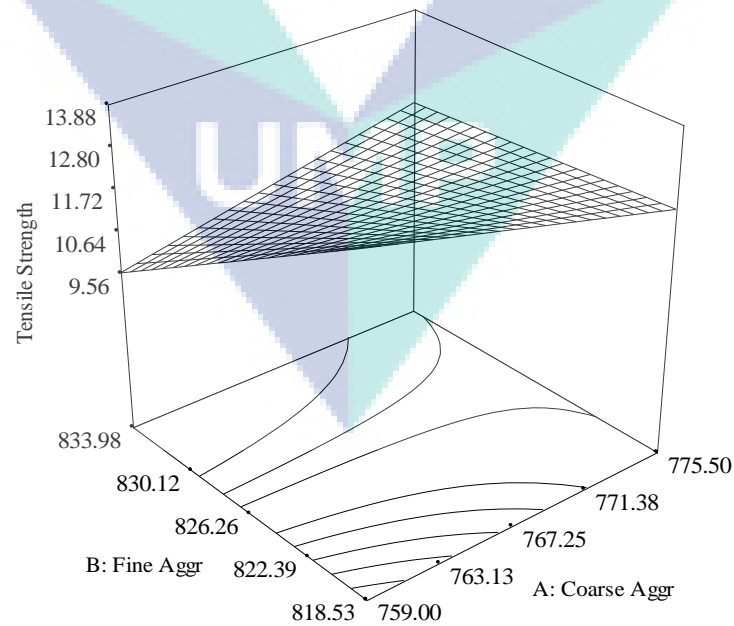
(a). Cement =538.29 kg, SF = 43.44 kg

Figure 5.15: Response surface of tensile strength
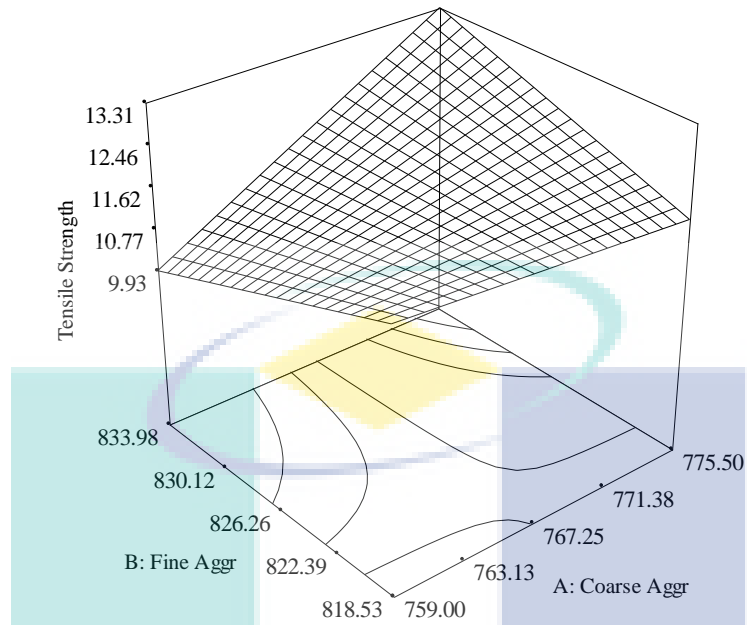
(b). Cement = 545.99 kg, SF = 43.44 kg

Figure 5.15: Response surface of tensile strength
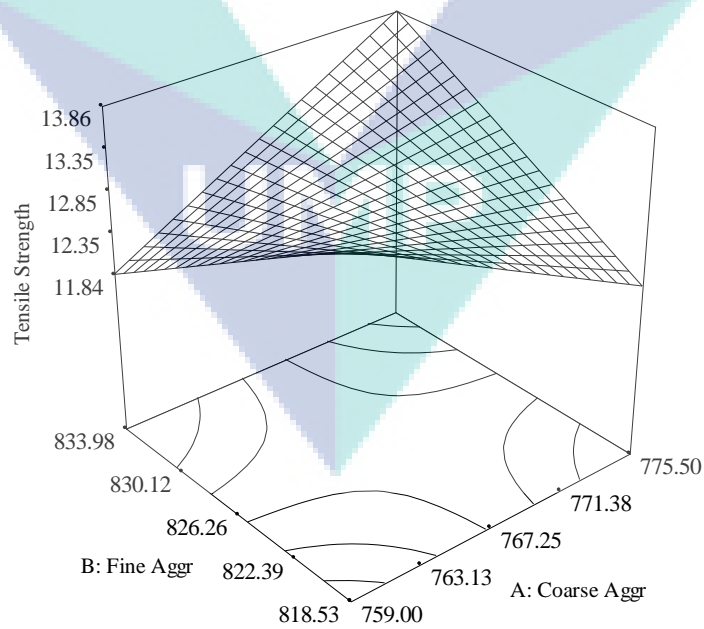
(c). Cement = 545.99 kg, SF= 45.20 kg

Figure 5.15: Response surface of tensile strength

iii.   Flexural strength

The response surface of flexural strength is shown in Figure 5.16. The same orientation and shape of the response surface in Figures 5.16(a) and (b) shows that silica fume has no effect on flexural strength. Nevertheless, the significant difference of orientation of the response surface in Figures 5.16 (b) and (c) indicates the high influence of cement content on flexural strength.

(a). Cement = 538.29 kg, SF = 43.44 kg
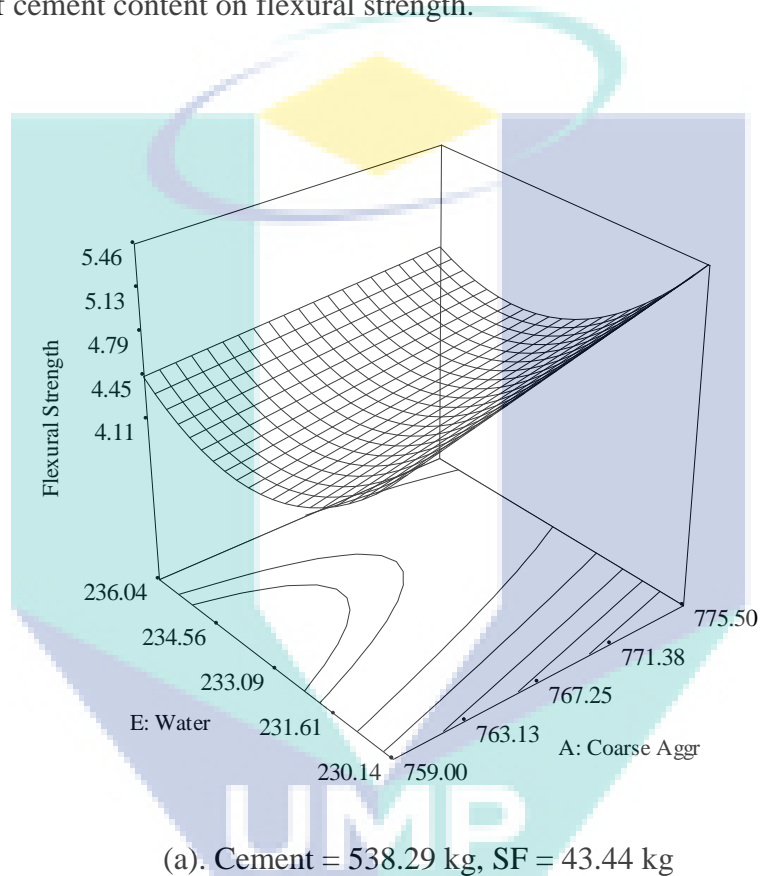
Figure 5.16: Response surface of flexural strength
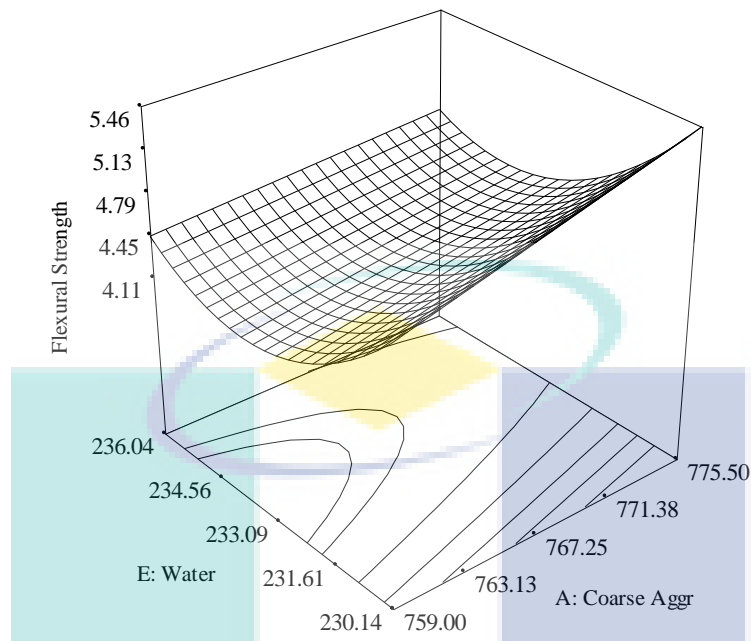
(b). Cement = 538.29 kg, SF = 47.26 kg

Figure 5.16: Response surface of flexural strength
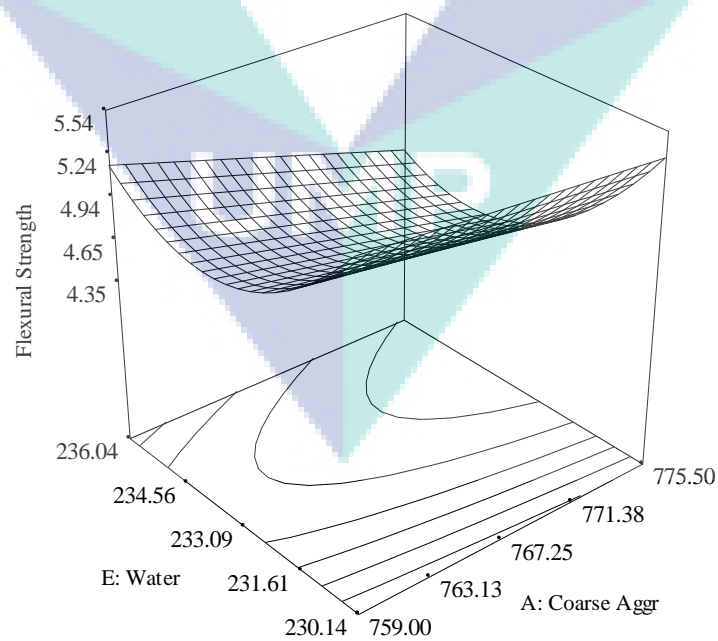
(c). Cement = 554.11 kg, SF= 47.26 kg

Figure 5.16: Response surface of flexural strength

5.5   ENHANCED MODELLING OF SCC

In this research, enhanced modelling, Smooth Supprt Vector Regression (SSVR) is used to model the fresh properties and hardened properties. To implement the SSVR model, SSVR-Matlab (Lee, et.al. 2005) is applied.

To assess the utility of the SSVR based modelling approach for predicting the properties of self-compacting concrete, eighteen data sets taken from laboratory experiments were used. To predict the material properties of SCC, coarse aggregate, fine aggregate, cement, silica fume, water, and superplasticizer were used as input parameters, whereas four responses were used as output for the fresh stage (slump flow, flow time, V-funnel, L-box and segregation resistance) and three responses (compressive, tensile, and flexural strength) for the hardened properties.

The first step to implement the SSVR is choosing the optimal parameter. Parameter selection is one of the important steps in SSVR to improve the performance of the model. Three parameters must be tuned in this parameter selection: the penalty of estimation error (C), the value of ε-Insensitive (ε) and the RBF parameter (γ). The Taguchi design approach is applied to select the optimal parameter (see Chapter 3). The obtained optimal parameters are C= 30, $\varepsilon = 0,01$ and $\gamma = 6$. These values are used to predict both the fresh and hardened properties. The results of SSVR prediction are described as follows.

The actual and predicted values of other fresh properties (flow time, blocking ratio, V-funnel and segregation resistance) and hardened properties (compressive strength, splitting strength, flexural strength) are presented in Table 5.16 to 5.22. Two performance evaluations are used to evaluate the SSVR method. The coefficient of determination (R^2) and mean square error (*MSE*). All properties show a high R^2 value and a very low *MSE*.

Table 5.16: Actual and predicted values for slump flow

Exp No	Actual slump flow (mm)	Predicted slump flow (mm)
1	665	665.20
2	720	718.41
3	740	737.76
4	690	689.37
5	710	708.73
6	737.5	735.34
7	680	679.70
8	700	699.05
9	695	694.21
10	720	718.41
11	735	732.92
12	740	737.76
13	710	708.73
14	705	703.89
15	720	718.41
16	717.5	715.99
17	695	694.21
18	690	689.37
	R^2	0.9954
	MSE	2.0217

Table 5.17: Actual and predicted values of flow time

Exp No	Actual Flow time (second)	Predicted Flow time (second)
1	4.95	4.91
2	3.81	3.83
3	2.9	2.95
4	5.28	5.23
5	3.31	3.34
6	3.54	3.56
7	5.2	5.15
8	5.48	5.42
9	4.23	4.21
10	3.84	3.85
11	3.09	3.13
12	3.09	3.13
13	5.07	5.03
14	5.1	5.05
15	2.76	2.81
16	4.32	4.30
17	4.38	4.36
18	5.73	5.66
	R^2	0.9982
	MSE	0.0016

Table 5.18: Actual and predicted values of Blocking Ratio

Exp No	Actual Blocking Ratio	Predicted Blocking Ratio
1	0.99	0.98
2	0.87	0.86
3	0.84	0.84
4	0.92	0.91
5	0.87	0.86
6	0.88	0.87
7	0.80	0.81
8	0.89	0.88
9	0.83	0.84
10	0.90	0.89
11	0.91	0.90
12	0.98	0.97
13	0.90	0.89
14	0.91	0.90
15	0.86	0.85
16	0.89	0.88
17	0.87	0.86
18	0.98	0.97
	R^2	0.9468
	MSE	0.000131

Table 5.19: Actual and predicted values of V-funnel

Exp No	Actual V-funnel (second)	Predicted V-funnel (second)
1	11.78	11.74
2	10.52	10.54
3	12.09	12.04
4	8.69	8.77
5	9.54	9.59
6	11.73	11.69
7	11.65	11.61
8	12.62	12.55
9	11.41	11.38
10	12.06	12.01
11	9.09	9.16
12	9.42	9.47
13	12.75	12.68
14	12.65	12.58
15	13.75	13.65
16	9.37	9.43
17	12.91	12.83
18	13.84	13.73
	R^2	0.9984
	MSE	0.0041

Table 5.20: Actual and predicted values of Segregation Resistance

Exp No	Actual Segregation Resistance %	Predicted Segregation Resistance %
1	0.12	0.11
2	0.09	0.09
3	0.05	0.06
4	0.14	0.13
5	0.07	0.08
6	0.08	0.09
7	0.14	0.13
8	0.14	0.13
9	0.09	0.09
10	0.09	0.09
11	0.07	0.08
12	0.06	0.07
13	0.14	0.13
14	0.13	0.12
15	0.05	0.06
16	0.09	0.09
17	0.10	0.09
18	0.15	0.14
	R^2	0.9145
	MSE	0.000092194

Table 5.21: Actual and predicted values of Compressive Strength

Exp No	Actual Compressive Strength (MPa)	Predicted Compressive Strength (MPa)
1	52.65	52.77
2	56.3	56.29
3	60.1	59.96
4	60.2	60.06
5	62.2	62.00
6	56.94	56.91
7	55.35	55.39
8	57.75	57.69
9	56.5	56.48
10	62.4	62.19
11	61.45	61.27
12	64.9	64.61
13	63.45	63.21
14	57.8	57.74
15	57.45	57.40
16	61.35	61.17
17	63.35	63.11
18	59.05	58.95
	R^2	0.9977
	MSE	0.0239

Table 5.22: Actual and predicted values of Splitting Strength

Exp No	Actual Splitting Strength (MPa)	Predicted Splitting Strength (MPa)
1	13.22	13.18
2	14.23	14.16
3	13.77	13.71
4	13.94	13.88
5	15.12	15.02
6	12.45	12.44
7	14.39	14.31
8	11.845	11.87
9	12.435	12.43
10	14.105	14.04
11	11.81	11.84
12	12.055	12.08
13	12.96	12.93
14	11.475	11.52
15	11.825	11.85
16	14.13	14.06
17	11.01	11.06
18	13.08	13.04
	R^2	0.998
	MSE	0.0027

Table 5.23: Actual and predicted values of Flexural Strength

Exp No	Actual Flexural Strength (MPa)	Predicted Flexural Strength (MPa)
1	5.36	5.33
2	4.30	4.32
3	5.04	5.02
4	4.67	4.67
5	4.80	4.79
6	5.18	5.15
7	4.63	4.64
8	5.56	5.52
9	4.13	4.16
10	4.97	4.95
11	4.72	4.71
12	5.49	5.45
13	5.06	5.04
14	5.16	5.13
15	4.66	4.67
16	4.98	4.96
17	5.47	5.43
18	4.82	4.81
	R^2	0.9962
	MSE	0.000558

5.5.1 Comparison Results of Regression Modelling and SSVR

The predicted values achieved through the proposed statistical second-order regression and SSVR formulations are compared with the experimental results for fresh properties (flow time, blocking ratio, V-funnel and segregation resistance) and the hardened properties (compressive strength, splitting strength, flexural strength) are presented in Figure 5.20 to 5.27. It was observed that the proposed SSVR formulation for the modelling properties of SCC closely follows the trend seen in the experimental data.
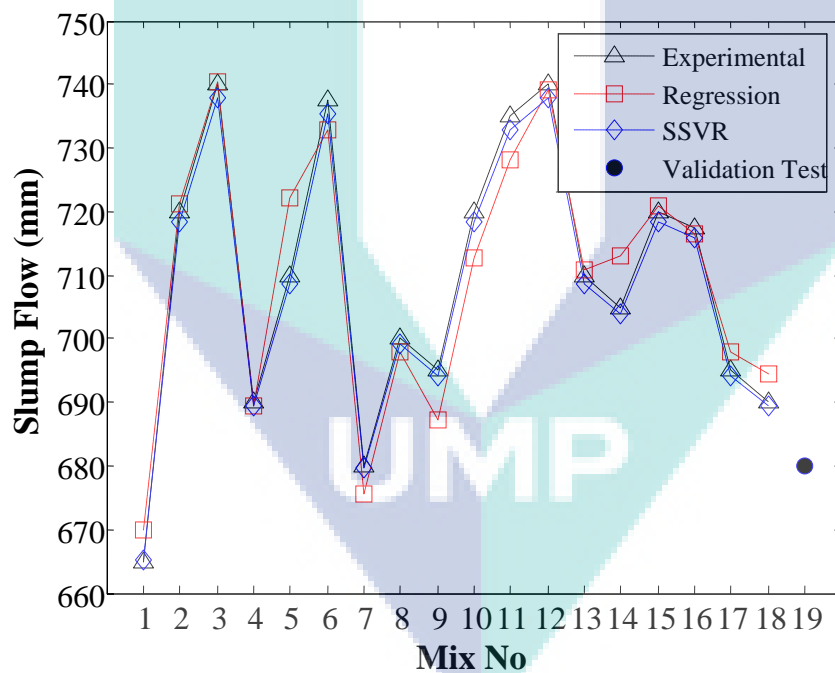
Figure 5.20: Comparison results of slump flow
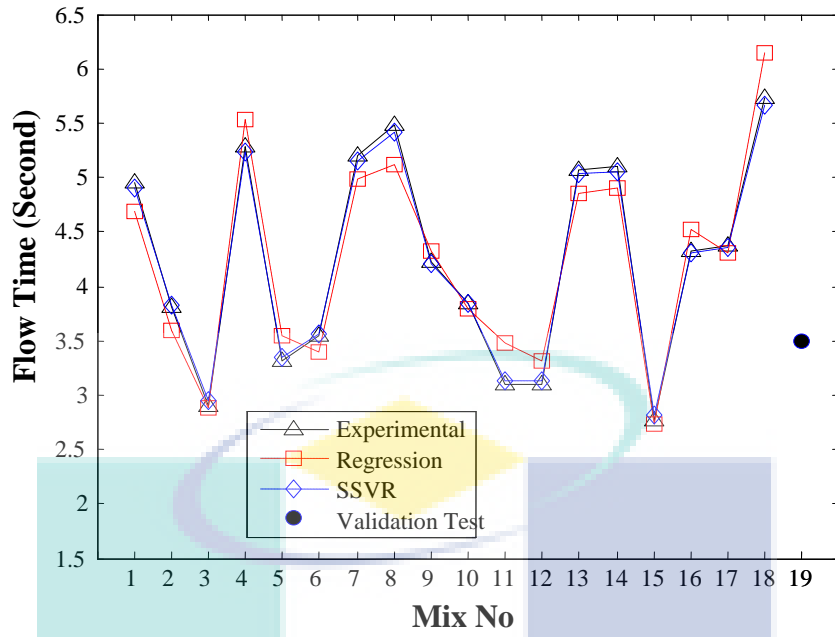
Figure 5.21: Comparison results of flow time
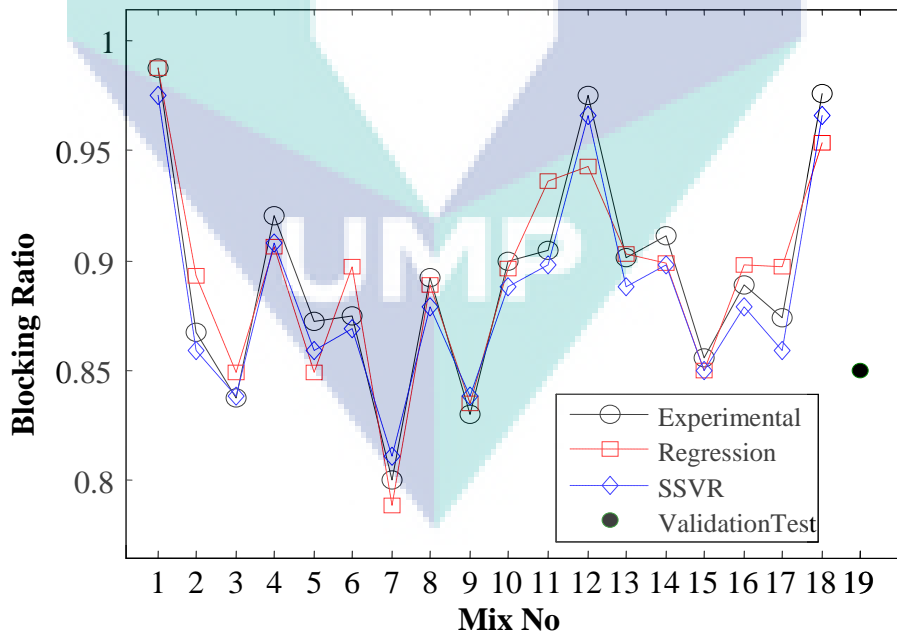
Figure 5.22: Comparison results of blocking ratio
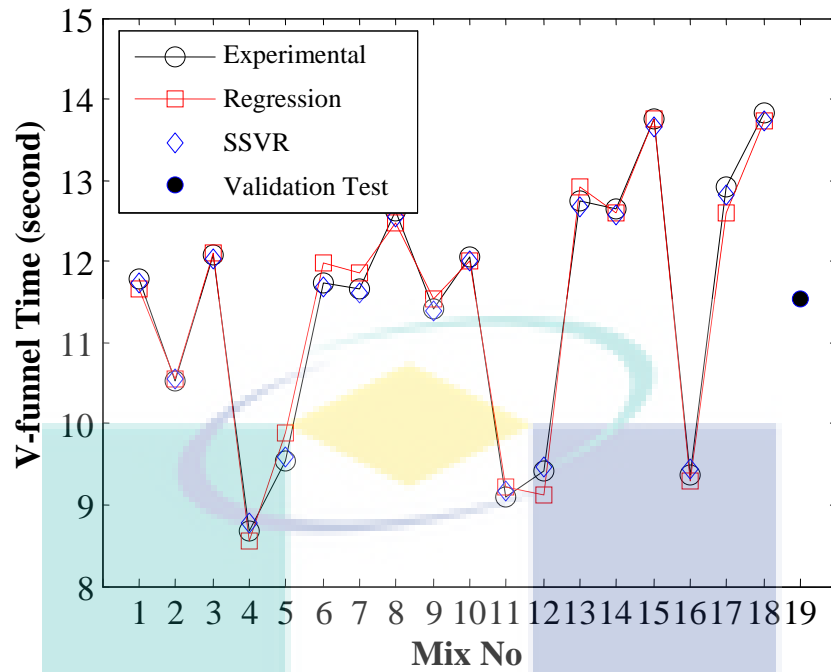
Figure 5.23: Comparison results of V-funnel time
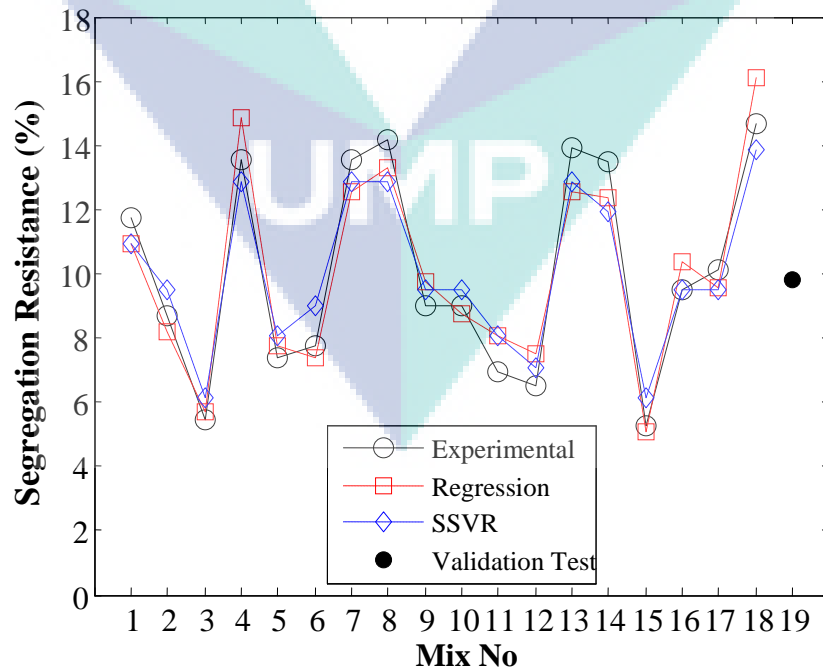
Figure 5.24: Comparison results of segregation resistance
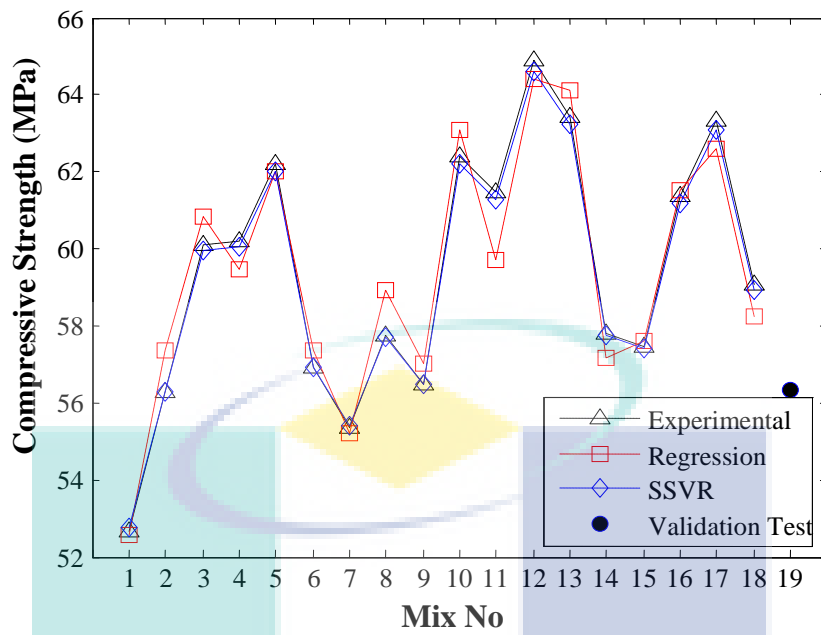
Figure 5.25: Comparison results of compressive strength
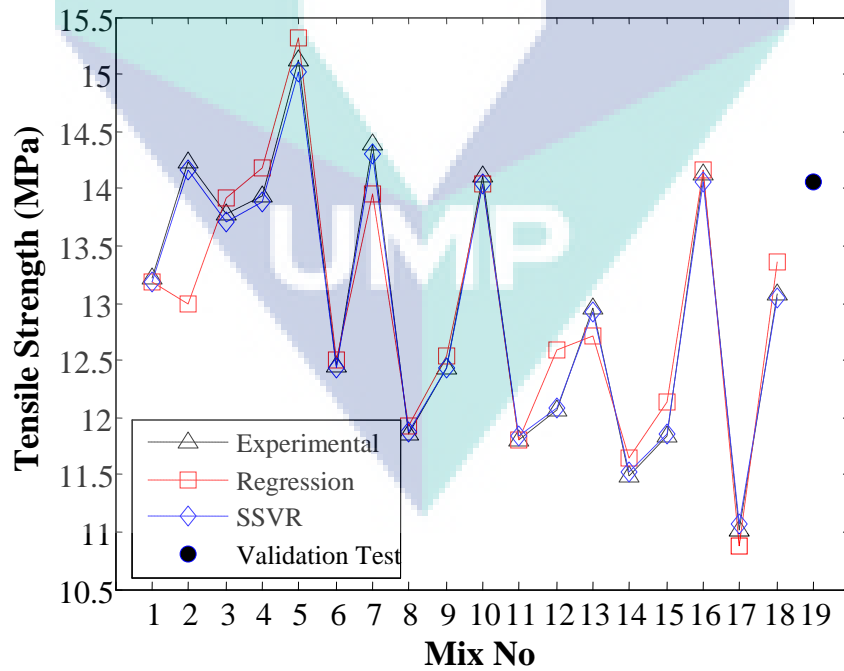
Figure 5.26: Comparison results of tensile strength
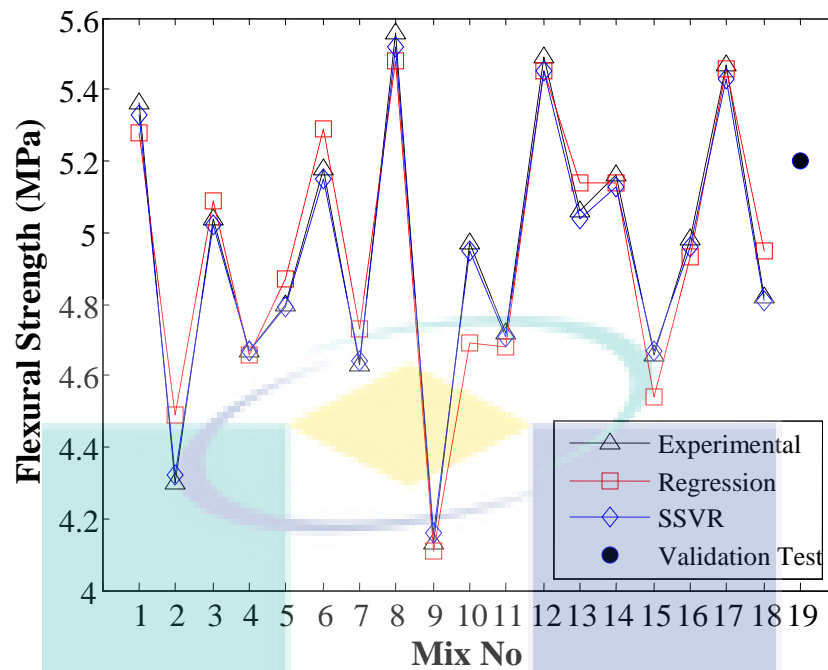
Figure 5.27: Comparison results of flexural strength

A performance summary of the regression and the SSVR formulations is given in Table 5.23 in which R^2 corresponds to the coefficient of correlation between the observed and modelled (predicted) data values; MSE or the mean square error is a frequently-used measure of the differences between values predicted by a model or an estimator and the values actually observed from the object being modelled or estimated. From Table 5.23 it can be concluded that the R^2 value in SSVR is higher than the R^2 value in regression and the MSE values in SSVR are smaller than the MSE values in regression. This means that the SSVR method shows a better performance than the regression method.

The accuracy of each of the proposed models was also determined by comparing the predicted-to-measured values obtained with the eighteen mixtures presented in Figure 5.28 for regression and Figure 5.29 for SSVR. Figure 5.29 shows that most points lie on or are very close to the straight-line with slope 1, this reflects that most of the predicted values are in relatively close agreement with the measured values. The result also illustrate that the SSVR models possess high interpolation ability.

Table 5.24: Performance comparison of regression and SSVR

Model	Regression		SSVR	
	R^2	*MSE*	R^2	*MSE*
Slump flow	0.9386	53.460	0.9954	2.0217
Flow time	0.9393	0.1100	0.9982	0.0016
V-funnel	0.9892	0.0090	0.9984	0.0041
Blocking ratio	0.8723	0.0006	0.9468	0.0001
Segregation Resistance	0.8673	0.0003	0.9145	0.0001
Compr. Strength	0.9712	1.0800	0.9977	0.0239
Tensile strength	0.8983	0.2700	0.9980	0.0027
Flexural strength	0.9351	0.0300	0.9962	0.0001
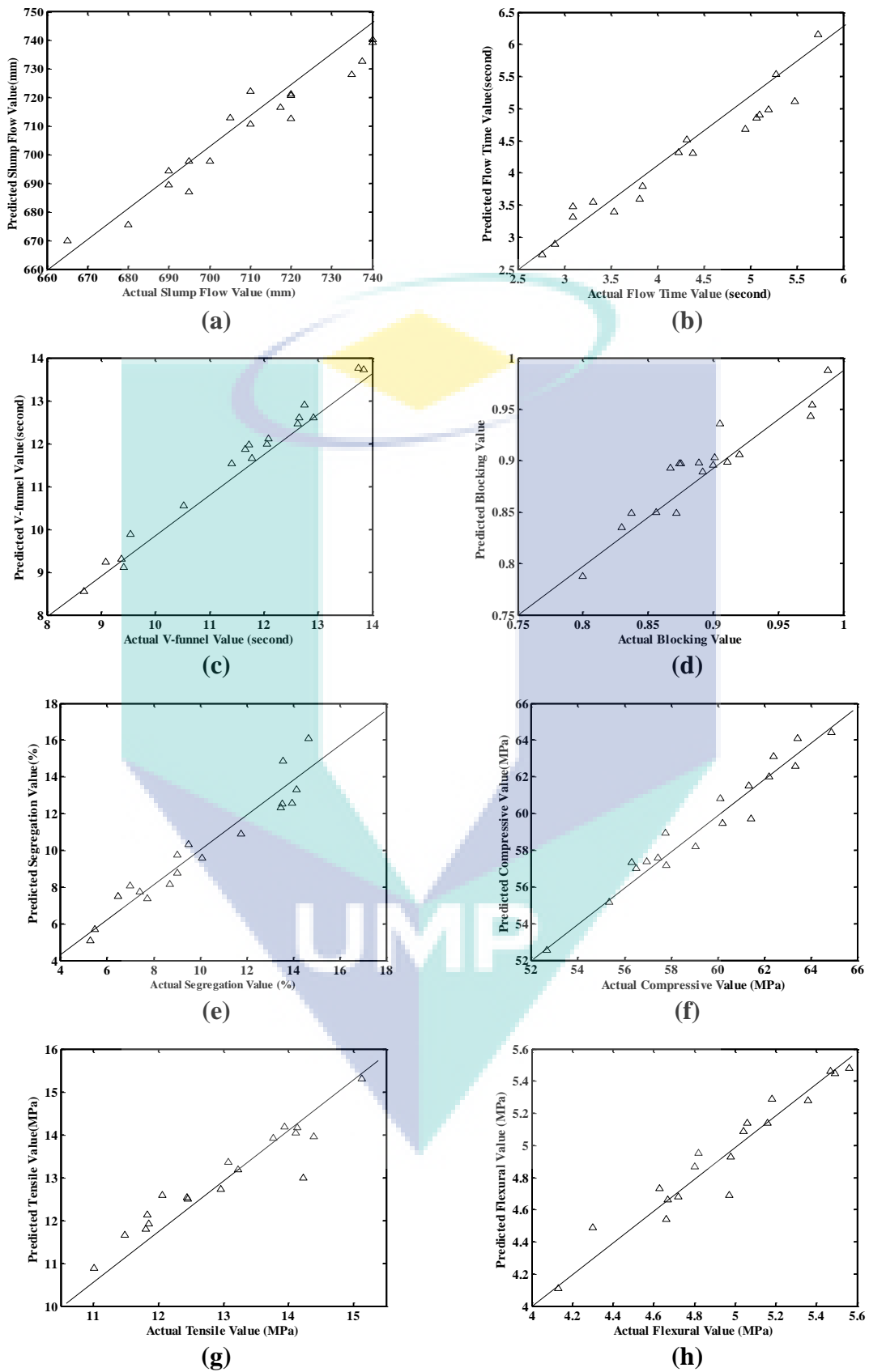
Figure 5.28: Actual-Predicted using Regression
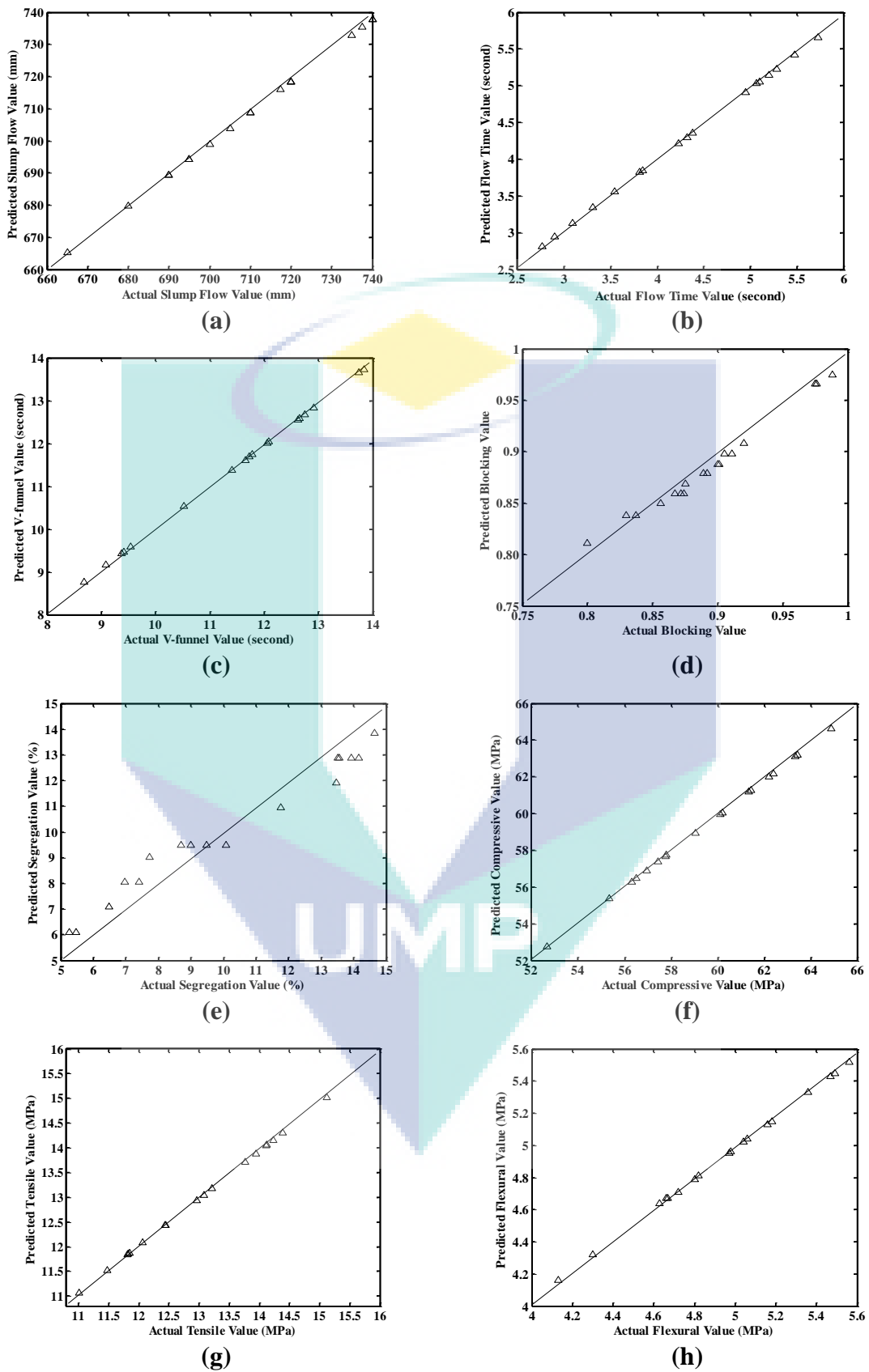
Figure 5.29: Actual-Predicted using SSVR

5.6   VALIDATION OF EXPERIMENTS

To validate the statistical and enhanced model, verification tests were conducted under optimal condition (Table 5.4 and 5.5) which were determined by the Taguchi method. The materials used in this verification tests were identical to those used in the experiment. Type I cement, tap water, crushed gravel, natural sand, silica fume, and naphthalene-sulfonate-based superplasticizer. Table 5.25 presents the verification test results. The table shows the differences between the predicted values by the SSVR and that the results measured from the experiments were small. Hence, the SSVR model is very useful for predicting the SCC properties.

Table 5.25: Validation test results

Concrete Property	Prediction		Observed Values
	Second order	SSVR	
Slump flow (mm)	706.24	690	680
Flow time (second)	3.56	3.52	3.5
L-box ratio	0.934	0.87	0.85
V-funnel time (second)	9.064	10.98	11.54
Segregation Resistance (%)	7.73	9.5	9.8
Compressive strength (MPa)	61.25	58.50	56.34
Splitting strength (MPa)	13.3	14.15	14.05
Flexural strength (MPa)	5.48	5.35	5.20

This work presents a promising smooth support vector regression (SSVR) technique for predictions of self-compacting concrete. The performance of the proposed method is verified by comparing the predicted levels with the actual values. However, the estimated results by SSVR produce remarkably fewer estimation errors compared to those of regression. From the results it can be concluded that the SSVR method can predict the properties of SCC with higher estimation accuracy. It is expected that the prediction of slump flow by the SSVR method will also play an important role in future slump flow level predictions. Moreover, field engineers can utilise the SSVR method, it

does not require any procedure to determine the explicit form, unlike the regression analysis techniques.

5.7. CRITICAL ANALYSIS

5.7.1. Effect of Mix Proportioning on Workabilty

Several factors influence the design of a structural element of SCC. As previously mentioned, many factors affect the mix design and should be considered; therefore, a cause-effect diagram, also known as an ''Ishikawa Diagram'', was used in this study to identify the main factors, as shown in Figure 5.30.
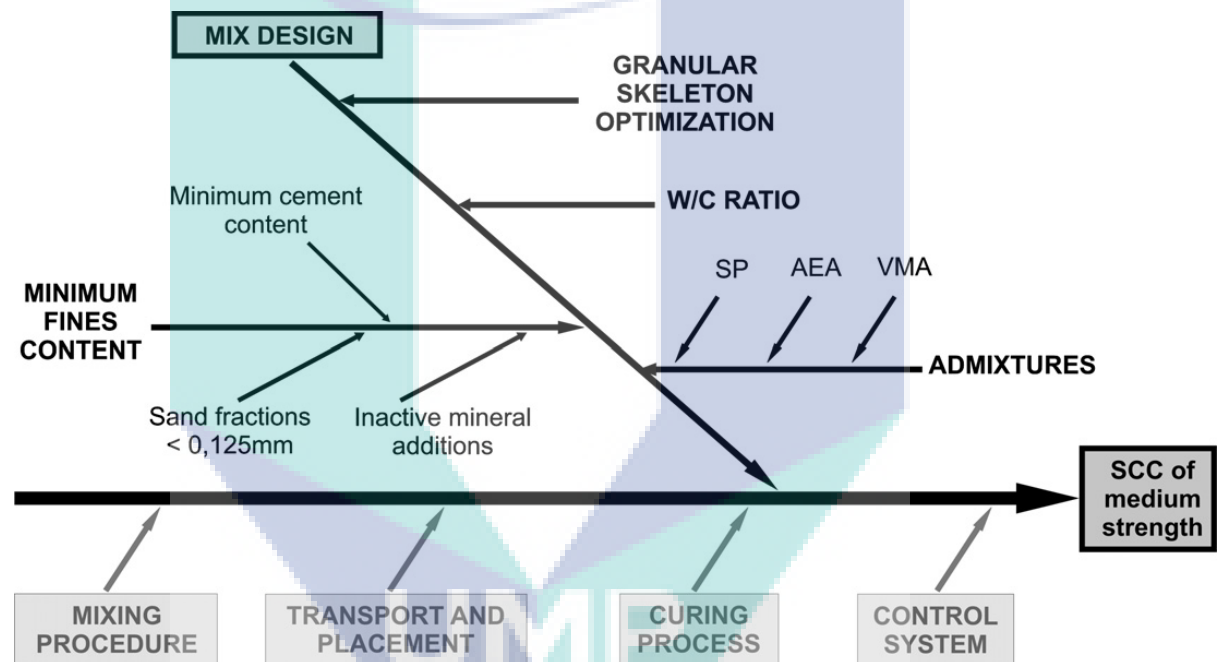
Figure 5.30: Ishikawa Diagram of SCC.

Cementitious Materials

The inclusion of cementitious materials (CMs) in the proportioning of SCC mixes is recommended not only to reduce the greater heat of hydration produced by the large amount of cementitious material incorporated in this type of concrete, but also to increase the workability of fresh concrete (Sonebi and Bartos, 2001). The mix design, which did not incorporate any SCM, showed a poor workability and an overall inferior performance. Furthermore, the inclusion of SCMs in the mix design of the SCC

improves the durability properties of the concrete, including the resistance to chloride permeability (Westerholm et al., 2002).

Aggregates

The size and gradation of the aggregates were considered the most important factors affecting the performance of the SCC mixes. Hence, not only the individual gradation of each aggregate, but also the combined gradation of both coarse and fine aggregates should be taken into account when designing a workable SCC mix.

The mixes with the best performance showed a lower percentage of stones retained on large size sieves than those mixes with a poor performance. This was intuitive: the larger the size of the stone used, the greater the blockage potential of the mix when flowing through congested reinforcement. These results confirmed Ramage et al.'s (2006) studies, which had proposed SCC mixes with blended aggregates because they performed the best in fresh state testing.

Chemical Admixes

All superplasticizer agents used proved to effectively reduce the yield stress of the concrete paste. However, the effectiveness of a given dosage rate in producing self compacting abilities in a mix was completely dependent on the type of superplasticizer and the specific proportioning of the mix, including w/cm and aggregate gradation. Based on the response surface model the flow time decreases as the dosage of superplasticizer increases. This is consistent with the finding by Faroug, et.al (1999).

5.7.1. Interrelationship of fresh properties

The results from the slump flow, L-box, V-funnel, and flow time tests are shown in Figures. 5.31 and 5.32. In Figure 5.31, the dashed line denotes the critical value of h_2/h_1 suggested by EFNARC, and the domain of $h_2/h_1 > 0.8$ is called the self-flow zone. Figure 5.30 shows that all of the mixtures satisfy the workability requirement for SCC based on the L-box and flow time tests.

In Figure 5.32, the domain surrounded by $8 \leq Tv \leq 14s$ and $650 \leq$ Slump Flow ≤ 800 mm is called the self-flow zone. Figure 5.31 reveals that all of the mixtures also satisfy the workability requirement for SCC based on the V-funnel and slump flow tests.

Therefore, all of the mixtures are of have a high fluidity, deformability, passing ability, and filling ability.
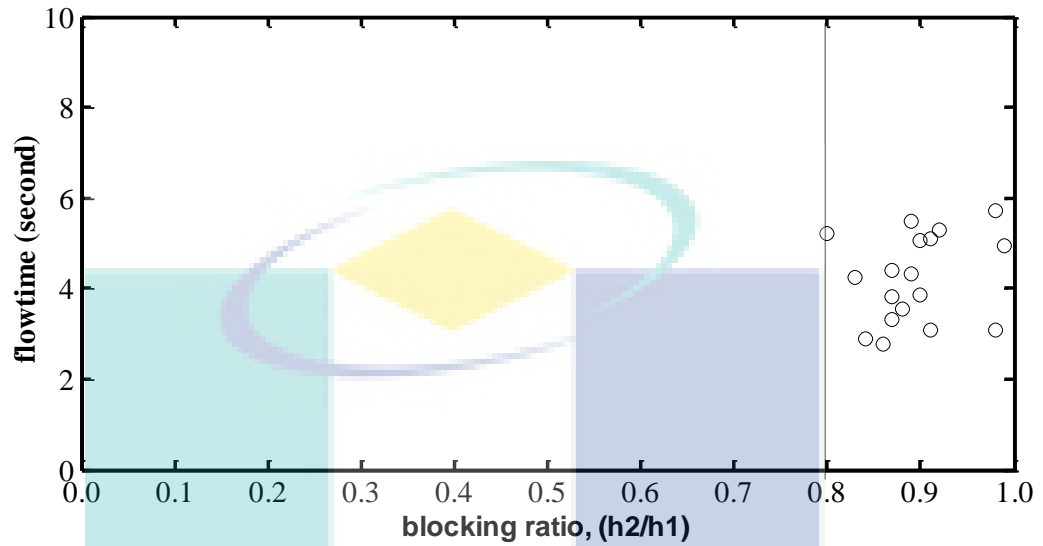
Figure 5.31: Self-flow zone for blocking ratio criteria
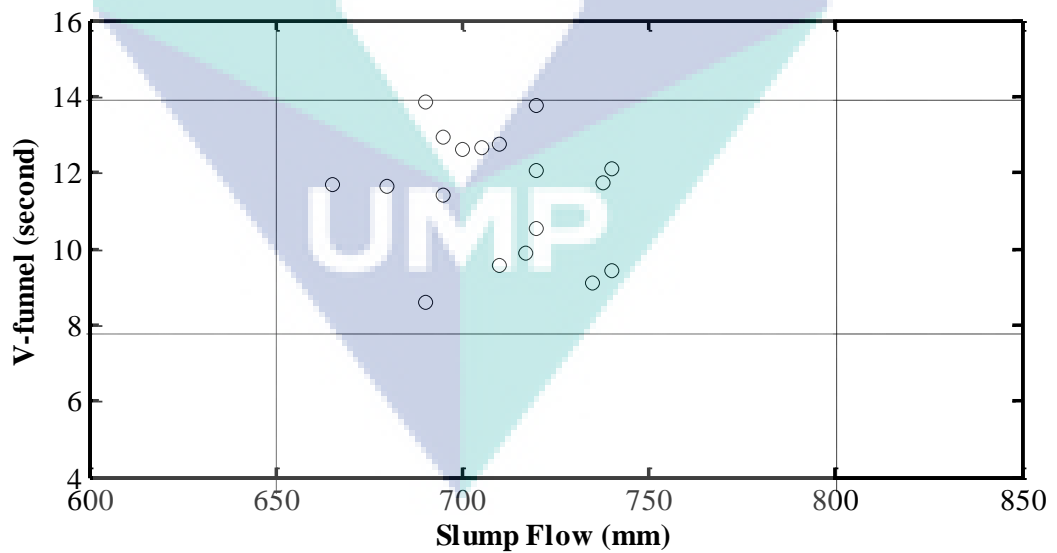
Figure 5.32: Self-flow zone for slump-flow criteria

CHAPTER 6

CONCLUSIONS AND RECOMMENDATIONS

6.1   SUMMARY OF CONCLUSIONS

Self-Compacting Conceret (SCC) consists of many components, including coarse aggregate, fine aggregate, cement, silica fume, water and super plasticizer. Systematic approaches to identify and investigate the optimal mix of the most effective factor on SCC properties under a set of constraints have been used. Taguchi method with L_{18} (3^6) orthogonal array is applied in this work to evaluate the valuable variables and most excellent possible mixture combinations of SCC's properties.

In this study, 18 concrete mixes were evaluated to investigate properties of self-compacting concrete. Six factors, namely; coarse aggregate, fine aggregate, cement, silica fume, water and super plasticizer were used in this study. Four responses for fresh stage (flow time, slump flow, L-box, V-funnel, and segregation resistance) and three responses (compressive, tensile, and flexural strength) for hardened properties were evaluated.

Initially, experimental design method based on the Taguchi approach was implemented to obtain a concrete mixture in accordance with the criteria of SCC fresh concrete on the slump diameter, flow time, V-funnel time, L-Bock ratio and resistance to segregation. Then, the response surface based on optimization technique was applied to obtain three-dimensional graphical visualization variables in response to input variables. Finally, new method of prediction based on Smooth Support Vector Regression (SSVR) was introduced to resolve the properties modelling of self-compacting concrete (SCC).

6.2   DETAILS OF CONCLUSIONS

Based on the results of this study, the following main conclusions are figured out:

1. Mix design on the SCC was very different from the mix design used for normal concrete. Mix design on the SCC should consider two conflicting natures of the concrete flow ability, and at the same time keep up the concrete compressive strength. In this study, the procedure underlying Nan Su Mix design method was used with the application of efficiency factor. The alternative mix design for SCC is proposed. The mix design is called Modified Nan Su Mix design for SCC.

2. Taguchi method could be used to optimize the proportion of SCC mixtures to get the properties of fresh and hardened concrete. Taguchi method was so simple that it reduced the number of experiments and gave the optimal mix design proportions for fresh properties as shown in Table 5.4 for hardened properties in Table 5.5.

3. SCC was an extremely complex material made modelling a tricky task. This study was aimed at demonstrating possibilities of regression analysis and SSVR to predict the properties of SCC. The performance of the proposed method was evaluated using coefficient of determination (R^2) and mean square error (MSE). The model is called good performance if it has maximum R^2 and minimum MSE. The performance of the proposed method was also verified by comparing the predicted levels with actual values. Based on the findings of this study the following conclusion may be drawn:

   - All the R^2 values in all the properties of SCC (flow time, slump flow, V-funnel time, blocking ratio, segregation resistance, compressive strength, Tensile strength, and flexural strength) with SSVR approach had greater value when compared with conventional approaches. Mean Square error (MSE) of SSVR was also much less than that of regression. Therefore, the modelling of SCC properties based on SSVR was much better than that on the conventional analysis.

- Figure 5.29 shows that the majority of the points with actual results with SSVR scattered around a straight line with slope 1. This illustrates that the modelling results using SSVR are close to the value of the experimental results or the actual value.

6.3. RECOMMENDATIONS

The findings of the present study have shown the accuracy of the model; however, further works need to be carried out to improve some of the followings:

1. SCC mixture employing local available material used in this work was developed in laboratory; however, it would be better if the laboratory conclusions are again validated by performing the effect of type and shape of coarse aggregate of the SCC properties.

2. Despite using of silica fume as a cementitious material to gain appropriate strength. a systematic analysis of SCC mixture containing combination of cementitious material should have better understanding about its effect towards SCC properties, such as; fly ash, ground granulated blast slag, limestone powder.

3. SCC was developed using Ordinary Portland Cement (OPC) resulted in a moderate strength (50-60 MPa), yet other types of cement, such as rapid hardening cement can be evaluated in order that the SCC can be submitted in underwater concrete.

.4. Further tests should be completed to examine fresh properties, such as U-box, J-ring, Fill-box, Orimet,as well as hardened properties such like modulus of elasticity, bonding strength, drying shrinkage, and durability of concrete.

REFERENCES

Aitcin, P.C., 1998. "High Performance Concrete", E & FN Spon, London, 597p

Antony, J., Warwood, S., Fernandes, K., and Rowlands, H., 2001. Process Optimisation using Taguchi Methods of Experimental Design, Work Study, Vol. 50, No. 2, pp. 51-57

Assaad, J. J., and Khayat, K. H., 2006. "Effect of Mixture Consistency on Formwork Pressure Exerted by Highly Flowable Concrete", Journal of Materials in Civil Engineering, Vol. 18, No. 6.

Assaad, J.J., and Khayat, K.H., 2006. "Effect of Viscosity-Enhancing Admixtures on Formwork Pressure and Thixotropy of Self-Consolidating Concrete", ACI Materials Journal, Vol. 103, No. 4

Assie, S., Escadeillas, G., and Waller, V., 2006. "Estimates of self-compacting concrete 'potential' durability", Construction and Building Materials

Audenaert, K., Boel, V., and Schutter, G.D.,2002. "Carbonation of self compacting concrete", 6th International Symposium on High Strength/High Performance Concrete. Leipzig, pp. 853-862

Aydin, A.C., 2007. "Self compactability of high volume hybrid fiber reinforced concrete", Construction and Building Materials (21). pp. 1149–1154

Babu, K.G., and Prakahs, P.V.S., (1995). Efficiency of Silica Fume in Concrete, Cement and Concrete Research, 25 (6), pp. 1273-1283

Barros, J., Pereira, E., and Santos, S., 2007. "Lightweight Panels of Steel Fiber-Reinforced Self-Compacting Concrete", Journal of Materials in Civil Engineering, ASCE.

Bassuoni, M.T., and Nehdi M.L. (2009). Durability of self-consolidating concrete to sulfate attack under combined cyclic environments and flexural loading. Cement and Concrete Research (39), pp. 206–226

Bassuoni, M.T., and Nehdi, M.L., 2007. "Resistance of self-consolidating concrete to sulfuric acid attack with consecutive pH reduction", Cement and Concrete Research (37), pp. 1070–1084

Bayramov, F.,Tasdemir, C. and Tasdemir, M.A. (2004). Optimisation of steel fibre reinforced concretes by means of statistical response surface method, *Cement & Concrete Composites* (26): pp. 665–675

Bouzoubaa, N., and Lachemi, M., 2001. "Self compacting concrete incorporating high volumes of class F fly ash: preliminary results", Cement and Concrete Research (31), pp. 413-420

Brouwers H J H., and Radix H J., (2005), "Self-compacting concrete: Theoretical and experimental study", Cement and Concrete Research, Vol. 35, pp.2116-2136

Castel, A., Vidal, T., Viriyametanont, K., and Francois, R., 2006. "Effect of Reinforcing Bar Orientation and Location on Bondwith Self-Consolidating Concrete", ACI Structural Journal, V. 103, No. 4.

Chen, B.T., Chang, T.P., Shih, J.Y., and Wang, J.J. (2009). Estimation of exposed temperature for fire-damaged concrete using support vector machine. *Computational Materials Science* (44) pp. 913–920

Choi, Y.W., Kim, Y.J., Shin, H.C., and Moon, H.Y., 2006. "An experimental research on the fluidity and mechanical properties of high-strength lightweight self-compacting concrete", Cement and Concrete Research (36) 1595– 1602

Cunha, V.M.C.F., Barros, J.A.O., and Cruz, J.S., 2007. "Modelling the influence of age of steel fibre reinforced self-compacting concrete on its compressive behaviour", Materials and Structures, RILEM

Dehn, F., Holschemacher, K., and Weibe, D., 2000. "Self-Compacting Concrete (SCC) Time Development of the Material Properties and the Bond Behaviour", LACER (5) pp 115-125

Dibike, Y.B., Velickov, S., Solomatine, D., and Abbott, M.B. 2001. Model Induction with Support Vector Machines: Introduction and Applications. *Journal of Computing in Civil Engineering*, Vol. 15, No. 3. pp. 208-216

Ding,Y., Zhang,Y. and Thomas, A., 2007. The investigation on strength and flexural toughness of fibre cocktail reinforced self-compacting high performance concrete. Construction and Building Materials.

Domone, P.L., and Jin, J. 1999. Properties of mortar for self-compacting concrete. In: Skarendahl A, Petersson O, editors. Proceedings of the 1st International RILEM symposium on self-compacting concrete, pp. 109–200.

Druta, C., 2003. Tensile Strength and Bonding Characteristics of Self-Compacting Concrete. MSc Thesis. Louisiana State Unversity. 125p

EFNARC, 2002. "Specification and Guidelines for Self-Compacting Concrete", 36p, http://www.efnarc.org/

EFNARC, 2005. "The European Guidelines for Self-Compacting Concrete: Specification, Production and Use, 68p

El-Chabib, H., and Nehdi, M., 2006. "Effect of Mixture Design Parameters on Segregation of Self-Consolidating Concrete", ACI Materials Journal, V. 103, No. 5.

Elinwa, A.U., Ejeh, S.P., and Mamuda, A.M., 2007. "Assessing of the fresh concrete properties of self-compacting concrete containing sawdust ash", Construction and Building Materials

Faroug, F., Szwabowski, J., and Wild, S. (1999). Influence of Superplasticizers on Workability of Concrete, Journal of Materials in Civil Engineering, Vol. 11, No. 2, pp. 151-157

Felekoglu, B, 2006. "A comparative study on the performance of sands rich and poor in fines in self-compacting concrete", Construction and Building Materials

Felekoglu, B., and Sarikahya, H., 2007. "Effect of chemical structure of polycarboxylate-based superplasticizers on workability retention of self-compacting concrete", Construction and Building Materials

Felekoglu,B., Turkel, S., and Baradan, B., 2007. "Effect of water/cement ratio on the fresh and hardened properties of self-compacting concrete", Building and Environment (42), pp.1795–1802

Ferraris, C.; Browner, L.; Ozyildirim, C.; and Daczko, J., 2000. "Workability of Self- Compacting Concrete," Proceedings of PCI/FHWA/FIB International Symposium on High-Performance Concrete: The Economical Solution for Durable Bridges and Transportation Structures; Orlando, FL; pp. 398-407.

Geikera,M.R., Brandla, M., Thranea,L.N., Bagerb, D.H., and Wallevikc, O., 2002. "The effect of measuring procedure on the apparent rheological properties of self-compacting concrete", Cement and Concrete Research (32) 1791–1795

Grauers, M, 2000. "Rational Production and Improved Working Environment through using Self Compacting Concrete", Brite EuRam-Final Technical Report

Grube, H. and Rickert J 2002. Self compacting concrete – another stage in the development of the 5-component system of concrete. Today's Concrete Technology, 10p

Guang, N.H., and Zong, W.J., 2000. Prediction of compressive strength of concrete by neural networks. Cement and Concrete Research (30), pp. 1245- 1250

Holschemacher, K. and Klug, Y., 2002. A Database for the Evaluation of Hardened Properties of SCC. LACER No. 7, pp. 123-134

Holschemacher, K. and Klug, Y., 2002. Properties of SCC in comparison with normal vibrated concrete. Today's Concrete Technology, 10p

Hwang, S.D., Khayat, K.H., and Bonneau, O., 2006. "Performance-Based Specifications of Self-Consolidating Concrete Used in Structural Applications", ACI Materials Journal, pp. 121-129

JSCE, 1999. "Recommendation for Self Compacting Concrete," JSCE Concrete Engineering Series 31, T., Omoto and K., Ozawa, eds., 77p

Kapoor, Y.P., Munn, C., and Charif, K., 2003. "Self Compacting Concrete-an Economic Approach", 7th International Conference on Concrete in Hot & Aggressive Environments, Bahrain, pp. 509-592

Khatib, J.M., 2007. "Performance of self-compacting concrete containing fly ash", Construction and Building Materials

Khayat, K. H., 1999. "Workability, Testing and Performance of Self-Consolidating Concrete", ACI Materials Journal, v.96, No. 3, pp. 346-353.

Khayat, K.H., and Assaad, J.J., 2006. "Effect of w/cm and High-Range Water-Reducing Admixture on Formwork Pressure and Thixotropy of Self-Consolidating Concrete", ACI Materials Journal, V. 103, No. 3.

Kim, J.I., Kim, D.K., Feng, M.Q., and Yazdani, F., 2004. Application of Neural Networks for Estimation of Concrete Strength. Journal of Materials in Civil Engineering, Vol. 16, No. 3, pp. 257-265

Lachemi, M., Hossain, K.M.A., and Lambros, V.B., 2006. "Axial Load Behavior of Self-Consolidating Concrete-Filled Steel Tube Columns in Construction and Service Stages", ACI Structural Journal, V. 103, No. 1.

Lee, Y.J., and Mangasarian, O. L. (2001). SSVM: A Smooth Support Vector Machine for Classification. *Computational Optimization and Applications* (20) pp 5-22.

Lee, Y.J., Hsieh, W.F. and Huang, C.M., (2005). ε-SSVR: A Smooth Support Vector Machine for ε-Insensitive Regression. *IEEE Transactions on Knowledge and Data Engineering*, Vol. 17, No. 5.pp. 678-685

Marsh, D., 2002, "Spreading the Word on Self-Consolidating Concrete" ConcreteProducts,<concreteproducts.com/ar/concrete_spreading_word_selfc onsolidating>

Mijnsbergen, J.P.G. 2000. Tensile strength as design parameter. Brite EuRam-Technical Report, 28p

Mnahoncakova, E., Pavlikova, M., Grzeszczyk, S., Rovnanikova, P. and Cerny, R., 2007. "Hydric, thermal and mechanical properties of self-compactingconcrete containing different fillers", Construction and Building Materials

Montgomery, D. C., 2004. Design and Analysis of Experiments, 6th Edition, John Wiley & Sons, USA.

Nehdi, M., Pardhan, M., and Koshowski, S., 2004. "Durability of self consolidating concrete incorporating high volume replacement composite cements", Cement and Concrete Research (34), pp. 2103-2112

Noumowe, A., Carre, H., Daoud, A., and Toutanji, H., 2006. "High-Strength Self-Compacting Concrete Exposed to Fire Test", Journal of Materials in Civil Engineering, Vol. 18, No. 6.

NRMCA, 2004. "Concrete in Practice (CIP37): Self Compacting Concrete", NRMCA (National Ready Mixed Concrete Association), Technical Information, http://www.nrmca.org

Nunes, S., Figueiras, H., Oliveira, P.M., Coutinho, J.S., and Figueiras, J., 2006 . "A Methodology to Assess Robustness of SCC Mixtures", Cement and Concrete Research (36) 2115-2122

O'Brien, R. M., 2007. "A Caution Regarding Rules of Thumb for Variance Inflation Factors," Quality and Quantity 41 (5), pp. 673-690.

Okamura, H, 1997. "Self-Compacting High-Performance Concrete", Concrete International, pp.50-54

Okamura, H. and Ozawa,K., 1995. "Mix design for self-compacting concrete", Concrete Library of JSCE, 25, pp.107-120

Okamura, H., and Ouchi, M., 1999. "Self-Compacting Concrete", Proceedings of the First International RILEM Symposium, pp. 3-14., Edited by A. Skarendahl and O. Petersson

Okamura, H., and Ouchi, M., 2003. "Self Compacting Concrete", Journal of Advanced Concrete Technology, Vol.1. No.1. pp.5-15

Oliveira, L.A.P., Gomes,J.P.C., and Pereira, C.N.G., 2006. "Study of Sorptivity of Self-Compacting Concrete with Mineral Additives", Journal of Civil Engineering and Management, Lithuaniae, Vol XII, No 3, pp. 215–220

Oniyah, L.C. (2009). Design and Analysis of Experiments: Classical and Regression Approaches with SAS. CRC Press. USA. 822p.

Ouchi, M., Hibino,M., Sugamata, T., and Okamura, H., 2001. "A quantitative evalution method for effect of superplasticizer in self compacting concrete", Transactions of JCI, pp. 15-20

Ouchi, M., Nakamura, S., Otsterberg, T., Hallberg, S.E., and Lwin, M., 2003 . "Applications of Self-Compacting Concrete in Japan, Europe and the United States", ISHPC (International Symposium on High Performance Concrete), pp.1-20

Ozbay, E., Gesoglu, M., and Guneyisi, E., 2007. 'Empirical modeling of fresh and hardened properties of self-compacting concretes by genetic programming", Construction and Building Materials

Patel, R., Hossain, K.M.A., Shehata, M., Bouzouba, N., and Lachemi, M., 2004. "Development of statistical models for mixture design of high volume fly ash self consolidating concrete", ACI Materials Journal (101), pp. 294-302

PCI, 2003. "Interim Guidelines for the Use of Self-Consolidating Concrete in Precast/Prestressed Concrete Institute Member Plants", Precast/Prestressed Concrete Institute, Chicago USA, 165pp

Peter, J.A., Lakshmanan, N., and Manoharan, P.D., 2006. "Investigations on the Static Behavior of Self-Compacting Concrete Under-Reamed Piles", Journal of Materials in Civil Engineering, Vol. 18, No. 3.

Petit, J.Y., Wirquin, E., Vanhove, Y., and Khayat, K.H., 2007. "Yield stress and viscosity equations for mortars and self-consolidating concrete", Cement and Concrete Research (37) 655–670.

Ramage, B..; Kahn, L.; and Kurtis, K.(2006). "Evaluation of Self-Consolidating Concrete for Bridge Structure Applications: Task 1 Report," Structural Engineering Mechanics and Material Special.

Ravindrarajah, R.S., Siladyi, D., and Adamopoulos, B. (2003). Development of High-Strength Self-Compacting Concrete with Reduced Segregation Potential. Proceedings of the 3rd International RILEM Symposium, Reykjavik, Iceland, Edited by O. Wallevik and I. Nielsson , (RILEM Publications), Vol. 1, 1048 p

Reinhardt, H.W., and Stegmaier, M, 2006a. "Influence of heat curing on the pore structure and compressive strength of self-compacting concrete (SCC)", Cement and Concrete Research (36) 879–885

Reinhardt, H.W., and Stegmaier, M., 2006b. "Self-Consolidating Concrete in Fire", ACI Materials Journal, Vol. 103, No. 2.

Roussel, N., 2006. "A thixotropy model for fresh fluid concretes: Theory, validation and applications", Cement and Concrete Research (36) 1797–1806

Roy, R. 1990. A Primer on the Taguchi Method, Van Nostrand Reinhold, USA

Roziere, E., Granger, S., Turcry,Ph., and Loukili, A., 2007. "Influence of paste volume on shrinkage cracking and fracture properties of self-compacting concrete", Cement & Concrete Composites (29) 626–636

Safiuddin, M., FitzGerald, G.R., West, J.S., and Soudki, K.A., 2006. "Air-Void Stability in Fresh Self-Consolidating Concretes Incorporating Rice Husk

Ash", Advances in Engineering Structures, Mechanics & Construction, pp. 129–138.

Sahmaran, M., and Yaman, I.O., 2007."Hybrid fiber reinforced self-compacting concrete with a high-volume coarse fly ash", Construction and Building Materials (21), pp. 150–156

Sakata, N., Yanai, S., Yokozeki, K., and Maruyama, K., 2003. "Study on New Viscosity Agent for Combinatioon use Type of Self Compacting Concrete", Journal of Advanced Concrete Technology Vol.1., No. 1. pp.37-41

Schindler, A.K., Barnes, R.W., Roberts, J.B., and Rodriguez, S., 2007. "Properties of Self-Consolidating Concrete for Prestressed Members", ACI Materials Journal, Vol. 104, No. 1.

Schutter, G.,D., and Audenaert, K., 2004. "Evaluation of water absorption of concrete as a measure for resistance against carbonation and chloride migration", Materials and Structures (37), pp 591-596.

Schutter, G.D., 2005a "Guidelines for Testing Fresh Self-Compacting Concrete", European Research Project Report

Schutter, G.D., 2005b. "Measurement of Properties of Fresh Self-Compacting Concrete", European Research Project Report, pp.1-23

Sekhar, T.S. and Rao, P.S., 2008. Relationship between Compressive, Split Tensile, Flexural Strength of Self Compacted Concrete. International Journal of Mechanics and Solids. 3 (2). pp.157-168

Shi, C., Wu, Y., and Riefler, C., 2006. "Self-Consolidating Lightweight Concrete:A field demonstration using insulating concrete forms", Concrete international

Shindoh, T. and Matsuoka, Y. 2003. "Development of Combination-Type Self-Compacting Concrete and Evalution Test Methods", Journal of Advanced Concrete Technology Vol.1., No. 1. pp.26-36

Skarendahl,A., and Petersson, O., 2000."Self-Compacting Concrete - State-of-the-Art", Report of RILEM TC 174-SCC, 168p, http://www.rilem.net/

Sonebi, M., Grünewald, S., and Walraven, J., 2007. "Filling Ability and Passing Ability of Self-Consolidating Concrete", ACI Materials Journal, V. 104, No. 2.

Sonebi, M.; and Bartos, P. J. M. 2001. "Performance of Reinforced Columns Cast with Self-Compacting Concrete," Proceedings for the Fifth CANMET/ACI International Conference on Recent Advances in Concrete Technology, SP-200, Singapore, Ed.V. M. Malhortra, pp.415-431.

Srinivasan,C.B., Narasimhan,N.L., and Ilango, S.V. 2003. Development of rapid-set high-strength cement using statistical experimental design. Cement and Concrete Research (33) pp. 1287–1292

Su N., Hsu K C., and Chai H W., 2001, "A simple mix design method for self-compacting concrete", Cement and Concrete Research, Vol. 31, pp. 1799-1807

Su, N., Miao, B., (2003). A new method for the mix design of medium strength flowing concrete with low cement content. *Cement and Concrete Composites* (25): pp. 215– 222.

Sukumar, B., Nagamani, K., and Raghavan, R.S., 2007. "Evaluation of strength at early ages of self-compacting concrete with high volume fly ash", Construction and Building Materials

Tanyildizi, H. 2008. Effect of temperature, carbon fibers, and silica fume on the mechanical properties of lightweight concretes. New Carbon Materials, 23(4). p. 339–344.

Tanyildizi, H., and Coskun, A., 2008. Performance of lightweight concrete with silica fume after high temperature. Construction and Building Materials (22). pp. 2124–2129.

Torrijos, M.C., Barragan, B.E., and Zerbino, R.L., 2007. "Physical–mechanical properties, and mesostructure of plain and fibre reinforced self-compacting concrete", Construction and Building Materials

Tumidajski, P. J and Gong B. 2006. Effect of coarse aggregate size on strength and workability of concrete. Canadian Journal of Civil Engineering; (33), 2 pp. 206-213

Turcry, P., and Loukili, A., 2006. "Evaluation of Plastic Shrinkage Cracking of Self-Consolidating Concrete", ACI Materials Journal, V. 103, No. 4.

Turcry, P., Loukili, A., Haidar, H., Cabot, G.P., and Belarbi, A., 2006. "Cracking Tendency of Self-Compacting Concrete Subjected to Restrained Shrinkage: Experimental Study and Modeling", Journal of Materials in Civil Engineering, Vol. 18, No. 1.

Turkmena, I., and Kantarci, A., 2007. "Effects of expanded perlite aggregate and different curing conditions on the physical and mechanical properties of self-compacting concrete", Building and Environment (42) 2378–2383

Turkmena, I., Gul, R., and Celik, C. 2008. A Taguchi approach for investigation of some physical properties of concrete produced from mineral admixtures, Building and Environment (43) p. 1127–1137

Unal, R., and Dean, E.B., 1991. Taguchi Approach to Design Optimization for Quality and Cost: An Overview, Annual Conference of the International Society of Parametric Analysts, pp. 1-10

Vapnik, V.N., (1995). *The Nature of Statistical Learning Theory*. New York: Springer-Verlag.

Vapnik, V.N., (1998). An Overview of statistical learning theory. *IEEE Transaction on Neural Network*, vol. 10, no. 5, pp. 988–999.

Vapnik, V.N., Golowich, S.E., and Smola, A., (1996). "Support vector method for function approximation, regression estimation and signal processing". in *Advances in Neural Information Processing Systems. Cambridge*, MA: MIT Press, Vol. 9, pp. 281–287.

Westerholm, M., P. Skoglund and J. Trägårdh, 2002. "Chloride Transport and Related Microstructure of Self-Consolidating Concrete", Proceedings of the First North American Conference on the Design and Use of Self-Consolidating Concrete, Hanley-Wood, LLC, Illinois, USA, pp: 319-324.

Westphal, K, 2006. "Comparison of Guidelines for SCC", Course Material-Nordic SCC Network Workshop.

Wustholz, T. and Reinhardt, H.W., 2006. "Deformation behaviour of self-compacting concrete under tensile loading", Materials and Structures

Yanzhong, L., Xuhong, L., and Xiaojian, S., 2007. Short-Term Traffic Flow Prediction Based on Lagrange Support Vector Regression. International Conference on Transportation Engineering 2007 (ICTE 2007), pp. 1249-1254

Yazıcı, H., 2007. "The effect of silica fume and high-volume Class C fly ash on mechanical properties, chloride penetration and freeze–thaw resistance of self-compacting concrete", Construction and Building Materials

Yeh, I.C., 1998a. Modeling Concrete Strength with Augment-Neuron Networks. Journal of Materials in Civil Engineering, Vol. 10, No. 4, pp. 263-268

Yeh, I.C., 1998b. Modeling of strength of high-performance concrete using artificial neural networks. Cement and Concrete Research, Vol. 28, No. 12, pp. 1797–1808

Yeh, I.C., 1999. Design of high-performance concrete mixture using neural networks and nonlinear programming. Journal of computing in civil engineering, Vol. 13, No. 1, pp. 36-42

Yeh, I.C., 2006. Exploring Concrete Slump Model Using Artificial Neural Networks. Journal of Computing in Civil Engineering, Vol. 20, No. 3, pp.217-222

Yeh, I.C., 2007. "Modeling slump flow of concrete using second-order regressions and artificial neural networks", Cement & Concrete Composites (29) 474–480

Zaina,M.F.M., Mahmud, H.B. , Ilhama, A. and Faizala, M. 2002. Prediction of splitting tensile strength of high-performance concrete. Cement and Concrete Research (32) pp.1251–1258

Zhang, J., Sato, T., and Iai, S. 2006. Support vector regression for on-line health monitoring of large-scale structures. *Structural Safety* (28) pp. 392–406

Zhu, W., and Bartos P.J.M., 2003." Permeation properties of self compacting concrete", Cement & Concrete Research (33), pp. 921-926
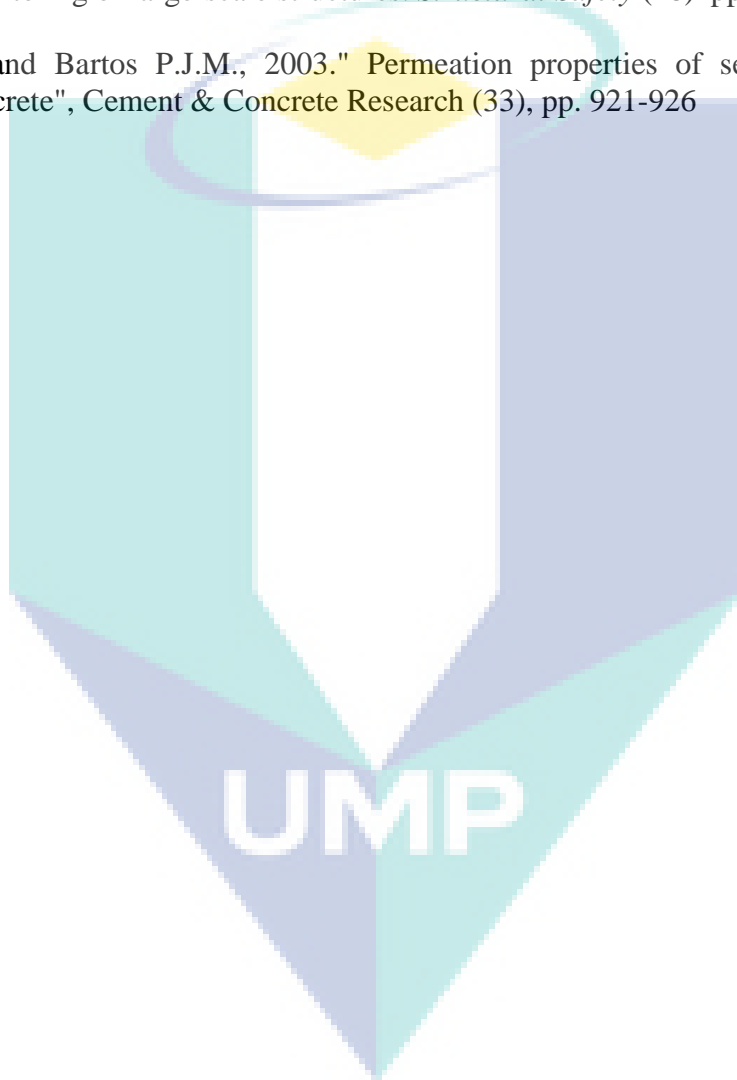
Appendix A

LIST OF PUBLICATIONS

No.	Paper/Journal Title
1	**Regression Modeling of Self Compacting Concrete Slump Flow** International Conference on Civil Engineering 2008 (ICCE'08), Kuantan, Malaysia, 12-14th May 2008,
2	**Workability Modeling of Self Compacting Concrete using Support Vector Regression** The 4th IMT-GT Conference on Mathematics, Statistics and Applications (ICMSA), Banda Aceh-Indonesia, 9-11 June 2008
3	**Review of Testing Methods for Self Compacting Concrete** International Conference on Construction and Building Technology (ISSBT2008), Kuala Lumpur Malaysia, 16-18 June 2008
4	**Effect of Packing Factor for SCC Mix Design** International Graduate Conference on Engineering and Science (IGCES 2008), Johor Bahru, Malaysia, 23-24 Dec 2008
5	**Effect Superplasticizer and Water-Binder Ratio on Freshened Properties and Compressive Strength Of SCC** Journal of Engineering and Applied Sciences 4 (3): 232-235, 2009 ISSN: 1816-949X, Medwell Journals, Pakistan, 2009
6	**Taguchi Experiment Design for Investigation of Freshened Properties of Self-Compacting Concrete** American Journal of Engineering and Applied Sciences, 3 (2): 300-306, 2010, ISSN: 1941-7020, Science Publications, USA, 2010

Appendix B

PHOTOS OF TESTING APPARATUS

Figure B.1. V-funnel test apparatus
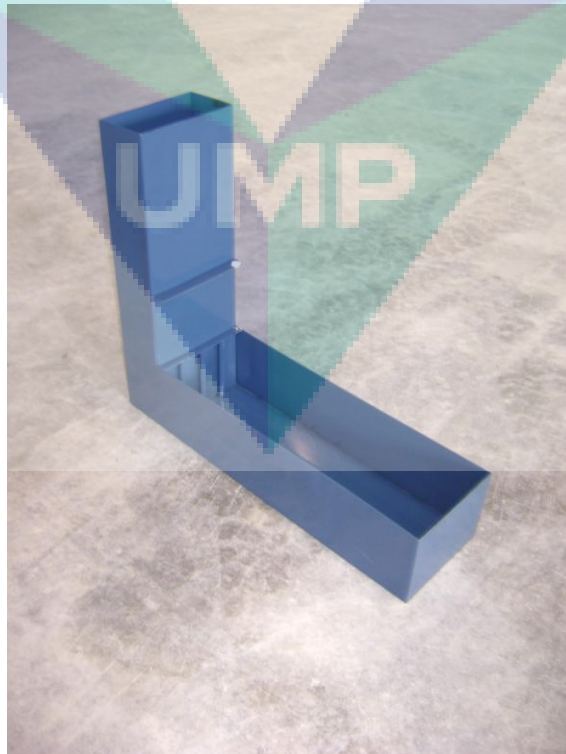
Figure B.2. L-box test Apparatus
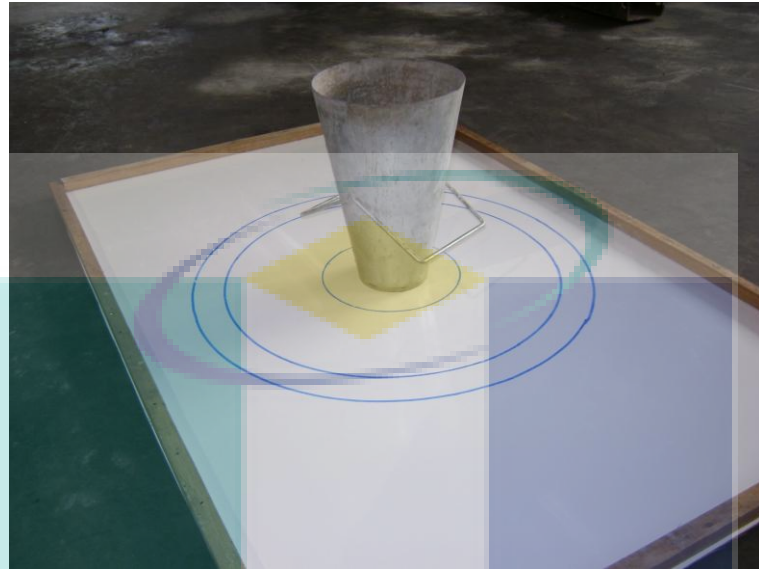
Figure B.3. Slump flow test apparatus

Figure B.4. Slump flow

Figure B.5. Compressive test apparatus

Figure B.6. Flexural test apparatus

Appendix C

STATISTICAL *F*-TABLE

TABLE A.3

F Distribution: Critical Values of F (5% significance level)

v_1	1	2	3	4	5	6	7	8	9	10	12	14	16	18	20
v_2															
1	161.45	199.50	215.71	224.58	230.16	233.99	236.77	238.88	240.54	241.88	243.91	245.36	246.46	247.32	248.01
2	18.51	19.00	19.16	19.25	19.30	19.33	19.35	19.37	19.38	19.40	19.41	19.42	19.43	19.44	19.45
3	10.13	9.55	9.28	9.12	9.01	8.94	8.89	8.85	8.81	8.79	8.74	8.71	8.69	8.67	8.66
4	7.71	6.94	6.59	6.39	6.26	6.16	6.09	6.04	6.00	5.96	5.91	5.87	5.84	5.82	5.80
5	6.61	5.79	5.41	5.19	5.05	4.95	4.88	4.82	4.77	4.74	4.68	4.64	4.60	4.58	4.56
6	5.99	5.14	4.76	4.53	4.39	4.28	4.21	4.15	4.10	4.06	4.00	3.96	3.92	3.90	3.87
7	5.59	4.74	4.35	4.12	3.97	3.87	3.79	3.73	3.68	3.64	3.57	3.53	3.49	3.47	3.44
8	5.32	4.46	4.07	3.84	3.69	3.58	3.50	3.44	3.39	3.35	3.28	3.24	3.20	3.17	3.15
9	5.12	4.26	3.86	3.63	3.48	3.37	3.29	3.23	3.18	3.14	3.07	3.03	2.99	2.96	2.94
10	4.96	4.10	3.71	3.48	3.33	3.22	3.14	3.07	3.02	2.98	2.91	2.86	2.83	2.80	2.77
11	4.84	3.98	3.59	3.36	3.20	3.09	3.01	2.95	2.90	2.85	2.79	2.74	2.70	2.67	2.65
12	4.75	3.89	3.49	3.26	3.11	3.00	2.91	2.85	2.80	2.75	2.69	2.64	2.60	2.57	2.54
13	4.67	3.81	3.41	3.18	3.03	2.92	2.83	2.77	2.71	2.67	2.60	2.55	2.51	2.48	2.46
14	4.60	3.74	3.34	3.11	2.96	2.85	2.76	2.70	2.65	2.60	2.53	2.48	2.44	2.41	2.39
15	4.54	3.68	3.29	3.06	2.90	2.79	2.71	2.64	2.59	2.54	2.48	2.42	2.38	2.35	2.33
16	4.49	3.63	3.24	3.01	2.85	2.74	2.66	2.59	2.54	2.49	2.42	2.37	2.33	2.30	2.28
17	4.45	3.59	3.20	2.96	2.81	2.70	2.61	2.55	2.49	2.45	2.38	2.33	2.29	2.26	2.23
18	4.41	3.55	3.16	2.93	2.77	2.66	2.58	2.51	2.46	2.41	2.34	2.29	2.25	2.22	2.19
19	4.38	3.52	3.13	2.90	2.74	2.63	2.54	2.48	2.42	2.38	2.31	2.26	2.21	2.18	2.16
20	4.35	3.49	3.10	2.87	2.71	2.60	2.51	2.45	2.39	2.35	2.28	2.22	2.18	2.15	2.12
21	4.32	3.47	3.07	2.84	2.68	2.57	2.49	2.42	2.37	2.32	2.25	2.20	2.16	2.12	2.10
22	4.30	3.44	3.05	2.82	2.66	2.55	2.46	2.40	2.34	2.30	2.23	2.17	2.13	2.10	2.07
23	4.28	3.42	3.03	2.80	2.64	2.53	2.44	2.37	2.32	2.27	2.20	2.15	2.11	2.08	2.05
24	4.26	3.40	3.01	2.78	2.62	2.51	2.42	2.36	2.30	2.25	2.18	2.13	2.09	2.05	2.03
25	4.24	3.39	2.99	2.76	2.60	2.49	2.40	2.34	2.28	2.24	2.16	2.11	2.07	2.04	2.01
26	4.22	3.37	2.98	2.74	2.59	2.47	2.39	2.32	2.27	2.22	2.15	2.09	2.05	2.02	1.99
27	4.21	3.35	2.96	2.73	2.57	2.46	2.37	2.31	2.25	2.20	2.13	2.08	2.04	2.00	1.97
28	4.20	3.34	2.95	2.71	2.56	2.45	2.36	2.29	2.24	2.19	2.12	2.06	2.02	1.99	1.96
29	4.18	3.33	2.93	2.70	2.55	2.43	2.35	2.28	2.22	2.18	2.10	2.05	2.01	1.97	1.94
30	4.17	3.32	2.92	2.69	2.53	2.42	2.33	2.27	2.21	2.16	2.09	2.04	1.99	1.96	1.93
35	4.12	3.27	2.87	2.64	2.49	2.37	2.29	2.22	2.16	2.11	2.04	1.99	1.94	1.91	1.88
40	4.08	3.23	2.84	2.61	2.45	2.34	2.25	2.18	2.12	2.08	2.00	1.95	1.90	1.87	1.84
50	4.03	3.18	2.79	2.56	2.40	2.29	2.20	2.13	2.07	2.03	1.95	1.89	1.85	1.81	1.78
60	4.00	3.15	2.76	2.53	2.37	2.25	2.17	2.10	2.04	1.99	1.92	1.86	1.82	1.78	1.75
70	3.98	3.13	2.74	2.50	2.35	2.23	2.14	2.07	2.02	1.97	1.89	1.84	1.79	1.75	1.72
80	3.96	3.11	2.72	2.49	2.33	2.21	2.13	2.06	2.00	1.95	1.88	1.82	1.77	1.73	1.70
90	3.95	3.10	2.71	2.47	2.32	2.20	2.11	2.04	1.99	1.94	1.86	1.80	1.76	1.72	1.69
100	3.94	3.09	2.70	2.46	2.31	2.19	2.10	2.03	1.97	1.93	1.85	1.79	1.75	1.71	1.68
120	3.92	3.07	2.68	2.45	2.29	2.18	2.09	2.02	1.96	1.91	1.83	1.78	1.73	1.69	1.66
150	3.90	3.06	2.66	2.43	2.27	2.16	2.07	2.00	1.94	1.89	1.82	1.76	1.71	1.67	1.64
200	3.89	3.04	2.65	2.42	2.26	2.14	2.06	1.98	1.93	1.88	1.80	1.74	1.69	1.66	1.62
250	3.88	3.03	2.64	2.41	2.25	2.13	2.05	1.98	1.92	1.87	1.79	1.73	1.68	1.65	1.61
300	3.87	3.03	2.63	2.40	2.24	2.13	2.04	1.97	1.91	1.86	1.78	1.72	1.68	1.64	1.61
400	3.86	3.02	2.63	2.39	2.24	2.12	2.03	1.96	1.90	1.85	1.78	1.72	1.67	1.63	1.60
500	3.86	3.01	2.62	2.39	2.23	2.12	2.03	1.96	1.90	1.85	1.77	1.71	1.66	1.62	1.59
600	3.86	3.01	2.62	2.39	2.23	2.11	2.02	1.95	1.90	1.85	1.77	1.71	1.66	1.62	1.59
750	3.85	3.01	2.62	2.38	2.23	2.11	2.02	1.95	1.89	1.84	1.77	1.70	1.66	1.62	1.58
1000	3.85	3.00	2.61	2.38	2.22	2.11	2.02	1.95	1.89	1.84	1.76	1.70	1.65	1.61	1.58

Table A.3 (continued)

F Distribution: Critical Values of F (5% significance level)

v_1	25	30	35	40	50	60	75	100	150	200
v_2										
1	249.26	250.10	250.69	251.14	251.77	252.20	252.62	253.04	253.46	253.68
2	19.46	19.46	19.47	19.47	19.48	19.48	19.48	19.49	19.49	19.49
3	8.63	8.62	8.60	8.59	8.58	8.57	8.56	8.55	8.54	8.54
4	5.77	5.75	5.73	5.72	5.70	5.69	5.68	5.66	5.65	5.65
5	4.52	4.50	4.48	4.46	4.44	4.43	4.42	4.41	4.39	4.39
6	3.83	3.81	3.79	3.77	3.75	3.74	3.73	3.71	3.70	3.69
7	3.40	3.38	3.36	3.34	3.32	3.30	3.29	3.27	3.26	3.25
8	3.11	3.08	3.06	3.04	3.02	3.01	2.99	2.97	2.96	2.95
9	2.89	2.86	2.84	2.83	2.80	2.79	2.77	2.76	2.74	2.73
10	2.73	2.70	2.68	2.66	2.64	2.62	2.60	2.59	2.57	2.56
11	2.60	2.57	2.55	2.53	2.51	2.49	2.47	2.46	2.44	2.43
12	2.50	2.47	2.44	2.43	2.40	2.38	2.37	2.35	2.33	2.32
13	2.41	2.38	2.36	2.34	2.31	2.30	2.28	2.26	2.24	2.23
14	2.34	2.31	2.28	2.27	2.24	2.22	2.21	2.19	2.17	2.16
15	2.28	2.25	2.22	2.20	2.18	2.16	2.14	2.12	2.10	2.10
16	2.23	2.19	2.17	2.15	2.12	2.11	2.09	2.07	2.05	2.04
17	2.18	2.15	2.12	2.10	2.08	2.06	2.04	2.02	2.00	1.99
18	2.14	2.11	2.08	2.06	2.04	2.02	2.00	1.98	1.96	1.95
19	2.11	2.07	2.05	2.03	2.00	1.98	1.96	1.94	1.92	1.91
20	2.07	2.04	2.01	1.99	1.97	1.95	1.93	1.91	1.89	1.88
21	2.05	2.01	1.98	1.96	1.94	1.92	1.90	1.88	1.86	1.84
22	2.02	1.98	1.96	1.94	1.91	1.89	1.87	1.85	1.83	1.82
23	2.00	1.96	1.93	1.91	1.88	1.86	1.84	1.82	1.80	1.79
24	1.97	1.94	1.91	1.89	1.86	1.84	1.82	1.80	1.78	1.77
25	1.96	1.92	1.89	1.87	1.84	1.82	1.80	1.78	1.76	1.75
26	1.94	1.90	1.87	1.85	1.82	1.80	1.78	1.76	1.74	1.73
27	1.92	1.88	1.86	1.84	1.81	1.79	1.76	1.74	1.72	1.71
28	1.91	1.87	1.84	1.82	1.79	1.77	1.75	1.73	1.70	1.69
29	1.89	1.85	1.83	1.81	1.77	1.75	1.73	1.71	1.69	1.67
30	1.88	1.84	1.81	1.79	1.76	1.74	1.72	1.70	1.67	1.66
35	1.82	1.79	1.76	1.74	1.70	1.68	1.66	1.63	1.61	1.60
40	1.78	1.74	1.72	1.69	1.66	1.64	1.61	1.59	1.56	1.55
50	1.73	1.69	1.66	1.63	1.60	1.58	1.55	1.52	1.50	1.48
60	1.69	1.65	1.62	1.59	1.56	1.53	1.51	1.48	1.45	1.44
70	1.66	1.62	1.59	1.57	1.53	1.50	1.48	1.45	1.42	1.40
80	1.64	1.60	1.57	1.54	1.51	1.48	1.45	1.43	1.39	1.38
90	1.63	1.59	1.55	1.53	1.49	1.46	1.44	1.41	1.38	1.36
100	1.62	1.57	1.54	1.52	1.48	1.45	1.42	1.39	1.36	1.34
120	1.60	1.55	1.52	1.50	1.46	1.43	1.40	1.37	1.33	1.32
150	1.58	1.54	1.50	1.48	1.44	1.41	1.38	1.34	1.31	1.29
200	1.56	1.52	1.48	1.46	1.41	1.39	1.35	1.32	1.28	1.26
250	1.55	1.50	1.47	1.44	1.40	1.37	1.34	1.31	1.27	1.25
300	1.54	1.50	1.46	1.43	1.39	1.36	1.33	1.30	1.26	1.23
400	1.53	1.49	1.45	1.42	1.38	1.35	1.32	1.28	1.24	1.22
500	1.53	1.48	1.45	1.42	1.38	1.35	1.31	1.28	1.23	1.21
600	1.52	1.48	1.44	1.41	1.37	1.34	1.31	1.27	1.23	1.20
750	1.52	1.47	1.44	1.41	1.37	1.34	1.30	1.26	1.22	1.20
1000	1.52	1.47	1.43	1.41	1.36	1.33	1.30	1.26	1.22	1.19

TABLE A.3 (continued)

F Distribution: Critical Values of F (1% significance level)

v_2 \ v_1	1	2	3	4	5	6	7	8	9	10	12	14	16	18	20
1	4052.18	4999.50	5403.35	5624.58	5763.65	5858.99	5928.36	5981.07	6022.47	6055.85	6106.32	6142.67	6170.10	6191.53	6208.73
2	98.50	99.00	99.17	99.25	99.30	99.33	99.36	99.37	99.39	99.40	99.42	99.43	99.44	99.44	99.45
3	34.12	30.82	29.46	28.71	28.24	27.91	27.67	27.49	27.35	27.23	27.05	26.92	26.83	26.75	26.69
4	21.20	18.00	16.69	15.98	15.52	15.21	14.98	14.80	14.66	14.55	14.37	14.25	14.15	14.08	14.02
5	16.26	13.27	12.06	11.39	10.97	10.67	10.46	10.29	10.16	10.05	9.89	9.77	9.68	9.61	9.55
6	13.75	10.92	9.78	9.15	8.75	8.47	8.26	8.10	7.98	7.87	7.72	7.60	7.52	7.45	7.40
7	12.25	9.55	8.45	7.85	7.46	7.19	6.99	6.84	6.72	6.62	6.47	6.36	6.28	6.21	6.16
8	11.26	8.65	7.59	7.01	6.63	6.37	6.18	6.03	5.91	5.81	5.67	5.56	5.48	5.41	5.36
9	10.56	8.02	6.99	6.42	6.06	5.80	5.61	5.47	5.35	5.26	5.11	5.01	4.92	4.86	4.81
10	10.04	7.56	6.55	5.99	5.64	5.39	5.20	5.06	4.94	4.85	4.71	4.60	4.52	4.46	4.41
11	9.65	7.21	6.22	5.67	5.32	5.07	4.89	4.74	4.63	4.54	4.40	4.29	4.21	4.15	4.10
12	9.33	6.93	5.95	5.41	5.06	4.82	4.64	4.50	4.39	4.30	4.16	4.05	3.97	3.91	3.86
13	9.07	6.70	5.74	5.21	4.86	4.62	4.44	4.30	4.19	4.10	3.96	3.86	3.78	3.72	3.66
14	8.86	6.51	5.56	5.04	4.69	4.46	4.28	4.14	4.03	3.94	3.80	3.70	3.62	3.56	3.51
15	8.68	6.36	5.42	4.89	4.56	4.32	4.14	4.00	3.89	3.80	3.67	3.56	3.49	3.42	3.37
16	8.53	6.23	5.29	4.77	4.44	4.20	4.03	3.89	3.78	3.69	3.55	3.45	3.37	3.31	3.26
17	8.40	6.11	5.18	4.67	4.34	4.10	3.93	3.79	3.68	3.59	3.46	3.35	3.27	3.21	3.16
18	8.29	6.01	5.09	4.58	4.25	4.01	3.84	3.71	3.60	3.51	3.37	3.27	3.19	3.13	3.08
19	8.18	5.93	5.01	4.50	4.17	3.94	3.77	3.63	3.52	3.43	3.30	3.19	3.12	3.05	3.00
20	8.10	5.85	4.94	4.43	4.10	3.87	3.70	3.56	3.46	3.37	3.23	3.13	3.05	2.99	2.94
21	8.02	5.78	4.87	4.37	4.04	3.81	3.64	3.51	3.40	3.31	3.17	3.07	2.99	2.93	2.88
22	7.95	5.72	4.82	4.31	3.99	3.76	3.59	3.45	3.35	3.26	3.12	3.02	2.94	2.88	2.83
23	7.88	5.66	4.76	4.26	3.94	3.71	3.54	3.41	3.30	3.21	3.07	2.97	2.89	2.83	2.78
24	7.82	5.61	4.72	4.22	3.90	3.67	3.50	3.36	3.26	3.17	3.03	2.93	2.85	2.79	2.74
25	7.77	5.57	4.68	4.18	3.85	3.63	3.46	3.32	3.22	3.13	2.99	2.89	2.81	2.75	2.70
26	7.72	5.53	4.64	4.14	3.82	3.59	3.42	3.29	3.18	3.09	2.96	2.86	2.78	2.72	2.66
27	7.68	5.49	4.60	4.11	3.78	3.56	3.39	3.26	3.15	3.06	2.93	2.82	2.75	2.68	2.63
28	7.64	5.45	4.57	4.07	3.75	3.53	3.36	3.23	3.12	3.03	2.90	2.79	2.72	2.65	2.60
29	7.60	5.42	4.54	4.04	3.73	3.50	3.33	3.20	3.09	3.00	2.87	2.77	2.69	2.63	2.57
30	7.56	5.39	4.51	4.02	3.70	3.47	3.30	3.17	3.07	2.98	2.84	2.74	2.66	2.60	2.55
35	7.42	5.27	4.40	3.91	3.59	3.37	3.20	3.07	2.96	2.88	2.74	2.64	2.56	2.50	2.44
40	7.31	5.18	4.31	3.83	3.51	3.29	3.12	2.99	2.89	2.80	2.66	2.56	2.48	2.42	2.37
50	7.17	5.06	4.20	3.72	3.41	3.19	3.02	2.89	2.78	2.70	2.56	2.46	2.38	2.32	2.27
60	7.08	4.98	4.13	3.65	3.34	3.12	2.95	2.82	2.72	2.63	2.50	2.39	2.31	2.25	2.20
70	7.01	4.92	4.07	3.60	3.29	3.07	2.91	2.78	2.67	2.59	2.45	2.35	2.27	2.20	2.15
80	6.96	4.88	4.04	3.56	3.26	3.04	2.87	2.74	2.64	2.55	2.42	2.31	2.23	2.17	2.12
90	6.93	4.85	4.01	3.53	3.23	3.01	2.84	2.72	2.61	2.52	2.39	2.29	2.21	2.14	2.09
100	6.90	4.82	3.98	3.51	3.21	2.99	2.82	2.69	2.59	2.50	2.37	2.27	2.19	2.12	2.07
120	6.85	4.79	3.95	3.48	3.17	2.96	2.79	2.66	2.56	2.47	2.34	2.23	2.15	2.09	2.03
150	6.81	4.75	3.91	3.45	3.14	2.92	2.76	2.63	2.53	2.44	2.31	2.20	2.12	2.06	2.00
200	6.76	4.71	3.88	3.41	3.11	2.89	2.73	2.60	2.50	2.41	2.27	2.17	2.09	2.03	1.97
250	6.74	4.69	3.86	3.40	3.09	2.87	2.71	2.58	2.48	2.39	2.26	2.15	2.07	2.01	1.95
300	6.72	4.68	3.85	3.38	3.08	2.86	2.70	2.57	2.47	2.38	2.24	2.14	2.06	1.99	1.94
400	6.70	4.66	3.83	3.37	3.06	2.85	2.68	2.56	2.45	2.37	2.23	2.13	2.05	1.98	1.92
500	6.69	4.65	3.82	3.36	3.05	2.84	2.68	2.55	2.44	2.36	2.22	2.12	2.04	1.97	1.92
600	6.68	4.64	3.81	3.35	3.05	2.83	2.67	2.54	2.44	2.35	2.21	2.11	2.03	1.96	1.91
750	6.67	4.63	3.81	3.34	3.04	2.83	2.66	2.53	2.43	2.34	2.21	2.11	2.02	1.96	1.90
1000	6.66	4.63	3.80	3.34	3.04	2.82	2.66	2.53	2.43	2.34	2.20	2.10	2.02	1.95	1.90

TABLE A.3 (continued)

F Distribution: Critical Values of F (1% significance level)

v_2 \ v_1	25	30	35	40	50	60	75	100	150	200
1	6239.83	6260.65	6275.57	6286.78	6302.52	6313.03	6323.56	6334.11	6344.68	6349.97
2	99.46	99.47	99.47	99.47	99.48	99.48	99.49	99.49	99.49	99.49
3	26.58	26.50	26.45	26.41	26.35	26.32	26.28	26.24	26.20	26.18
4	13.91	13.84	13.79	13.75	13.69	13.65	13.61	13.58	13.54	13.52
5	9.45	9.38	9.33	9.29	9.24	9.20	9.17	9.13	9.09	9.08
6	7.30	7.23	7.18	7.14	7.09	7.06	7.02	6.99	6.95	6.93
7	6.06	5.99	5.94	5.91	5.86	5.82	5.79	5.75	5.72	5.70
8	5.26	5.20	5.15	5.12	5.07	5.03	5.00	4.96	4.93	4.91
9	4.71	4.65	4.60	4.57	4.52	4.48	4.45	4.41	4.38	4.36
10	4.31	4.25	4.20	4.17	4.12	4.08	4.05	4.01	3.98	3.96
11	4.01	3.94	3.89	3.86	3.81	3.78	3.74	3.71	3.67	3.66
12	3.76	3.70	3.65	3.62	3.57	3.54	3.50	3.47	3.43	3.41
13	3.57	3.51	3.46	3.43	3.38	3.34	3.31	3.27	3.24	3.22
14	3.41	3.35	3.30	3.27	3.22	3.18	3.15	3.11	3.08	3.06
15	3.28	3.21	3.17	3.13	3.08	3.05	3.01	2.98	2.94	2.92
16	3.16	3.10	3.05	3.02	2.97	2.93	2.90	2.86	2.83	2.81
17	3.07	3.00	2.96	2.92	2.87	2.83	2.80	2.76	2.73	2.71
18	2.98	2.92	2.87	2.84	2.78	2.75	2.71	2.68	2.64	2.62
19	2.91	2.84	2.80	2.76	2.71	2.67	2.64	2.60	2.57	2.55
20	2.84	2.78	2.73	2.69	2.64	2.61	2.57	2.54	2.50	2.48
21	2.79	2.72	2.67	2.64	2.58	2.55	2.51	2.48	2.44	2.42
22	2.73	2.67	2.62	2.58	2.53	2.50	2.46	2.42	2.38	2.36
23	2.69	2.62	2.57	2.54	2.48	2.45	2.41	2.37	2.34	2.32
24	2.64	2.58	2.53	2.49	2.44	2.40	2.37	2.33	2.29	2.27
25	2.60	2.54	2.49	2.45	2.40	2.36	2.33	2.29	2.25	2.23
26	2.57	2.50	2.45	2.42	2.36	2.33	2.29	2.25	2.21	2.19
27	2.54	2.47	2.42	2.38	2.33	2.29	2.26	2.22	2.18	2.16
28	2.51	2.44	2.39	2.35	2.30	2.26	2.23	2.19	2.15	2.13
29	2.48	2.41	2.36	2.33	2.27	2.23	2.20	2.16	2.12	2.10
30	2.45	2.39	2.34	2.30	2.25	2.21	2.17	2.13	2.09	2.07
35	2.35	2.28	2.23	2.19	2.14	2.10	2.06	2.02	1.98	1.96
40	2.27	2.20	2.15	2.11	2.06	2.02	1.98	1.94	1.90	1.87
50	2.17	2.10	2.05	2.01	1.95	1.91	1.87	1.82	1.78	1.76
60	2.10	2.03	1.98	1.94	1.88	1.84	1.79	1.75	1.70	1.68
70	2.05	1.98	1.93	1.89	1.83	1.78	1.74	1.70	1.65	1.62
80	2.01	1.94	1.89	1.85	1.79	1.75	1.70	1.65	1.61	1.58
90	1.99	1.92	1.86	1.82	1.76	1.72	1.67	1.62	1.57	1.55
100	1.97	1.89	1.84	1.80	1.74	1.69	1.65	1.60	1.55	1.52
120	1.93	1.86	1.81	1.76	1.70	1.66	1.61	1.56	1.51	1.48
150	1.90	1.83	1.77	1.73	1.66	1.62	1.57	1.52	1.46	1.43
200	1.87	1.79	1.74	1.69	1.63	1.58	1.53	1.48	1.42	1.39
250	1.85	1.77	1.72	1.67	1.61	1.56	1.51	1.46	1.40	1.36
300	1.84	1.76	1.70	1.66	1.59	1.55	1.50	1.44	1.38	1.35
400	1.82	1.75	1.69	1.64	1.58	1.53	1.48	1.42	1.36	1.32
500	1.81	1.74	1.68	1.63	1.57	1.52	1.47	1.41	1.34	1.31
600	1.80	1.73	1.67	1.63	1.56	1.51	1.46	1.40	1.34	1.30
750	1.80	1.72	1.66	1.62	1.55	1.50	1.45	1.39	1.33	1.29
1000	1.79	1.72	1.66	1.61	1.54	1.50	1.44	1.38	1.32	1.28

Appendix D

SAMPLE MIX DESIGN CALCULATION

Code :   Date :

Data :	f'c	50	MPa
	fcr	54.69	MPa
	Specific gravity of coarse aggregate	2.65	
	The bulk density of coarse aggregate (WgL)	1300	kg/m3
	Specific gravity of fine aggregate	2.64	
	The bulk density of fine aggregate (WsL)	1300	kg/m3
	Specific gravity of cement	3.15	
	Specific gravity of SilicaFume (SF)	2.2	
	Specific gravity of Superplasticizer (SP)	1.064	
	S/a	0.52	

Step 1:   Determine the coarse and fine aggregate contents

Fine aggregate content

Assume PF   1.233

$$W_{\mathrm{s}} = \mathrm{PF} \times W_{\mathrm{sL}} \times \frac{S}{a}$$ **833.51**   kg/m3

Coarse aggregate content

$$W_{\mathrm{g}} = \mathrm{PF} \times W_{\mathrm{gL}} \left(1 - \frac{S}{a}\right)$$ **769.39**   kg/m3

Step 2   Determine the cement content

                                                X   0.105

$$C = \frac{f'_{\mathrm{c}}}{x}$$ C =   **520.86**   kg/m3

Step 3   Determine the mixing water content required by cement

                                        w/c   0.4

$$W_{\mathrm{wc}} = \left(\frac{W}{C}\right) C$$ Wwc =   208.3429   kg/m3

Step 4	Calculation of Silica Fume (SF) contents				
			Vca	0.2903	
			Vfa	0.3157	
			Vc	0.1654	
			Vw	0.2083	
			Va	0.0180	
			Vp	0.0022	
			Wpm=	0.0022	
				2200	
			Wpm=	4.9419	
		Efficiency factor =			
		0.15	Wsf=	**32.9463**	kg/m3

$$V_{\mathrm{Pf}} + V_{\mathrm{PB}} = 1 - \frac{W_{\mathrm{g}}}{1000 \times G_{\mathrm{g}}} - \frac{W_{\mathrm{s}}}{1000 \times G_{\mathrm{s}}} - \frac{C}{1000 \times G_{\mathrm{C}}} - \frac{W_{\mathrm{wc}}}{1000 \times G_{\mathrm{w}}} - V_{\mathrm{a}}$$

Step 5	Determine the mixing water content required for SF			
		Water content for SF Wsf = 0.55xWp =	49.419	kg/m3

Step 6	Determine the SP dosage			
		WSP = 0,01x(Cement+SF) =	**5.54**	kg/m3

Step 7	Adjustment of mixing water content needed in SCC			
	Amount of water in SP:			
		WwSP = (1-0.4)xWsp=	3.323	kg/m3
	Amount of mixing water needed in SCC:			
		W = Wwc + Wsf-WwSP =	**254.44**	kg/m3

Step 8	Trial batches and tests on SCC properties			
	Coarse Aggregate (kg)	769.39		
	Fine Aggregate (kg)	833.51		
	Cement (kg)	520.86		
	SF (kg)	32.95		
	Water (kg)	254.44		
	SP (kg)	5.54		

Appendix E

ORTHOGONAL ARRAY

Table E.1: Design of Experiment based on Orthogonal Array (Roy, 1990)

Array	Experimental Runs	Number of Factors	Number of Levels
$L_4(2^3)$	4	3	2
$L_8(2^7)$	8	7	2
$L_9(3^4)$	9	4	3
$L_{18}(2^1 \times 3^7)$*	18	1	2
		and 7	and 3
$L_{32}(2^1 \times 4^9)$*	32	1	2
		and 9	and 4

* Mixed level arrays

Table E.2: Orthogonal Array, $L_4(2^3)$ (2 levels, 3 factors)

$L_4(2^3)$	1	2	3
1	1	1	1
2	1	2	2
3	2	1	2
4	2	2	1

Table E.3: Orthogonal Array, $L_8(2^7)$ (2 levels, 7 factors)

$L_8(2^7)$	1	2	3	4	5	6	7
1	1	1	1	1	1	1	1
2	1	1	1	2	2	2	2
3	1	2	2	1	1	2	2
4	1	2	2	2	2	1	1
5	2	1	2	1	2	1	2
6	2	1	2	2	1	2	1
7	2	2	1	1	2	2	1
8	2	2	1	2	1	1	2

Table E.4: Orthogonal Array, $L_9(3^4)$ (3 levels, 4 factors)

	$L_9(3^4)$			
	1	2	3	4
1	1	1	1	1
2	1	2	2	2
3	1	3	3	3
4	2	1	2	3
5	2	2	3	1
6	2	3	1	2
7	3	1	3	2
8	3	2	1	3
9	3	3	2	1

Table E.5: Orthogonal Array, $L_{18}(2^1 \times 3^7)$ (2 levels 1 factors; 3 level 7 factors)

	$L_{18}(2^1 \times 3^7)$							
	1	2	3	4	5	6	7	8
1	1	1	1	1	1	1	1	1
2	1	1	2	2	2	2	2	2
3	1	1	3	3	3	3	3	3
4	1	2	1	1	2	2	3	3
5	1	2	2	2	3	3	1	1
6	1	2	3	3	1	1	2	2
7	1	3	1	2	1	3	2	3
8	1	3	2	3	2	1	3	1
9	1	3	3	1	3	2	1	2
10	2	1	1	3	3	2	2	1
11	2	1	2	1	1	3	3	2
12	2	1	3	2	2	1	1	3
13	2	2	1	3	3	1	3	2
14	2	2	2	1	1	2	1	3
15	2	2	3	2	2	3	2	1
16	2	3	1	2	2	3	1	2
17	2	3	2	3	3	1	2	3
18	2	3	3	1	1	2	3	1

Table E.6: Orthogonal Array, $L_{32}(2^1 \times 4^8)$ (2 levels 1 factors; 4 level 8 factors)

	$L_{32}(2^1 \times 4^8)$									
	1	2	3	4	5	6	7	8	9	10
1	1	1	1	1	1	1	1	1	1	1
2	1	1	2	2	2	2	2	2	2	2
3	1	1	3	3	3	3	3	3	3	3
4	1	1	4	4	4	4	4	4	4	4
5	1	2	1	1	2	2	3	3	4	4
6	1	2	2	2	1	1	4	4	3	3
7	1	2	3	3	4	4	1	1	2	2
8	1	2	4	4	3	3	2	2	1	1
9	1	3	1	2	3	4	1	2	3	4
10	1	3	2	1	4	3	2	1	4	3
11	1	3	3	4	1	2	3	4	1	2
12	1	3	4	3	2	1	4	3	2	1
13	1	4	1	2	4	3	3	4	2	1
14	1	4	2	1	3	4	4	3	1	2
15	1	4	3	4	2	1	1	2	4	3
16	1	4	4	3	1	2	2	1	3	4
17	2	1	1	4	1	4	2	3	2	3
18	2	1	2	3	2	3	1	4	1	4
19	2	1	3	2	3	2	4	1	4	1
20	2	1	4	1	4	1	3	2	3	2
21	2	2	1	4	2	3	4	1	3	2
22	2	2	2	3	1	4	3	2	4	1
23	2	2	3	2	4	1	2	3	1	4
24	2	2	4	1	3	2	1	4	2	3
25	2	3	1	3	3	1	2	4	4	2
26	2	3	2	4	4	2	1	3	3	1
27	2	3	3	1	1	3	4	2	2	4
28	2	3	4	2	2	4	3	1	1	3
29	2	4	1	3	4	2	4	2	1	3
30	2	4	2	4	3	1	3	1	2	4
31	2	4	3	1	2	4	2	4	3	1
32	2	4	4	2	1	3	1	3	4	2